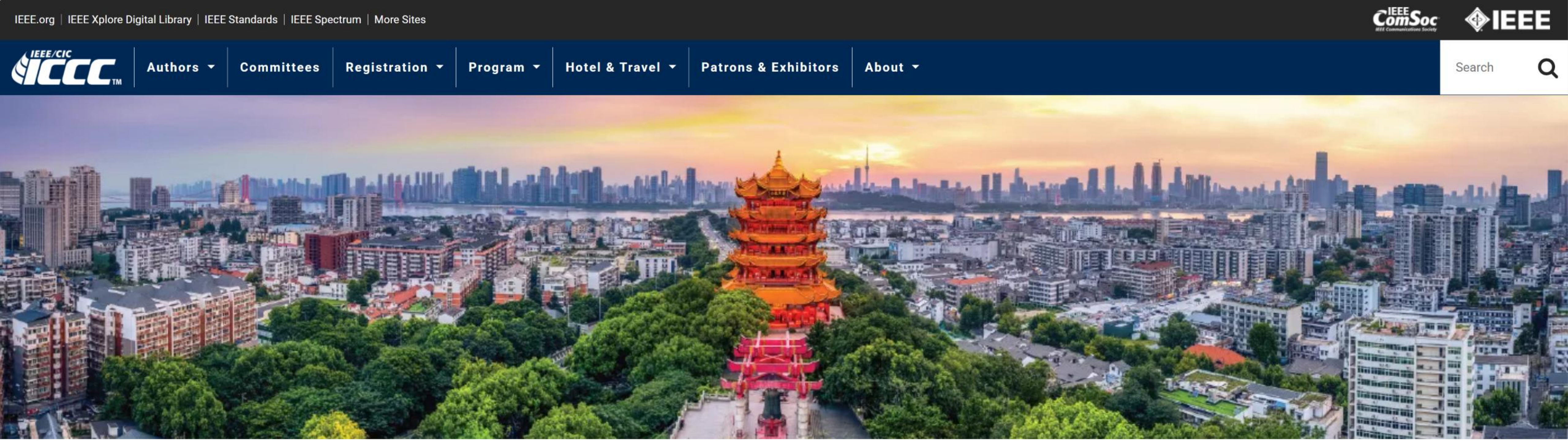

Near-Field Communications for 6G: Fundamentals, Potentials, Challenges, and Future Directions

Linglong Dai

Tsinghua University

7 August, 2026

Outline of the Tutorial

- Background of Near-Field Communications
- Fundamentals of Near-Field Communications
- Opportunities of Near-Field Communications
- Challenges of Near-Field Communications
- Future directions

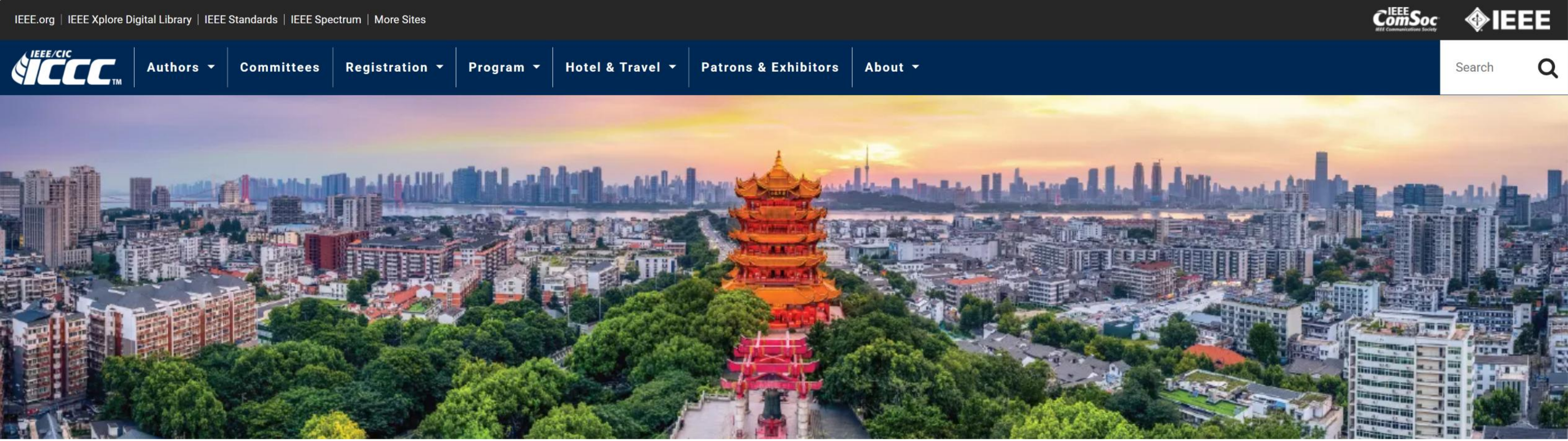

Part 1: Background of Near-Field Communications

Objectives of 6G Communications

- **New applications (e.g., holographic video) drive the upgrade from 5G to 6G**
- **Extended from 3 to 6 scenarios of IMT-2030 (6G): Compared with 5G, 3 new scenarios are ubiquitous connectivity, AI and communication, ISAC**

Holographic Video

Digital Replica

Extended Reality

Autonomous driving

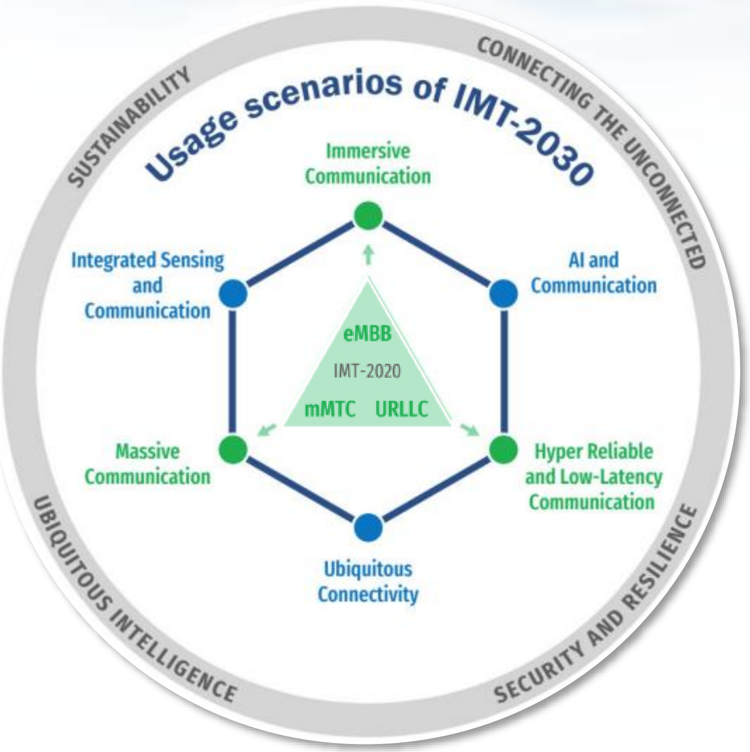

ITU-R WP 5D, "Framework and overall objectives of the future development of IMT for 2030 and beyond," Dec. 2023.

Key Performance Indicators (KPIs) of 6G

- **KPIs of 6G should be orders of magnitude higher than those of 5G, e.g., 10x data rate**
- **New capabilities should be considered, e.g., coverage, sensing/AI-related capabilities, …**

Coverage: 90%

Peak data rate: 1 Tbps

Low latency: 500 µs

Spectral efficiency: Kbps/Hz

Access density: 100 users/m^2

ITU-R WP 5D, "Framework and overall objectives of the future development of IMT for 2030 and beyond," Dec. 2023.

KPI 1: Spectral Efficiency

- **6G is expected to achieve 10 times higher spectral efficiency compared with 5G**
- **The higher spectral efficiency can be achieved exploiting spatial multiplexing, which requires significantly increased number of antennas**
  - ➢ **4G: 2-8 antennas → 5G: 64-256 antennas**
  - ➢ **6G: 1024+ antennas with ultra-massive MIMO (UM-MIMO) and cell-free massive MIMO (CF-MIMO)**

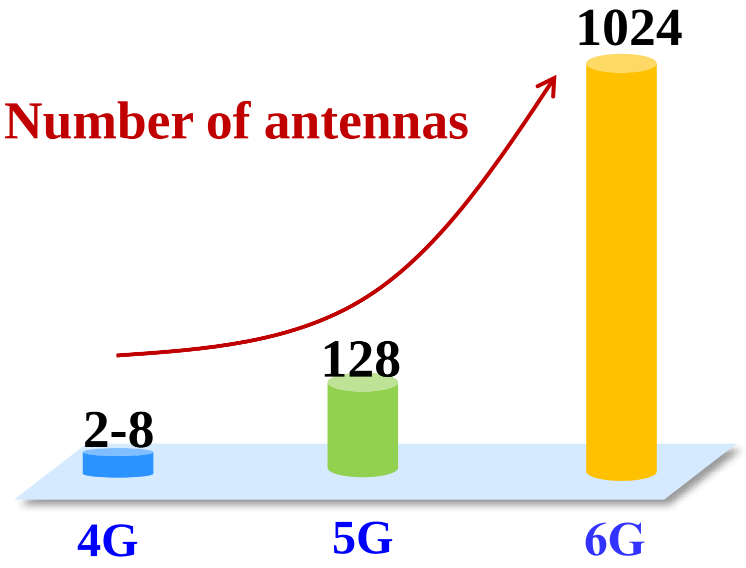

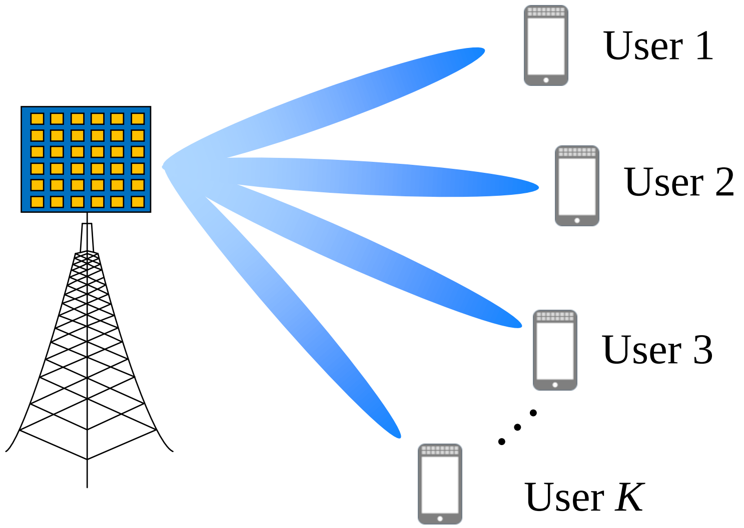

UM-MIMO

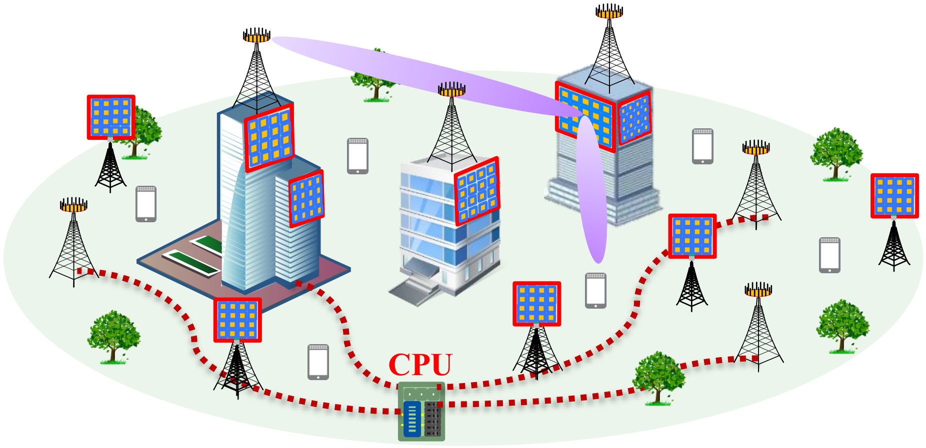

CF-MIMO

W. Jiang, B. Han, M. A. Habibi and H. D. Schotten, "The Road Towards 6G: A Comprehensive Survey," *IEEE Open J. Commun. Soc.*, vol. 2, pp. 334-366, Feb. 2021.

KPI 2: Peak Data Rate

- **100× peak data rate improvement for 6G**
  - **Using mmWave and THz can achieve this improvement with the abundant spectral resources**
  - **Very large antenna array is required to counteract the serious path loss in high-frequency band**

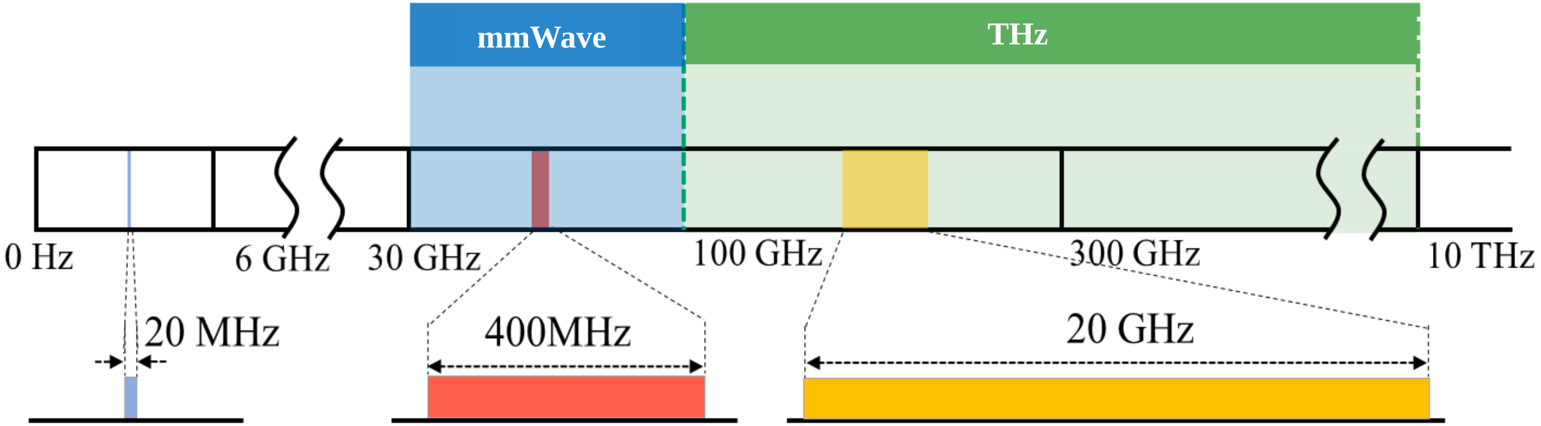

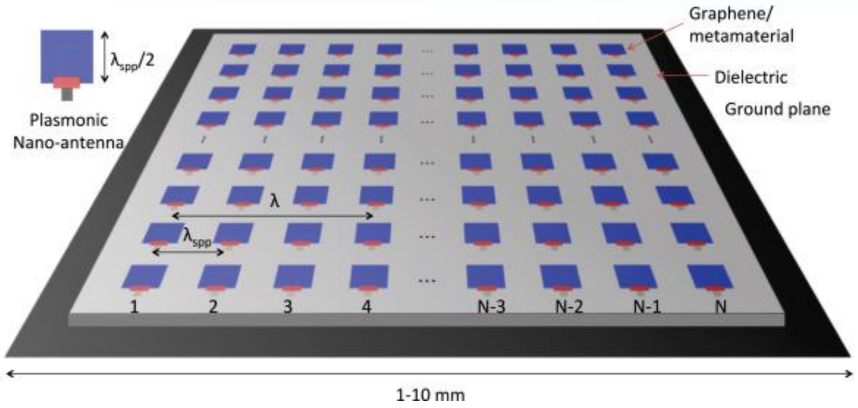

1024 ×1024 elements for THz band (0.06-10THz) [1]

I. F. Akyildiz, and J. M. Jornet, "Realizing ultra-massive MIMO (1024 ×1024) communication in the (0.06–10) terahertz band," *Nano Commun. Netw.*, vol. 8, pp. 46-54, Jun. 2016.

KPI 3: Coverage

- **By dynamically manipulating the transmission environment, reconfigurable intelligent surface (RIS) brings new possibilities for capacity and coverage enhancement**
- **Thousands of antennas are usually employed to overcome the “multiplicative fading” effect of RIS**

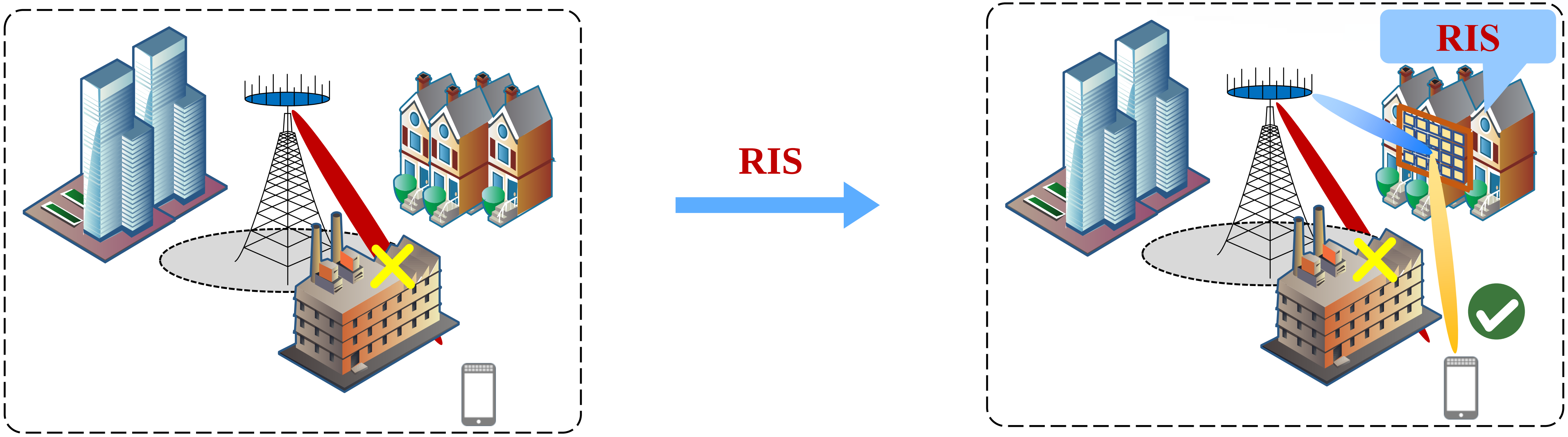

C. Huang, A. Zappone, G. C. Alexandropoulos, M. Debbah and C. Yuen, “Reconfigurable Intelligent Surfaces for Energy Efficiency in Wireless Communication,” *IEEE Trans. Wireless Commun.*, vol. 18, no. 8, pp. 4157-4170, Aug. 2019.

Extremely Large Antenna Arrays (ELAA)

- **ELAA** is the common feature for the above technologies

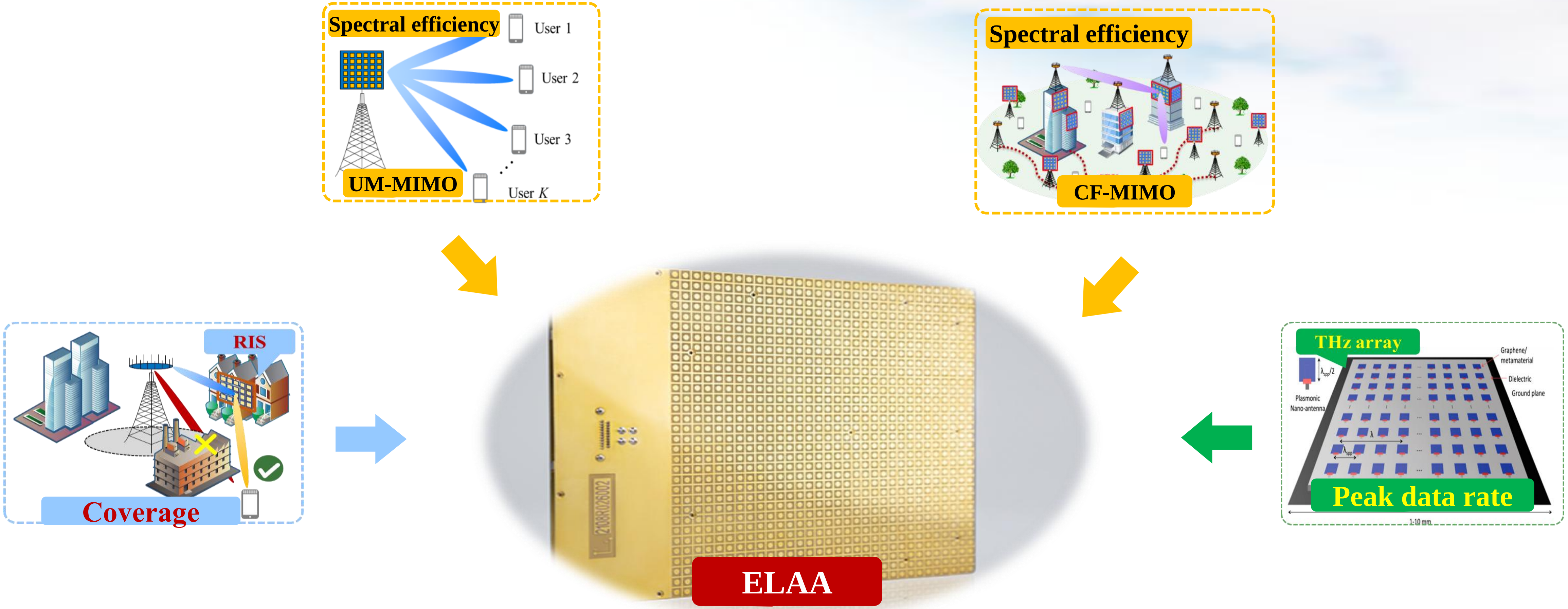

Massive MIMO vs. ELAA

	Massive MIMO	ELAA
Architecture	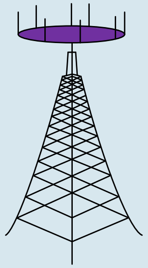	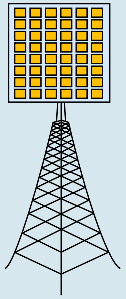
Number of antennas	**64 ~ 256**	**1000+**
Array aperture	**Big**	**Bigger**
Beam gain	**High**	**Higher**
Precoding complexity	**High**	**Higher**
Beam management	**Difficult**	**Very difficult**
Power consumption	**High**	**Higher**

Is there any fundamental change between the massive MIMO and ELAA

Electromagnetic Propagation: Near-Field vs. Far-Field

- **Electromagnetic (EM) propagation can be divided into far-field and near-field regions**
  - **Boundary of these regions is the Rayleigh distance**
  - **In far-field, EM propagation can be approximately modeled by the planar wave**
  - **In near-field, EM propagation has to be accurately modeled by the spherical wave**

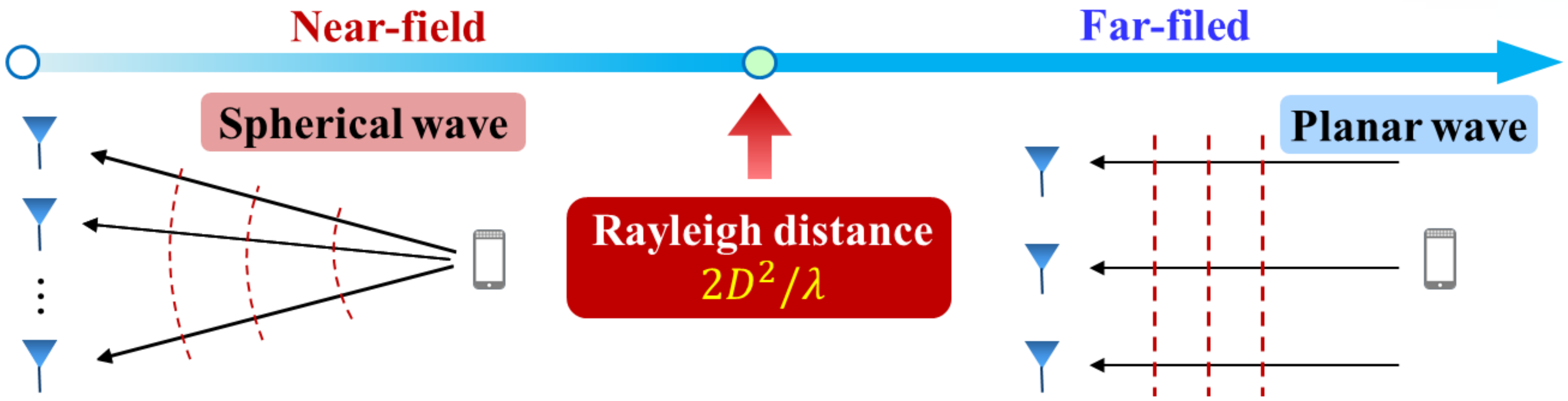

It has a critical difference of the EM characteristics between the near-field and far-field

M. Cui, Z. Wu, Y. Lu, X. Wei, and L. Dai, "Near-field MIMO communications for 6G: Fundamentals, challenges, potentials, and future directions," *IEEE Commun. Mag.*, vol. 61, no. 1, pp. 40-46, Jan. 2023.

Near-Field for ELAA

- **5G with massive MIMO: Users are located in the far-field region**
- **6G with ELAA: Users are more likely located in the near-field region**

Table I. Rayleigh distance [m] (Typical 5G cell radius: 150-250 m)

D \ *f*	3 GHz	7 GHz	28 GHz	142 GHz
0.5 m	5 m	12 m	47 m	237 m
1.6 m	51 m	119 m	476 m	/
3.0 m	180 m	420 m	/	/

Evolution from massive MIMO to ELAA results in fundamental change of spherical propagation model

M. Cui, Z. Wu, Y. Lu, X. Wei, and L. Dai, "Near-field MIMO communications for 6G: Fundamentals, challenges, potentials, and future directions," *IEEE Commun. Mag.*, vol. 61, no. 1, pp. 40-46, Jan. 2023.

Prototypes of ELAA for Near-Field Communications

- **MIT: 3200-element ELAA@2.4 GHz, Rayleigh distance 600 m**
- **Tsinghua: 2304-element ELAA@28 GHz, Rayleigh distance 25 m**
- **Qualcomm: 4096-element ELAA@13 GHz, Rayleigh distance 95 m**

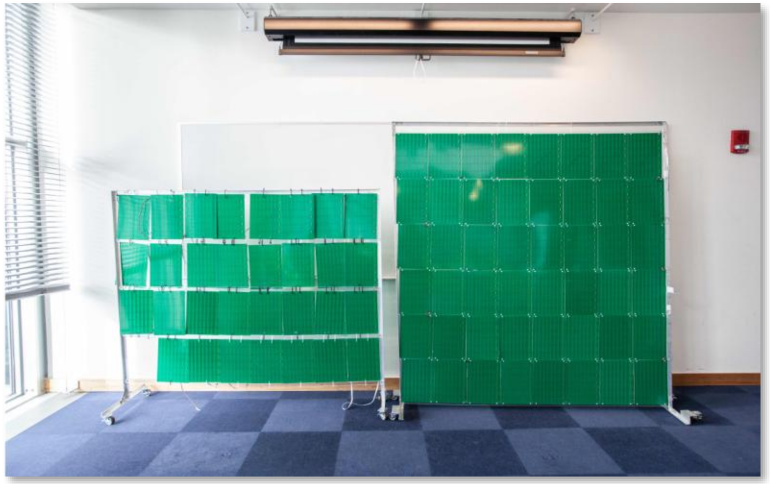

MIT: 3200-element ELAA

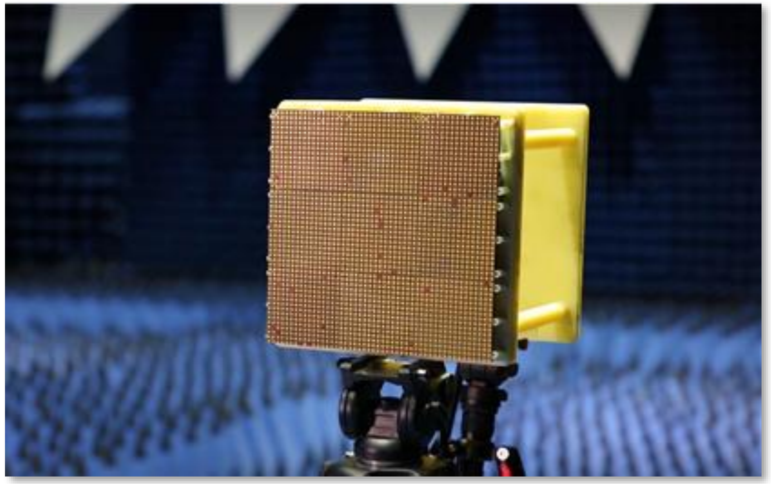

Tsinghua: 2304-element ELAA

Qualcomm: 4096-element ELAA

[1] M. Uusitalo, P. Rugeland, M. Boldi, E. C. Strinati, and Y. Zou, "RFocus: Beamforming using thousands of passive antennas," in *Proc. 17th USENIX Symposium on Networked Systems Design and Implementation (NSDI'20)*, Feb. 2020.

[2] M. Cui, Z. Wu, Y. Chen, S. Xu, F. Yang, and L. Dai, "Demo: Low-power communications based on RIS and AI for 6G," in *Proc. IEEE ICC*, May 2022. (**IEEE ICC 2022 Outstanding Demo Award**)

[3] Qualcomm, "MWC 2024: Wireless innovations enabling intelligent computing everywhere," Qualcomm, Feb. 2024. [Online]. Available: https://www.qualcomm.com/news/onq/2024/02/mwc-2024-wireless-innovations-enabling-intelligent-computing-everywhere.

Applications of Near-Field Communications

- **Near-field spherical waves enables near-field beamfocusing**

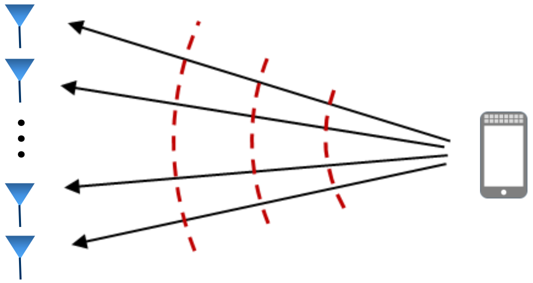

Near-Field Beamfocusing

Communications

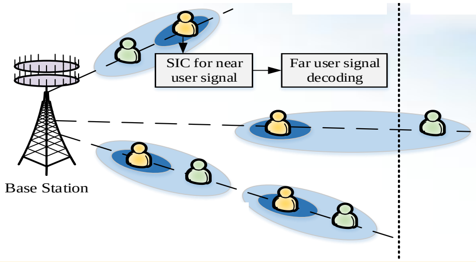

Increased capacity through signal focusing

Sensing and Localization

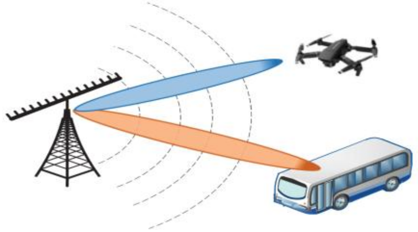

Higher accuracy through distance sensing

Wireless Power Transfer

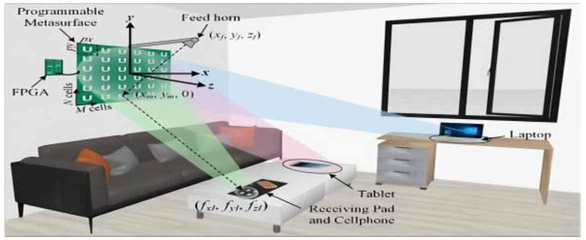

Improved efficiency through energy focusing

Recent Progress for Near-field Communications

- **In June 2025, 3GPP completed the standardization of the 7–24 GHz 6G mid-band near-field channel model in Release 19 [1].**
- **In April 2026, 3GPP formally recognized near-field propagation as a mandatory research component of future 6G design [2].**

Aug 2023: Initiation of 6G *Near-Field Technology White Paper* drafting, involving 206 experts from 73 institutions across 20 countries.

Dec 2023: 3GPP Rel-19 approves 7–24GHz channel measurement/modeling research, prioritizing near-field channel models.

Mar 2024: ZTE leads the establishment of the "Near-Field Models & Mechanisms Project" at ETSI ISG RIS.

Apr 2024: 6G Near-Field Technology White Paper released at Future 6G Summit's "New Tech & Materials" track.

Institute of Electronics hosts the 1st "Near-Field Communication Theory & Applications" forum, launching the "Joint Initiative for 6G Near-Field Tech R&D and

Apr 2024: ZTE partners with three major operators to launch a near-field research project under CCSA TC5WG6.

Series of Events: RIS, THz, and related activities.

(CAE Journal) hosts "6G Near-Field Communication Theory & Tech"

ksho

Mar 2025: 3GPP plenary 6G Workshop discusses key 6G technologies.

Mar 2025: Future 6G Summit releases 6G Near-Field Technology White Paper 2.0.

Mar 2025: Tsinghua, ZTE, BUPT, ZJU, and others co-found the "Near-Field Communication Task Force" under IMT2030.

Apr 2025: Chinese Institute of Electronics organizes the 2nd "Near-Field Communication Theory & Applications" forum.

Jun 2025: 3GPP 6G SI (Study Item) officially launches 6G standardization research.

[1] 3GPP TR 38.901 V19.0.0, Study on Channel Model for Frequencies from 0.5 to 100 GHz (Release 19), 3GPP, Jun. 2025.
[2] Chair notes RAN1#124bis_eom, 3GPP TSG RAN WG1 #124bis, Malta, MT, April 13th ~ 17th, 2026.

Recent Progress for Near-field Communications

- In March 2025, the IMT-2030 (6G) Promotion Group of China has officially established the “ Near-Field Communications Task Group”
- This task group is led by Tsinghua University with support from ZTE, China Mobile, Huawei, BUPT, ZJU, China Unicom. Over 40 universities and companies have joined this task group.

Lead Unit

Deputy Lead Units

Member Units

Over 40 universities and companies

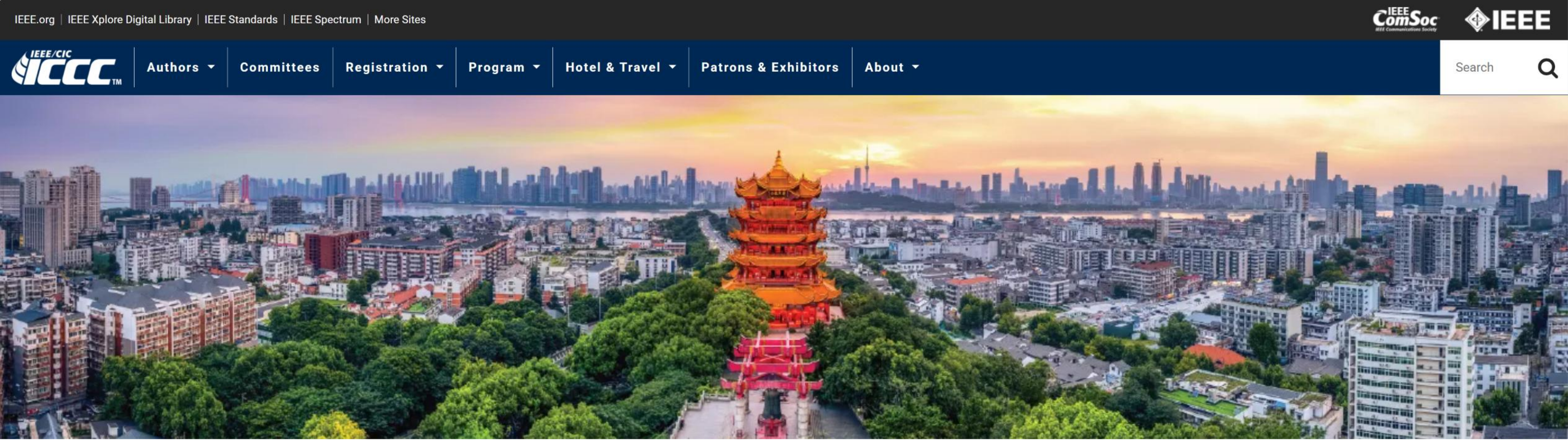

Part 2: Fundamentals of Near-Field Communications

Far-Field vs. Near-Field

- **Far-field: the EM waves impinging on the antenna array can be approximately modeled as planar waves, where the phase of the EM wave is a linear function of the antenna index**
- **Near-field: the EM waves have to be accurately modeled as spherical waves, where the phase of the EM wave is a non-linear function of the antenna index**

Far-field

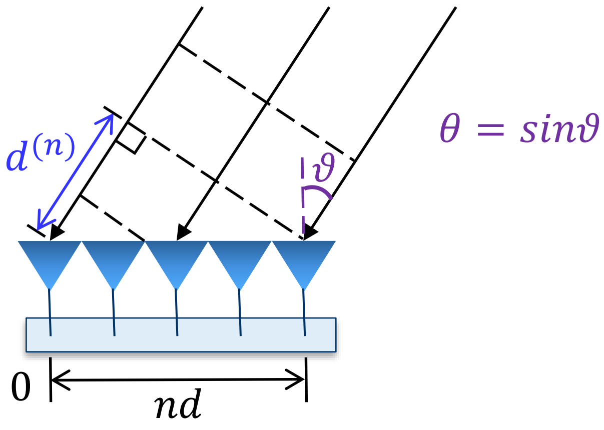

Near-field

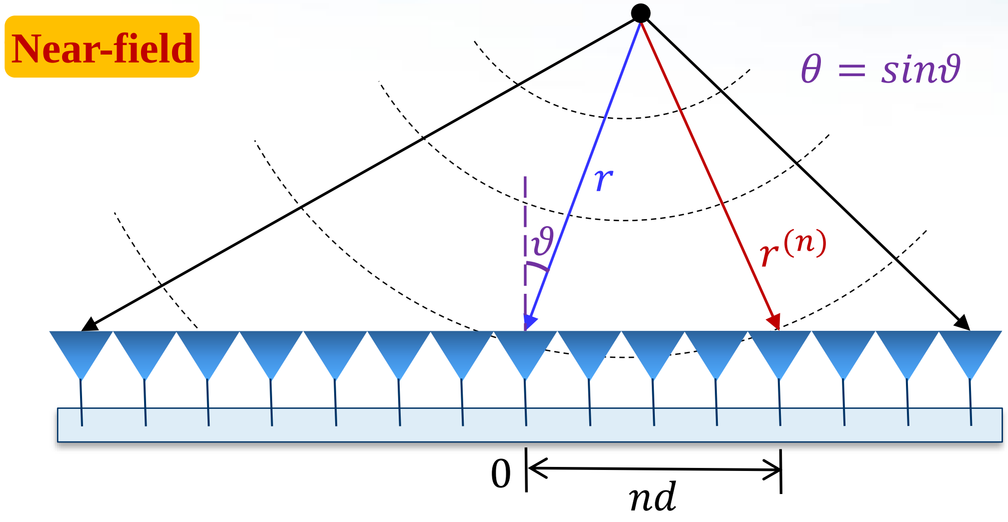

Distance: $d^{(n)} = nd\theta$ **Linear**

Phase: $\phi_n^{\text{far}} = -\frac{2\pi d^{(n)}}{\lambda} = -\frac{2\pi}{\lambda} nd\theta$

Distance: $r^{(n)} = \sqrt{r^2 + n^2 d^2 - 2ndr\theta}$ **Non-linear**

Phase: $\phi_n = \frac{2\pi\left(r^{(n)} - r\right)}{\lambda} = \frac{2\pi}{\lambda}\left(\sqrt{r^2 + n^2 d^2 - 2ndr\theta} - r\right)$

Antenna index: $n \in [-N, \cdots, 0, \cdots, N]$ **Antenna number:** $M = 2N + 1$

Definition of Rayleigh Distance

- The metric to determine the **boundary** between the far-field and near-field regions is the **Rayleigh distance**

Rayleigh distance: The planar waves are a long-distance approximation of the spherical waves. When the largest phase error $\Delta_n = \left|\phi_n - \phi_n^{\mathrm{far}}\right|$ between the accurate phase ϕ_n and the approximated phase ϕ_n^{far} is $\max_n \Delta_n = \pi/8$, then the Tx-Rx distance is the Rayleigh distance (RD), satisfying

$$\mathrm{RD} = \frac{2D^2}{\lambda},$$

where D denotes the array aperture, and λ is the wavelength.

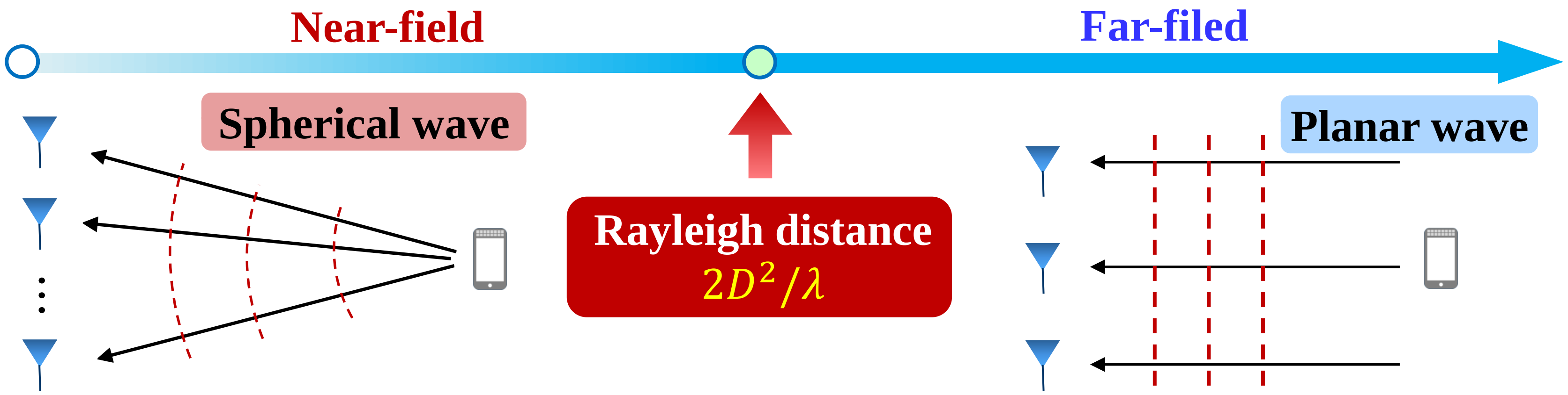

J. Sherman, "Properties of focused apertures in the Fresnel region," *IRE Trans. Antennas Propag.*, vol. 10, no. 4, pp. 399–408, Jul. 1962.

Derivation of Rayleigh Distance

- **To derive the Rayleigh distance, it is essential to derive the specific value of phase error $\Delta_n = \left|\phi_n - \phi_n^{\text{far}}\right|$, where $\phi_n = \frac{2\pi}{\lambda}\left(\sqrt{r^2 + n^2 d^2 - 2ndr\theta} - r\right)$ and $\phi_n^{\text{far}} = -\frac{2\pi}{\lambda} nd\theta$**

$$\phi_n = \frac{2\pi}{\lambda} r\left(\sqrt{1 + \frac{n^2 d^2}{r^2} - \frac{2nd\theta}{r}} - 1\right) = \frac{2\pi}{\lambda} r\left(1 - \frac{nd\theta}{r} + \frac{(1-\theta^2)n^2 d^2}{2r^2} + o\left(\frac{1}{r^2}\right) - 1\right)$$

$$= \underbrace{-\frac{2\pi}{\lambda} nd\theta}_{\textbf{Far-field phase } \phi_n^{\text{far}}} + \underbrace{\frac{1-\theta^2}{\lambda r}\pi n^2 d^2 + o\left(\frac{1}{r}\right)}_{\textbf{Phase error } \Delta_n}$$

$$\Rightarrow$$

Phase error $\Delta_n \approx \frac{1-\theta^2}{\lambda r}\pi n^2 d^2$

- **ϕ_n^{far} is the approximation of ϕ_n through first-order Taylor expansion. Therefore, the phase error Δ_n is mainly determined by the second-order Taylor expansion**
- **By maximizing the phase error Δ_n across the entire array**

$$\max_n \Delta_n = \frac{1-\theta^2}{\lambda r}\pi N^2 d^2 = \frac{1-\theta^2}{\lambda r}\frac{\pi D^2}{4} = \frac{\pi}{8} \Rightarrow r = \frac{2D^2(1-\theta^2)}{\lambda} \xrightarrow{\theta = 0} \text{RD} = \frac{2D^2}{\lambda}$$

Near-Field Ranges for Typical Scenarios

- **The near-field range of SIMO/MISO is exactly determined by the classical Rayleigh distance $\frac{2D^2}{\lambda}$**
- **For the MIMO scenario, both the BS array aperture D_1 and the UE array aperture D_2 contribute to the Rayleigh distance $\frac{2(D_1+D_2)^2}{\lambda}$**
- **For the RIS scenario, the near-field range is determined by the harmonic mean of the BS-RIS distance r_1 and RIS-UE distance r_2**

Communication scenario	**SIMO/MISO** 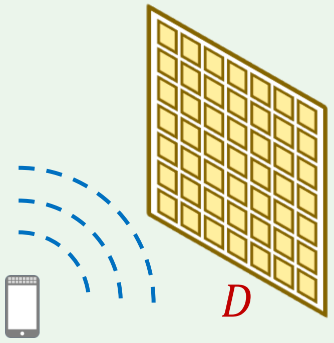 	**MIMO** 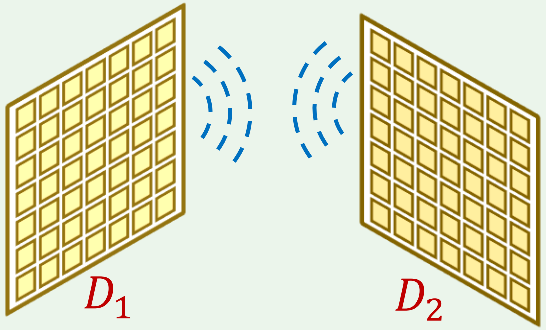 	**RIS** 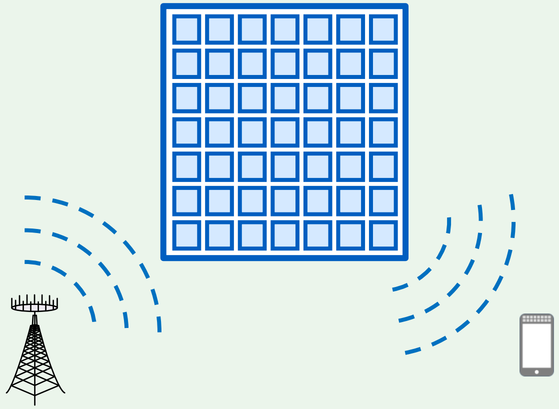
Near-field range	$r < \frac{2D^2}{\lambda}$	$r < \frac{2(D_1+D_2)^2}{\lambda}$	$\frac{r_1 r_2}{r_1+r_2} < \frac{2D^2}{\lambda}$

M. Cui, Z. Wu, Y. Lu, X. Wei, and L. Dai, "Near-field MIMO communications for 6G: Fundamentals, challenges, potentials, and future directions," *IEEE Commun. Mag.*, vol. 61, no. 1, pp. 40-46, Jan. 2023.

Near-Field LoS Channel Model

- **Base station (BS) antenna number $M = 2N + 1$, antenna spacing $d = \lambda/2$, array aperture $D = (M-1)d$, the location of the n-th antenna is $(0, nd)$, where $n \in [-N, \cdots, 0, \cdots, N]$**
- **The channel between the n-th antenna and the user located at $(r\cos\vartheta, r\sin\vartheta)$ is**

$$h_n = \boxed{\tilde{g}_n} e^{-j\frac{2\pi}{\lambda} r^{(n)}} = \boxed{g_n} e^{-j\boxed{\frac{2\pi}{\lambda}\left(r^{(n)} - r\right)}}$$

Complex gain

$g_n = \tilde{g}_n e^{j\frac{2\pi}{\lambda} r}$

Near-field phase ϕ_n

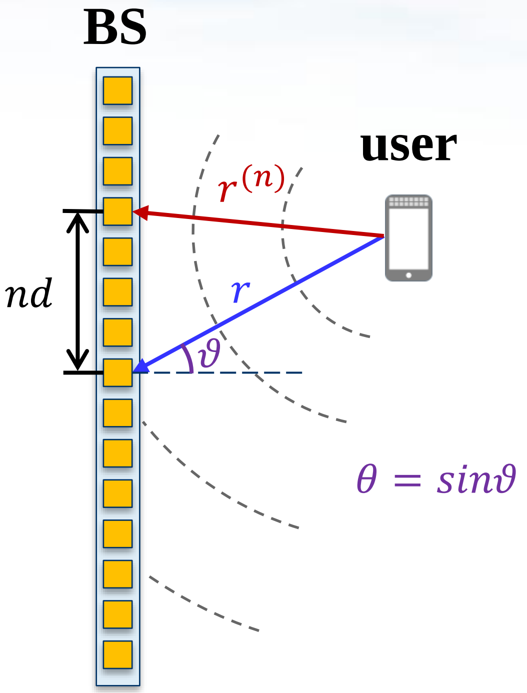

- **Generally, the complex gains are very similar when $r > 1.2D$**

$$g_{-N} \approx \cdots \approx g_0 \approx \cdots \approx g_N \approx g$$

- **Therefore, the LoS channel is**

$$\boldsymbol{h} = [h_{-N}, \cdots, h_0, \cdots, h_N]^T = g\left[e^{-j\frac{2\pi}{\lambda}\left(r^{(-N)} - r\right)}, \cdots, e^{-j\frac{2\pi}{\lambda}\left(r^{(N)} - r\right)}\right]^T$$
$$= g\boxed{\boldsymbol{a}(r, \theta)}$$

Near-field array response vector

E. Björnson, Ö. T. Demir, and L. Sanguinetti, "A primer on near-field beamforming for arrays and reconfigurable intelligent surfaces," in *Proc. 2021 55th Asilomar Conference on Signals, Systems, and Computers*, pp. 105-112, Oct. 2021.

Near-Field Multi-Path Channel Model

- **The multi-path channel can be represented as the sum of L near-field array response vectors.**

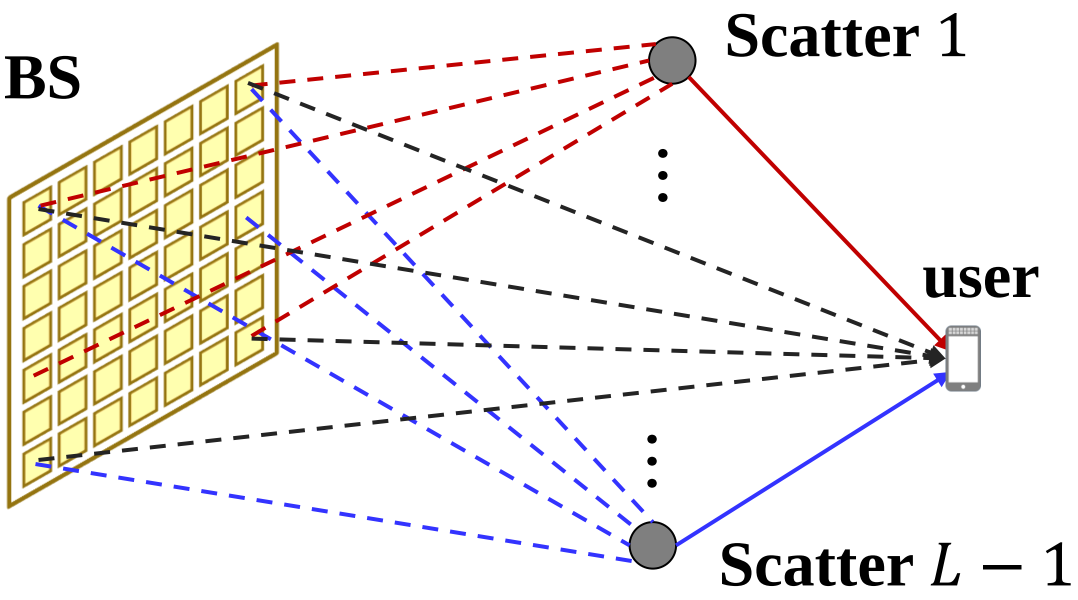

distance between the BS and the l-th scatter

$$\boldsymbol{h} = \underbrace{g_0 \boldsymbol{a}(r_0, \theta_0)}_{\text{LoS path}} + \underbrace{\sum_{l=1}^{L-1} g_l \boldsymbol{a}(\boxed{r_l}, \boxed{\theta_l})}_{\text{NLoS paths}}$$

angle between the BS and the l-th scatter

X. Yin, S. Wang, N. Zhang, and B. Ai, "Scatterer localization using large-scale antenna arrays based on a spherical wave-front parametric model," *IEEE Trans. Wireless Commun.*, vol. 16, no. 10, pp. 6543-6556, Oct. 2017.

Far-Field Beamsteering vs. Near-Field Beamfocusing

- **Far-field beamsteering (Far-field beamforming): the transmitter can only steer the radiated signal energy towards a specific angle**
- **Near-field beamfocusing (near-field beamforming): the spherical wave is able to focus the radiated signal energy in a specific spatial location**

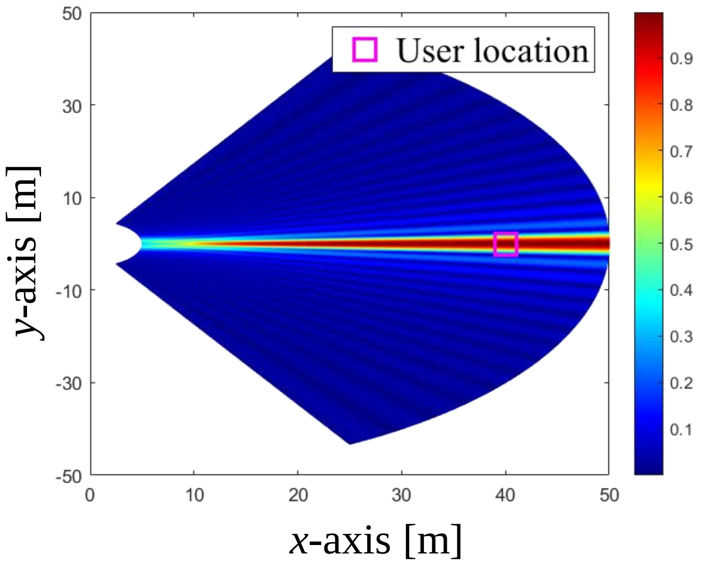

Far-Field Beamsteering

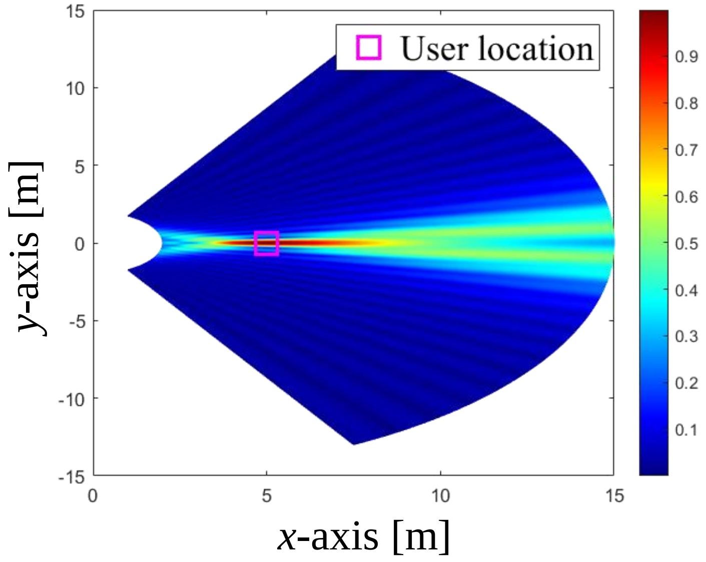

Near-Field Beamfocusing

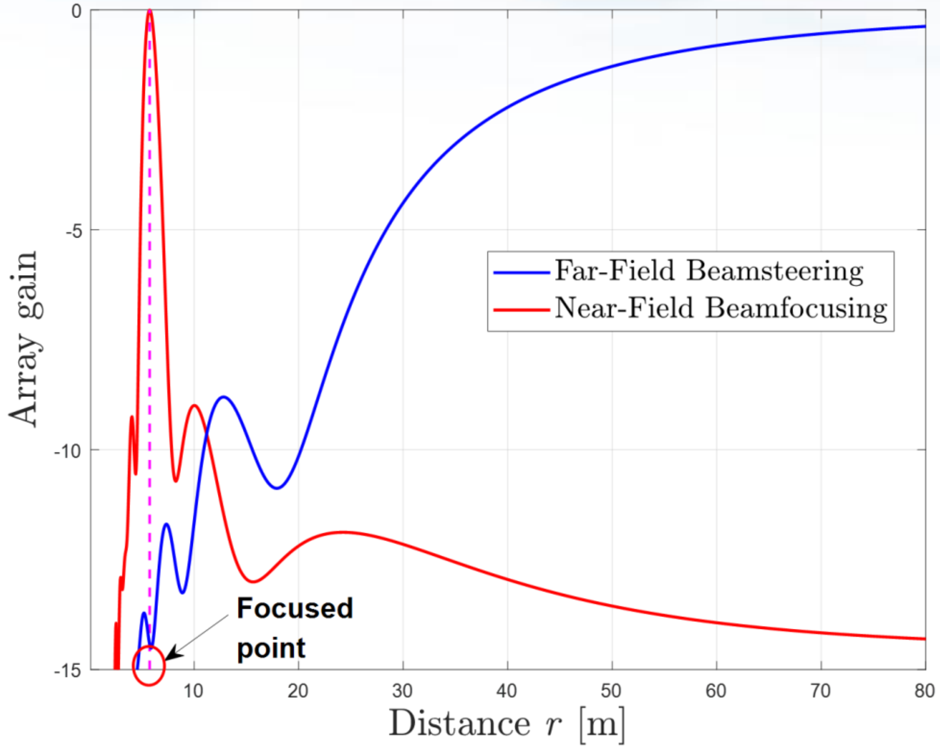

H. Zhang, N. Shlezinger, F. Guidi, D. Dardari, M. F. Imani, and Y. C. Eldar, "Beam focusing for near-field multiuser MIMO communications," *IEEE Trans. Wireless Commun.*, vol. 21, no. 9, pp. 7476–7490, Sep. 2022.

Array Gain of Near-Field Beamfocusing (1)

- **Array gain provided by beamfocusing on the same angle but different distances.**
  - **Assume a user is located at $(\bar{r}, \theta)$, then the corresponding LoS channel is**

$$\boldsymbol{h}(\bar{r}, \theta) = g\boldsymbol{a}(\bar{r}, \theta) = g\left[e^{-jk\left(\bar{r}^{(-N)}-\bar{r}\right)}, \cdots, e^{-jk\left(\bar{r}^{(0)}-\bar{r}\right)}, \cdots, e^{-jk\left(\bar{r}^{(N)}-\bar{r}\right)}\right]^T$$

  where $M = 2N + 1$ and $k = 2\pi/\lambda$ denote the wave number.

  - **The purpose of beamfocusing is to compensate for the phase variation between antennas, therefore, the beamfocusing vector aligned with the location $(\bar{r}, \theta)$ is**

$$\boldsymbol{w}(\bar{r}, \theta) = \frac{1}{\sqrt{M}}\boldsymbol{a}^*(\bar{r}, \theta) \ = \frac{1}{\sqrt{M}}\left[e^{jk\left(\bar{r}^{(-N)}-\bar{r}\right)}, \cdots, e^{jk\left(\bar{r}^{(0)}-\bar{r}\right)}, \cdots, e^{jk\left(\bar{r}^{(N)}-\bar{r}\right)}\right]^T$$

  - **Then, the normalized array gain achieved by $\boldsymbol{w} = \boldsymbol{a}^*(\bar{r}, \theta)$ at any other user located at (r, θ) is**

$$f(r, \bar{r}, \theta) = \frac{\left\|\boldsymbol{h}(r,\theta)^T\boldsymbol{w}(\bar{r},\theta)\right\|}{\|\boldsymbol{h}(r,\theta)\|\|\boldsymbol{w}(\bar{r},\theta)\|} = \frac{1}{M}\left|\sum_{n=-N}^{N} e^{jk\left(\bar{r}^{(n)}-r^{(n)}\right)}\right|$$

Array Gain of Near-field Beamfocusing (2)

Lemma 1: the normalized array gain achieved by $\boldsymbol{w} = \boldsymbol{a}^*(\bar{r},\theta)$ at the user location (r,θ) is obtained through Fresnel approximation as

$$f(r,\bar{r},\theta) = \frac{1}{M}\left|\sum_{n=-N}^{N} e^{jk(\bar{r}^{(n)}-r^{(n)})}\right| \approx |G(\beta)| = \left|\frac{C(\beta)+jS(\beta)}{\beta}\right|$$

where $\beta = \sqrt{\frac{M^2d^2(1-\theta^2)}{2\lambda}\left|\frac{1}{r}-\frac{1}{\bar{r}}\right|}$. $C(\beta) = \int_0^{\beta}\cos\left(\frac{\pi}{2}t^2\right)\mathrm{d}t$ **and** $S(\beta) = \int_0^{\beta}\sin\left(\frac{\pi}{2}t^2\right)\mathrm{d}t$ **are Fresnel functions.**

- **Proof:**
  - **Based on the second-order Tayler expansion, $\bar{r}^{(n)}$ and $r^{(n)}$ can be approximated as**

$$r^{(n)} = \sqrt{r^2 - 2ndr\theta + n^2d^2} \approx r - nd\theta + \frac{1-\theta^2}{2r}n^2d^2 \qquad \bar{r}^{(n)} \approx \bar{r} - nd\theta + \frac{1-\theta^2}{2\bar{r}}n^2d^2$$

  - **Then we have** $k\left(\bar{r}^{(n)} - \bar{r}\right) - k\left(r^{(n)} - r\right) = \pi n^2\frac{d^2(1-\theta^2)}{\lambda}\left(\frac{1}{\bar{r}}-\frac{1}{r}\right) = \pi n^2 x$**, therefore**

$$f(r,\bar{r},\theta) \approx \frac{1}{M}\left|\sum_{n=-N}^{N} e^{j\pi n^2 x}\right| \approx \frac{1}{2N}\left|\int_{-N}^{N} e^{j\pi n^2 x}\,\mathrm{d}n\right| = \left|\frac{\int_0^{\sqrt{2x}N} e^{j\frac{\pi}{2}t^2}\,\mathrm{d}t}{\sqrt{2x}N}\right| = \left|\frac{C(\beta)+jS(\beta)}{\beta}\right|$$

M. Cui and L. Dai, "Channel estimation for extremely large-scale MIMO: Far-field or near-field?," *IEEE Trans. Commun.*, vol. 70, no. 4, pp. 2663-2677, Apr. 2022.

Array Gain of Near-Field Beamfocusing (3)

- **Near-field array gain of planar arrays and RIS**
  - **A similar result with that of the linear arrays**

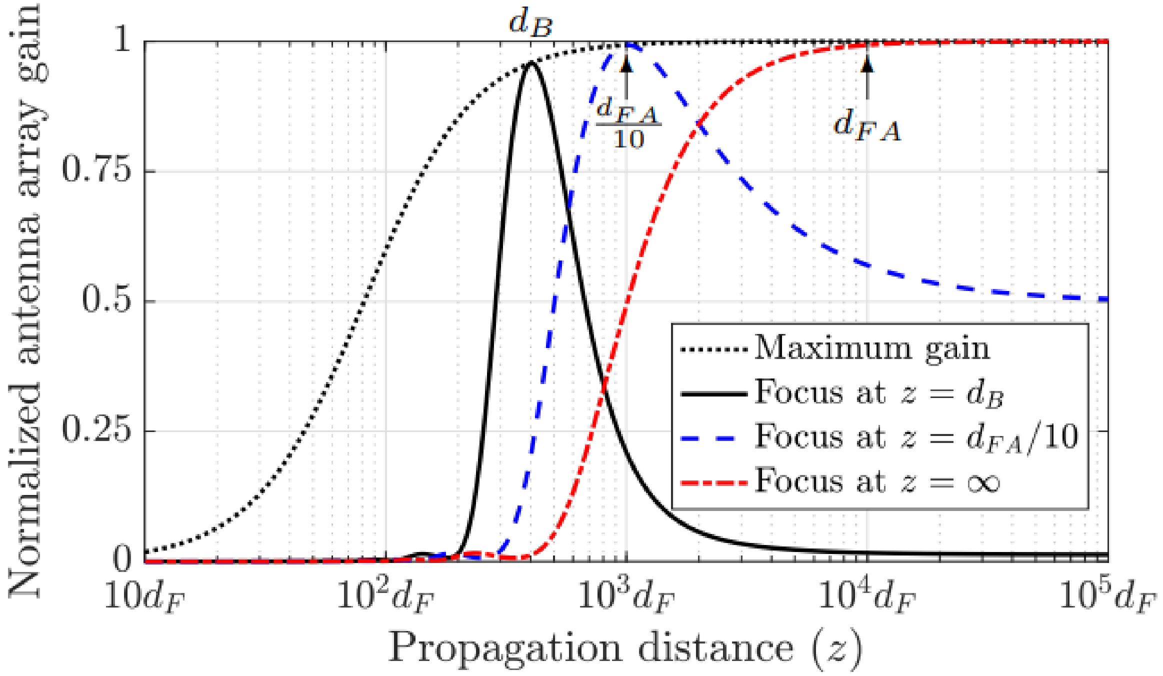

$$\begin{aligned} G_{\text{antenna}} &\approx \left(\frac{2}{D^2}\right)^2 \left| e^{-\mathrm{j}\frac{2\pi}{\lambda}z} \int_{\mathcal{A}} e^{-\mathrm{j}\frac{2\pi}{\lambda}\left(\frac{x^2}{2z}+\frac{y^2}{2z}\right)} dx\, dy \right|^2 \\ &= \left(\frac{2}{D^2}\right)^2 \left| \int_{-D/\sqrt{8}}^{D/\sqrt{8}} e^{-\mathrm{j}\frac{\pi}{\lambda}\frac{x^2}{z}} dx \right|^4 \\ &= \left(\frac{8z}{d_F}\right)^2 \boxed{\left(C^2\left(\sqrt{\frac{d_F}{8z}}\right) + S^2\left(\sqrt{\frac{d_F}{8z}}\right)\right)^2} \qquad (9) \end{aligned}$$

Fresnel functions

E. Björnson, Ö. T. Demir, and L. Sanguinetti, "A primer on near-field beamforming for arrays and reconfigurable intelligent surfaces," in *Proc. 2021 55th Asilomar Conference on Signals, Systems, and Computers*, pp. 105-112, Oct. 2021.

Characteristics of Near-Field Beamfocusing

- **The beamfocusing gain depends on the function $G(\beta) = \left|\frac{C(\beta)+S(\beta)}{\beta}\right|$ and the parameter β**

$$f(r,\bar{r},\theta) \approx G(\beta) = \left|\frac{C(\beta)+S(\beta)}{\beta}\right|$$

$$\beta = \sqrt{\frac{M^2 d^2 (1-\theta^2)}{2\lambda}\left|\frac{1}{r}-\frac{1}{\bar{r}}\right|}$$

- **Distance window**
  - $|G(\beta)|$ **shows a significant downward trend**
  - **To guarantee the array gain is larger than Γ, we have**

$$|G(\beta)| \geq \Gamma \quad \Rightarrow \quad \beta = \sqrt{\frac{M^2 d^2 (1-\theta^2)}{2\lambda}\left|\frac{1}{r}-\frac{1}{\bar{r}}\right|} \leq \beta_\Gamma \quad |G(\beta_\Gamma)| = \Gamma$$

$$\Downarrow$$

$$\left|\frac{1}{r}-\frac{1}{\bar{r}}\right| \leq \frac{2\lambda\beta_\Gamma^2}{M^2 d^2 (1-\theta^2)} = \frac{2\lambda\beta_\Gamma^2}{D^2 (1-\theta^2)} = \frac{4\beta_\Gamma^2}{\mathrm{RD}(1-\theta^2)}$$

distance window $$r \in \left[\frac{\bar{r}\mathrm{RD}(1-\theta^2)}{\mathrm{RD}(1-\theta^2)+4\beta_\Gamma^2\bar{r}}, \ \frac{\bar{r}\mathrm{RD}(1-\theta^2)}{\mathrm{RD}(1-\theta^2)-4\beta_\Gamma^2\bar{r}}\right]$$

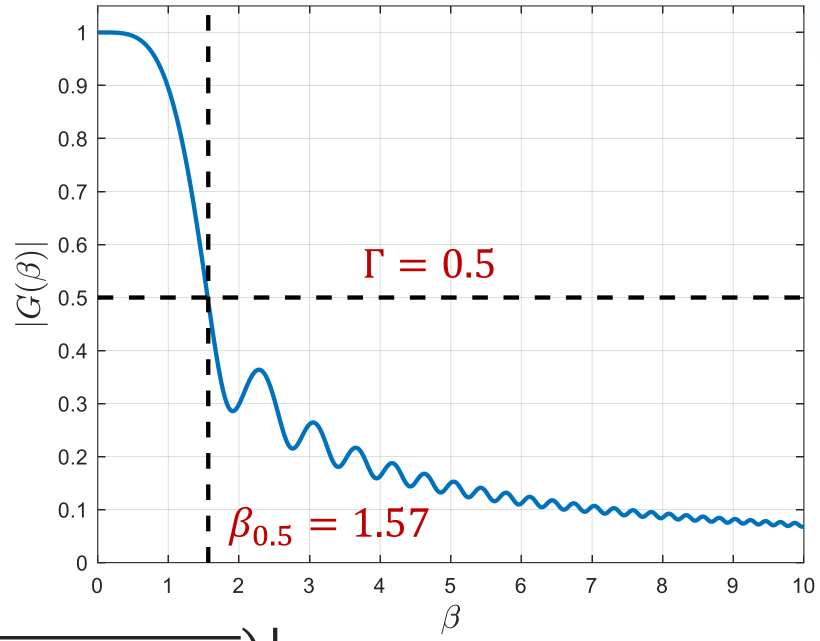

- **Limit performance analysis:**
  - **Array gain at zero distance:** $\lim_{r\to 0}|G(\beta)| = |G(+\infty)| = 0$
  - **Array gain at infinite distance:** $\lim_{r\to +\infty}|G(\beta)| = \left|G\left(\sqrt{M^2 d^2 (1-\theta^2)/(2\lambda\bar{r})}\right)\right|$

Simulation Results of Near-Field Beamfocusing

- **Limit performance analysis:**
  - **Array gain at zero distance:** $\lim_{r\to 0}|G(\beta)| = |G(+\infty)| = 0$
  - **Array gain at infinite distance:** $\lim_{r\to +\infty}|G(\beta)| = \left|G\left(\sqrt{M^2d^2(1-\theta^2)/(2\lambda\bar{r})}\right)\right|$
- **Distance window**

$$r \in \left[\frac{\bar{r}\mathrm{RD}(1-\theta^2)}{\mathrm{RD}(1-\theta^2)+4\beta_\Gamma^2\bar{r}}, \quad \frac{\bar{r}\mathrm{RD}(1-\theta^2)}{\mathrm{RD}(1-\theta^2)-4\beta_\Gamma^2\bar{r}}\right]$$

- **Parameters**

Parameters	**Values**
Carrier	**30 GHz**
Array structure	**256-ULA**
θ	$\pi/8$
$\bar{r}$	**15 meters**
Γ	**0.5**

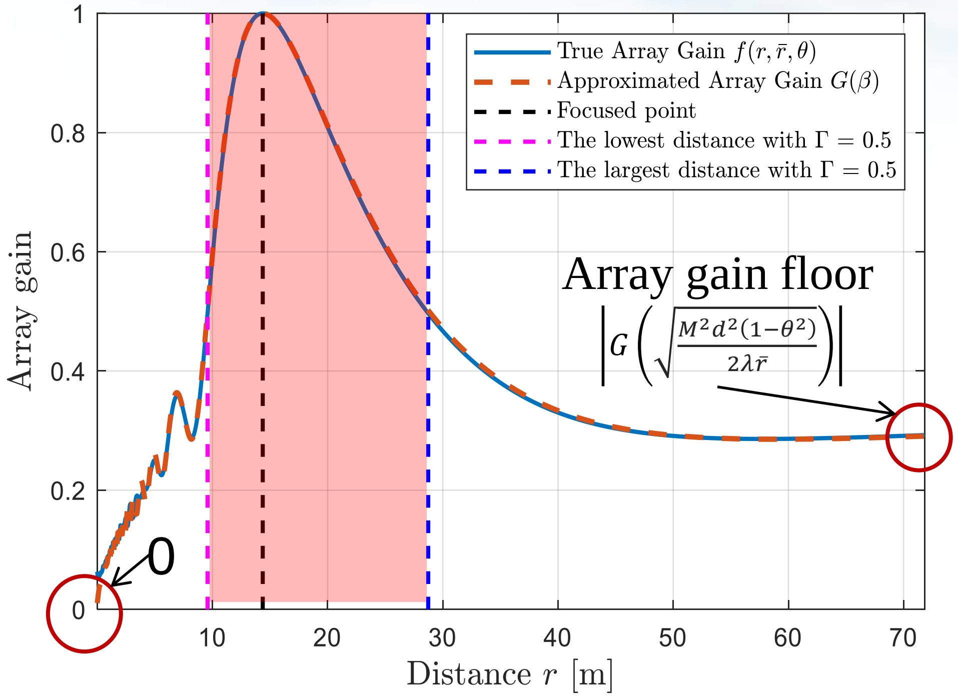

[1] M. Cui and L. Dai, "Channel estimation for extremely large-scale MIMO: Far-field or near-field?," *IEEE Trans. Commun.*, vol. 70, no. 4, pp. 2663-2677, Apr. 2022.

[2] E. Björnson, Ö. T. Demir, and L. Sanguinetti, "A primer on near-field beamforming for arrays and reconfigurable intelligent surfaces," in *Proc. 2021 55th Asilomar Conference on Signals, Systems, and Computers*, pp. 105-112, Oct. 2021.

Proposed Effective Rayleigh Distance

- **Derive the effective Rayleigh distance from the view of array gain loss**

Classical Rayleigh distance (RD)

- **Definition: When the largest phase error between the planar wave and spherical wave is $\pi/8$, the Tx-Rx distance is**

$$\mathrm{RD}=\frac{2D^2}{\lambda}$$

Effective Rayleigh distance (ERD)

- **Definition: When the array gain loss of the far-field beam in the near-field region is 5%, the Tx-Rx distance is**

$$\mathrm{ERD}=0.367\cos^2\vartheta\,\mathrm{RD}$$

Distance window

$$r\in\left[\frac{\bar{r}\mathrm{RD}\left(1-\theta^2\right)}{\mathrm{RD}\left(1-\theta^2\right)+4\beta_\Gamma^2\bar{r}},\ \frac{\bar{r}\mathrm{RD}\left(1-\theta^2\right)}{\mathrm{RD}\left(1-\theta^2\right)-4\beta_\Gamma^2\bar{r}}\right]$$

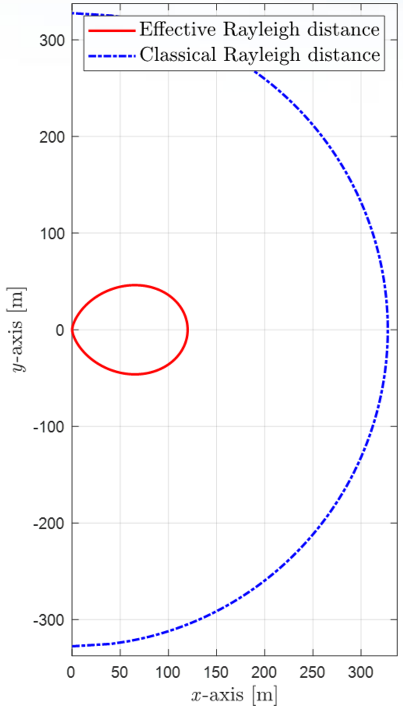

M. Cui, L. Dai, R. Schober, and L. Hanzo, "Near-field wideband beamforming for extremely large antenna array," *IEEE Trans. Wireless Commun.*, vol. 23, no. 10, pp. 13110-13124, Oct. 2024.

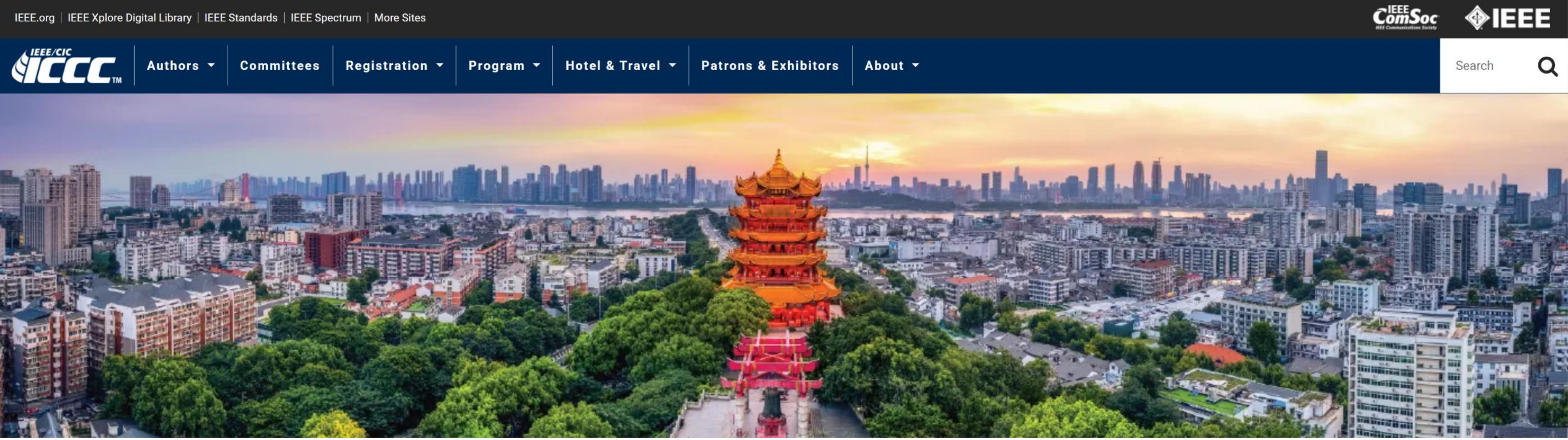

Part 3: Opportunities of Near-Field Communications

Outline of Part 3

- ☐ Near-Field Single-User MIMO Capacity Enhancement
- ☐ Near-Field Location Division Multiple Access
- ☐ Near-Field Airy Beam for Blockage Mitigation

Limited DoFs for Far-Field LoS Channel

- **Based on planar wave assumptions, degrees of freedom (DoF) are limited in line-of-sight (LoS) far-field channel**

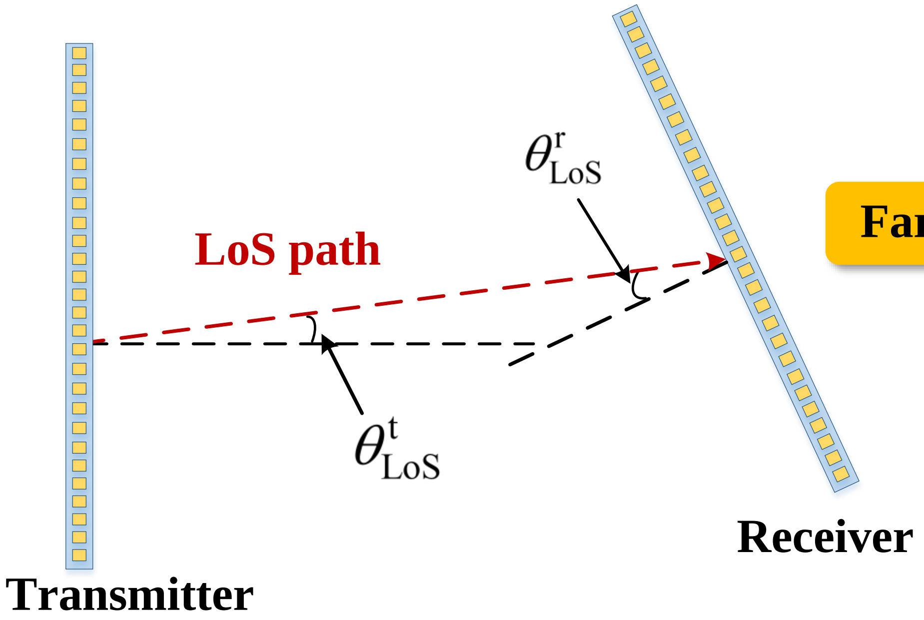

Far-field channel

Distance: $d^{(n)} = nd\theta$

Phase: $\phi_n^{\text{far}} = -\frac{2\pi d^{(n)}}{\lambda} = -\frac{2\pi}{\lambda} nd\theta$

Far-field steering vector

$$\mathbf{a}(\phi) = \frac{1}{\sqrt{N}}\left[1, e^{j\frac{2\pi}{\lambda}d\sin\phi}, \cdots, e^{j(2N)\frac{2\pi}{\lambda}d\sin\phi}\right]^T$$

$$\mathbf{H}_{\text{LoS}} = \alpha_{\text{LoS}} \underbrace{\mathbf{a}_{\text{r}}\left(\theta_{\text{LoS}}^{\text{r}}\right) \mathbf{a}_{\text{t}}^{H}\left(\theta_{\text{LoS}}^{t}\right)}_{\text{Rank-one matrix}}$$

The rank-one LoS channel can only support one data stream

O. Ayach, S. Rajagopal, S. Abu-Surra, Z. Pi, and R. W. Heath, "Spatially sparse precoding in millimeter wave MIMO systems," *IEEE Trans. Wireless Commun.*, vol. 13, no. 3, pp. 1499–1513, Jan. 2014.

From rank-one channel to highly ranked channel

- **The rank-one far-field LoS channel is not valid any more in the near-field region**
- **Based on spherical waves, the near-field LoS channel becomes highly ranked**

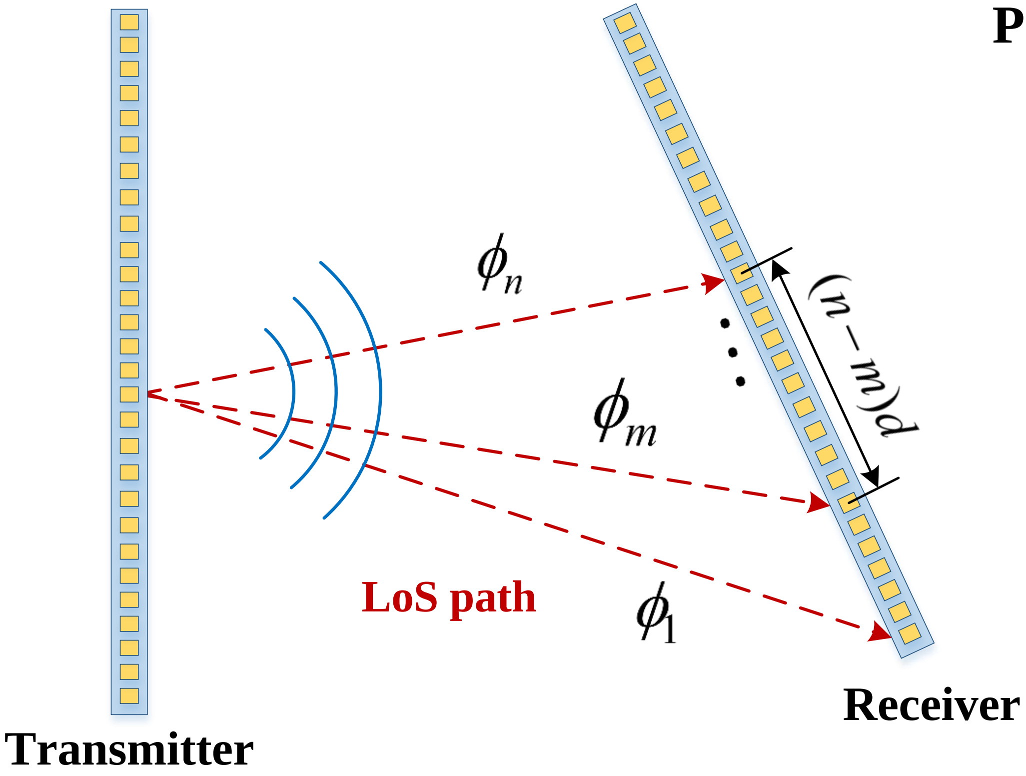

Near-field channel

Phase: $\phi_n = \frac{2\pi(r^{(n)}-r)}{\lambda} = \frac{2\pi}{\lambda}\left(\sqrt{r^2 - 2ndr\theta + n^2d^2} - r\right)$

$$\overset{r > \mathrm{RD}}{\approx} \underbrace{-\frac{2\pi}{\lambda} nd\theta}_{\text{Far-field phase } \phi_n^{\text{far}}}$$

✗ **Not valid in near-field region**

Near-field LoS channel

$$\underbrace{\mathbf{H}_{\mathrm{LoS}} = \begin{bmatrix} \alpha_{1,1} e^{-j2\pi r_{1,1}/\lambda} & \cdots & \alpha_{1,N_2} e^{-j2\pi r_{1,N_2}/\lambda} \\ \vdots & \ddots & \vdots \\ \alpha_{N_2,1} e^{-j2\pi r_{N2,1}/\lambda} & \cdots & \alpha_{N_2,N_1} e^{-j2\pi r_{N_2,N_1}/\lambda} \end{bmatrix}}_{\text{Significantly increased rank}}$$

Increased DoFs for Near-Field LoS Channel

- **The DoFs can significantly increase in the near-field region when both BS and UE are equipped with ELAAs**

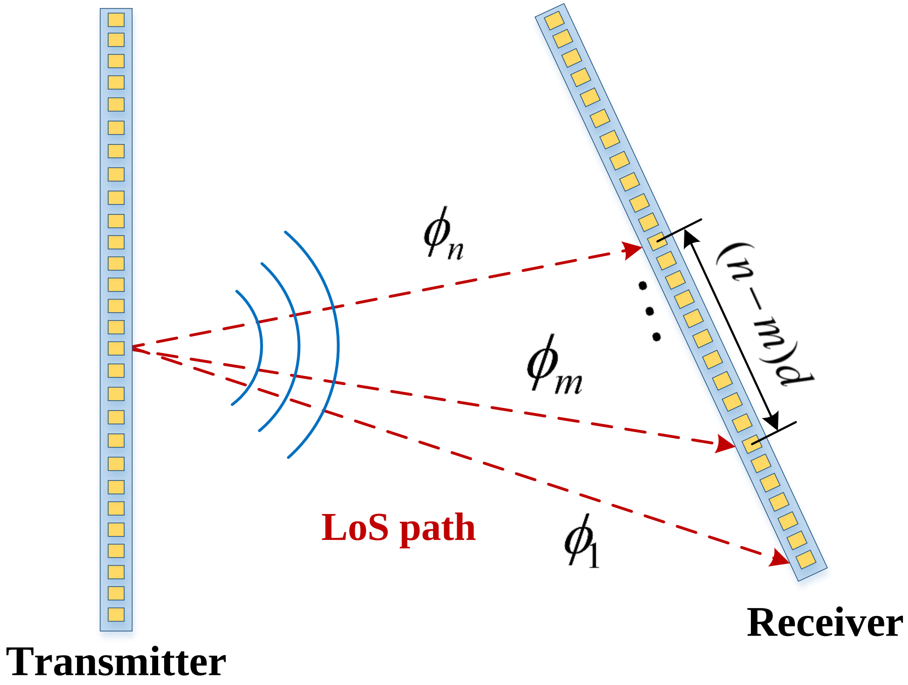

Near-field LoS channel

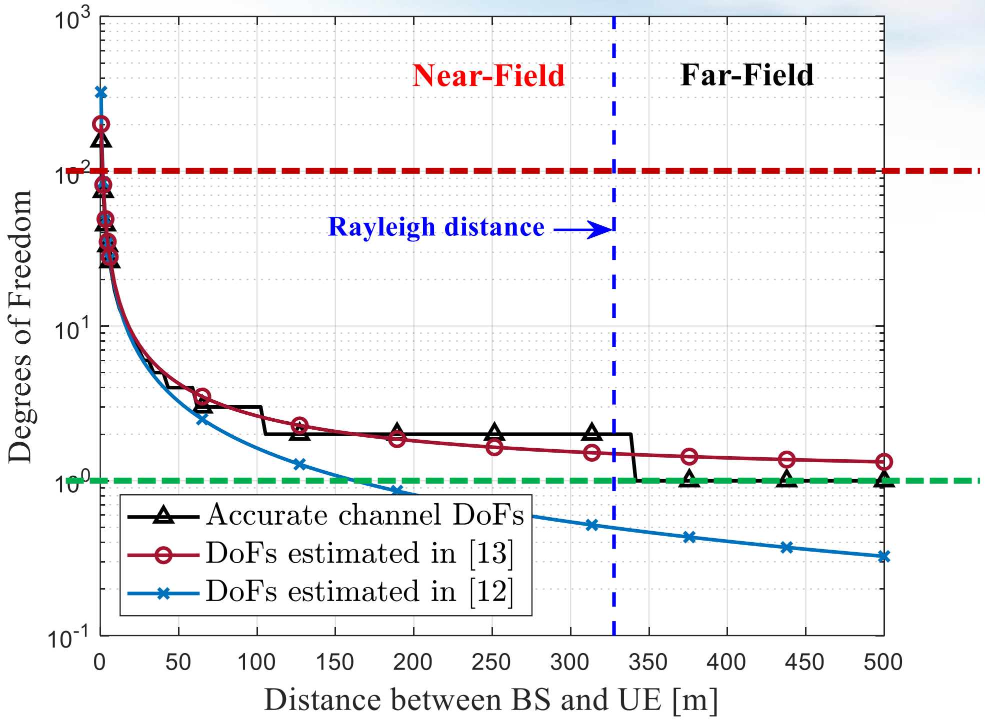

10^2 **DoFs in the near-field region**

↑

10^0 **DoFs in the far-field region**

The capacity is expected to be significantly enhanced with increased DoFs

[12] D. A. Miller, "Waves, modes, communications, and optics: A tutorial," *Adv. in Opt. and Photon.*, vol. 11, no. 3, pp. 679–825, Sep. 2019.

[13] N. Decarli and D. Dardari, "Communication modes with large intelligent surfaces in the near field," *IEEE Access*, vol. 9, pp. 165 648–165 666, Sep. 2021.

Limitation of hybrid precoding architecture

- However, limited by the small number of RF chains, the classical hybrid precoding can not efficiently utilize the increased DoFs to enhance the capacity

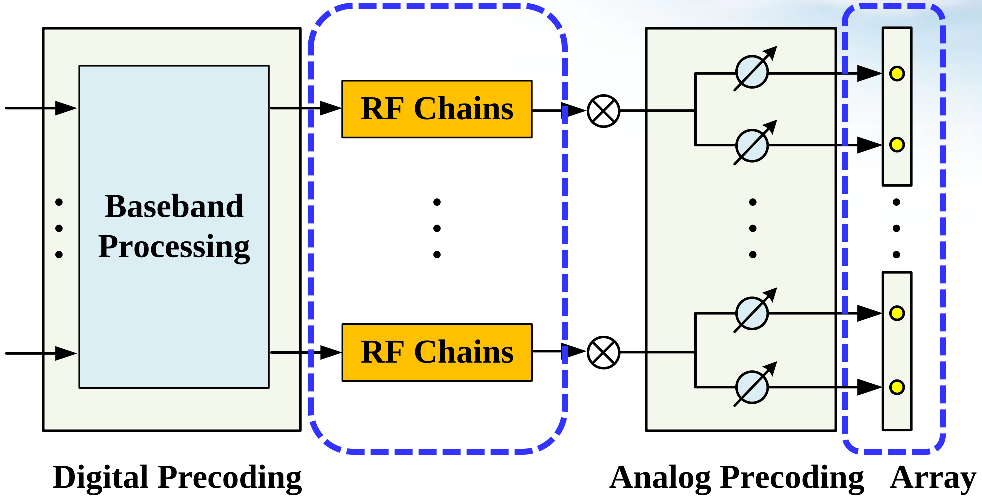

Precoding	Region	Spatial DoFs	RF chains	Spectral Efficiency
Hybrid Precoding	Far-Field	Low	RF Chains ≈ DoFs	Near Optimal
	Near-Field	High	RF Chains ≪ Distance-Related DoFs	Far From Optimal

How to efficiently utilize the significantly increased DoFs in near field

Distance-Aware Precoding Architecture

- **Based on the distance-related DoFs in the near-field region, the distance-aware precoding architecture is proposed**
- **The number of activated RF chains can be configured to match the increased DoFs in the near-field region**

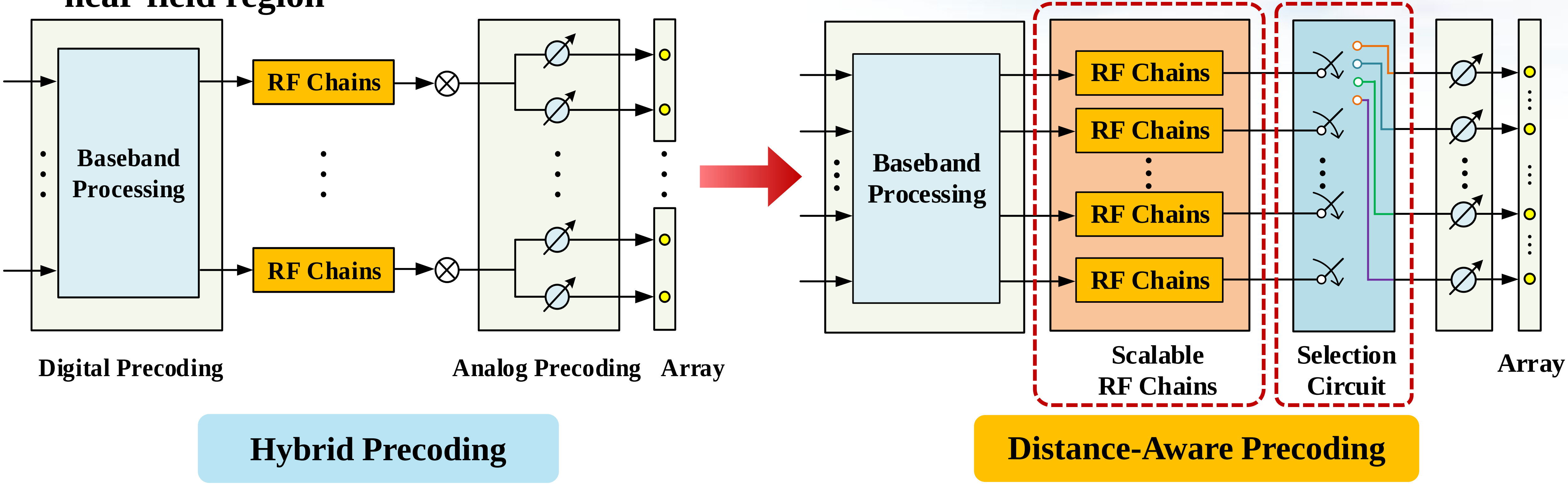

Z. Wu, M. Cui, Z. Zhang, and L. Dai, "Distance-aware precoding for near-field capacity improvement in XL-MIMO," in *Proc. IEEE 95th Veh. Technol. Conf. (IEEE VTC'22 Spring)*, Helsinki, Finland, Jun. 2022.

Simulation Results

- **In the distance-aware precoding architecture, the number of RF chains can be flexibly adjusted to match the spatial DoFs**
- **The spectral efficiency can be significantly enhanced in the near-field region**

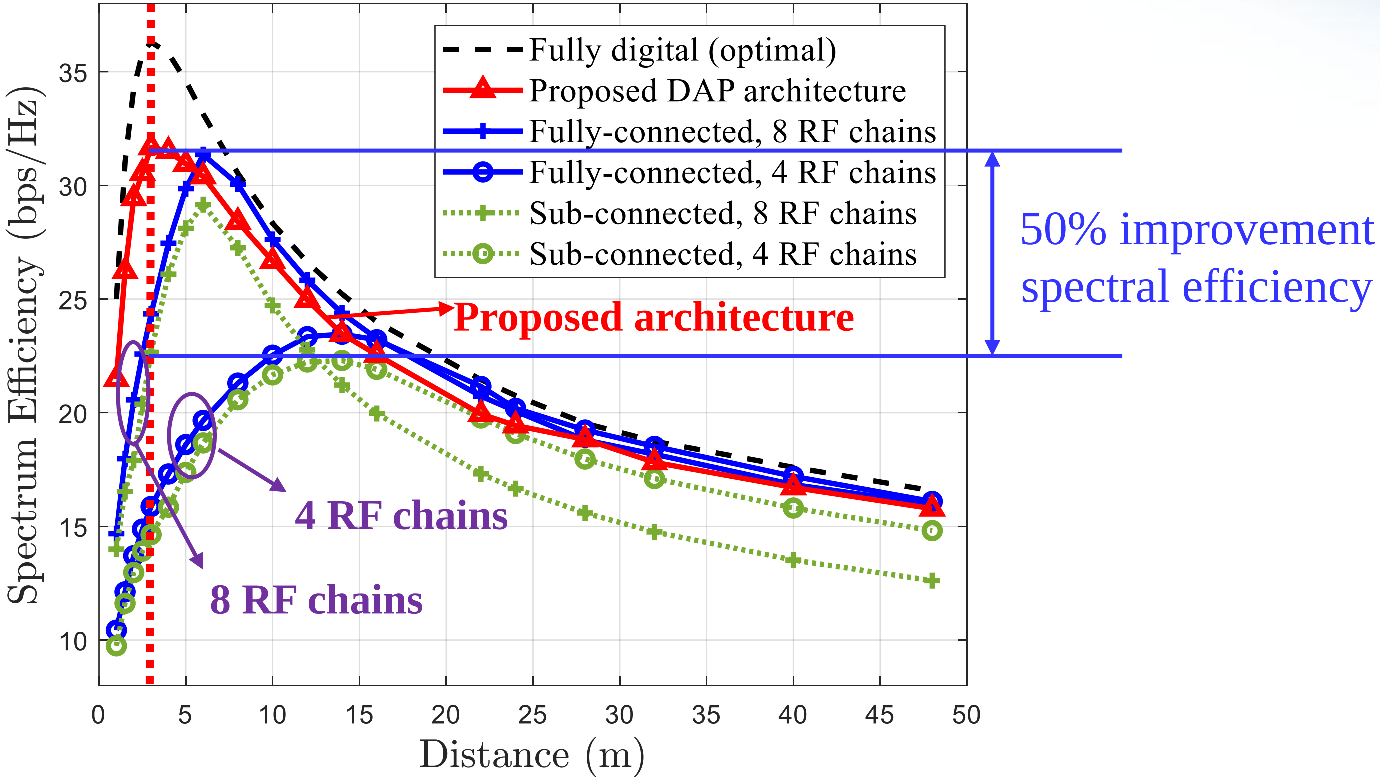

Proposed architecture

4 RF chains

8 RF chains

50% improvement spectral efficiency

Parameters	**Values**
Carrier	**100 GHz**
BS antennas	**256**
MS antennas	**256**
SNR	**30 dB**

---

[1] X. Gao, L. Dai, S. Han, C.-L. I, and R. W. Heath, "Energy-efficient hybrid analog and digital precoding for mmwave MIMO systems with large antenna arrays," *IEEE J. Sel. Areas Commun.*, vol. 34, no. 4, pp.998–1009, Apr. 2016.

[2] X. Yu, J. Z. J. Shen, and K. B. Letaief, "Alternating minimization algorithms for hybrid precoding in millimeter wave MIMO systems," *IEEE J. Sel. Areas Commun.*, vol. 10, no. 3, pp. 485–500, Apr. 2016.

Outline of Part 3

- ☐ **Near-Field Single-User MIMO Capacity Enhancement**
- ☐ **Near-Field Location Division Multiple Access**
- ☐ **Near-Field Airy Beam for Blockage Mitigation**

Challenge of SDMA for Far-Field Communication

- **Spatial division multiple access (SDMA) is employed by massive MIMO to multiplex data streams to different users for improving spectral efficiency**
- **In massive MIMO systems, far-field beamsteering vectors only focus on specific angles, which enables the multiple access for users at different angles**

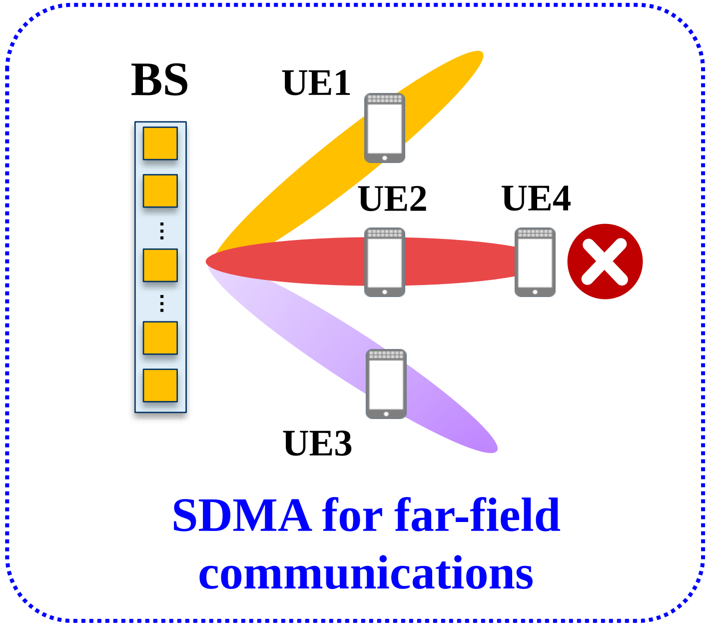

SDMA for far-field communications

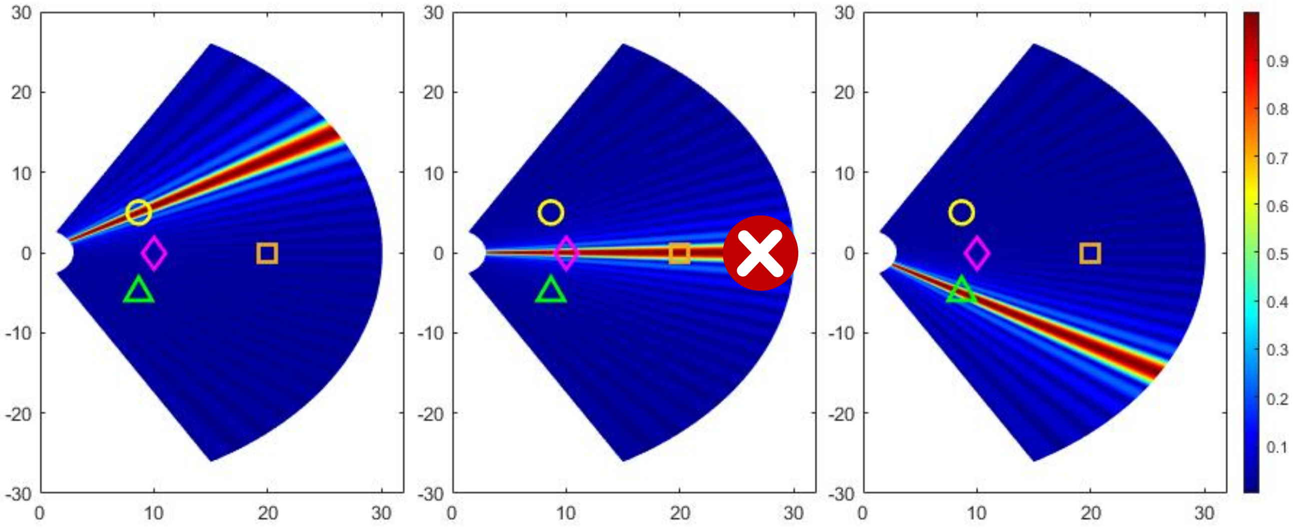

Users at the same angle cannot be simultaneously served by massive MIMO with SDMA

Mitigated Interference with Near-Field Beamfocusing

- **Far-field beamsteering vectors focus on specific spatial angle**
- **Near-field beamfocusing is capable to focus on specific location, which could be leveraged to mitigate inter-user interferences**

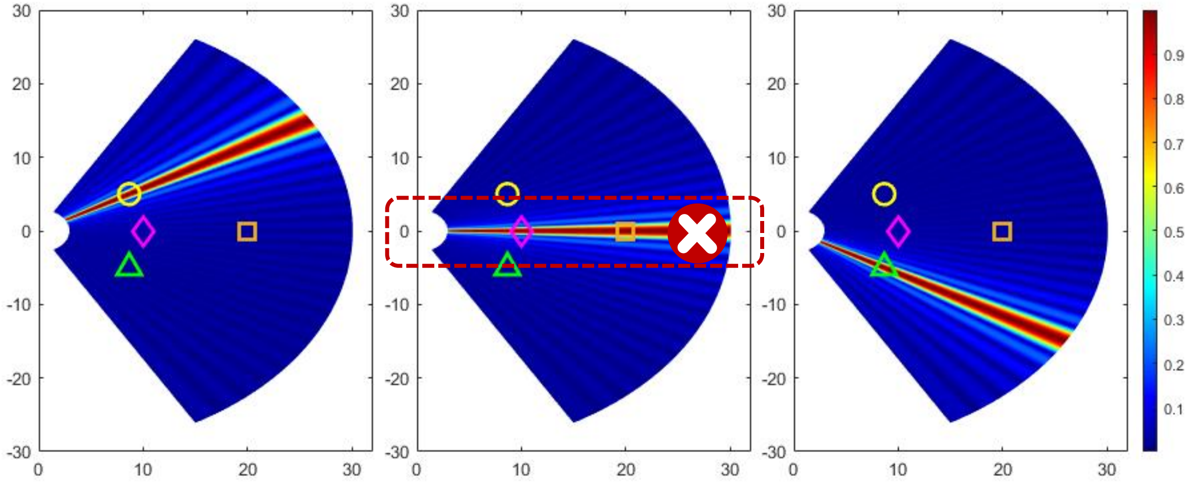

Far-field beamsteering

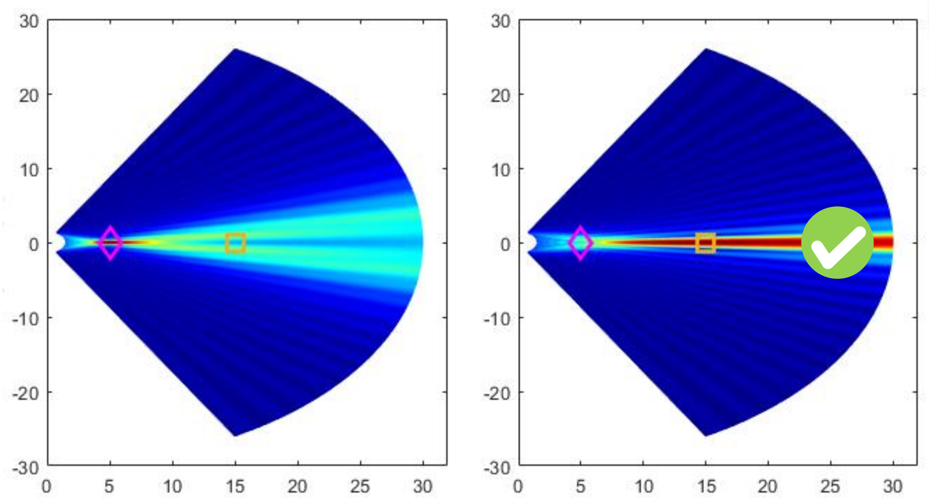

Near-field beamfocusing

Near-field beamfocusing has the potential to serve users at the same spatial angle

H. Zhang, N. Shlezinger, F. Guidi, D. Dardari, M. F. Imani, and Y. C. Eldar, "Beam focusing for near-field multiuser MIMO communications," *IEEE Trans. Wireless Commun.*, vol. 21, no. 9, pp. 7476–7490, Sep. 2022.

Multiple Access for Near-Field Communications: SDMA or LDMA?

- **Far-field SDMA**: Users at different **angles** can be served by orthogonal far-field beams
- **Near-field location division multiple access (LDMA)**: Users at different **locations** can be simultaneously served due to property of near-field beam focusing

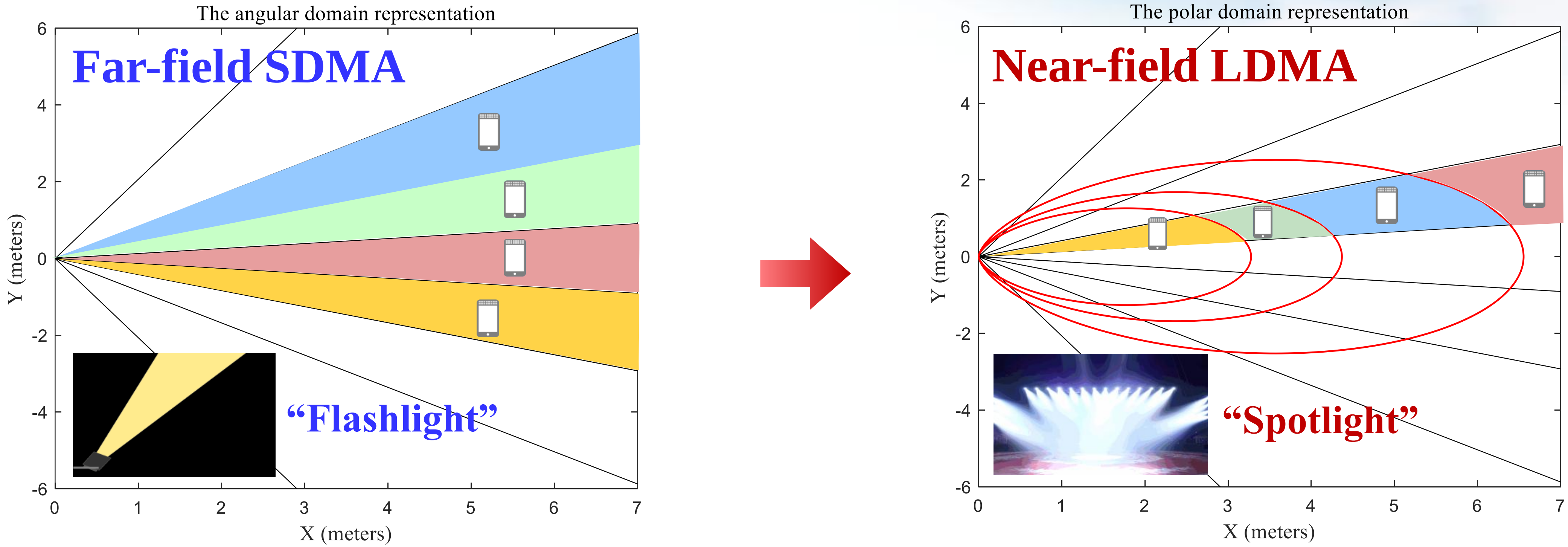

Compared with far-field SDMA, near-field LDMA provides a new dimension for capacity improvement

Z. Wu and L. Dai, “Multiple access for near-field communications: SDMA or LDMA? ” *IEEE J. Sel. Areas Commun.*, vol. 41, no. 6, pp. 1918-1935, Jun. 2023.

Distance Domain Asymptotic Orthogonality

- **Far-field orthogonality in angular domain**

Phase: $\phi_n^{\text{far}}(\theta) = -\frac{2\pi}{\lambda} nd\theta$

Correlation: $f^{\text{far}} = |\mathbf{a}^H(\theta_1)\mathbf{a}(\theta_2)| = \frac{1}{N}\left|\frac{\sin(\frac{1}{2}Nkd(\sin\theta_1 - \sin\theta_2))}{\sin(\frac{1}{2}kd(\sin\theta_1 - \sin\theta_2))}\right|$

As $N \rightarrow \infty$, interference from different angles $I^{\text{far}} \rightarrow 0$ $(\theta_1 \neq \theta_2)$

- **Lemma 2: Near-field orthogonality in distance domain**

Phase: $\phi_n^{\text{near}}(\theta) = -\frac{2\pi}{\lambda} nd\theta + \frac{1-\theta^2}{\lambda r}\pi n^2 d^2$

Correlation: $f^{\text{near}} = |\mathbf{a}^H(\theta, r_1)\mathbf{a}(\theta, r_2)| \approx |G(\beta)| = \left|\frac{C(\beta)+jS(\beta)}{\beta}\right|$

where $\beta = \sqrt{\frac{N^2 d^2(1-\theta^2)}{2\lambda}\left|\frac{1}{r} - \frac{1}{\bar{r}}\right|}$

As $N \rightarrow \infty$, interference from different distances $I^{\text{near}} \rightarrow 0$ $(\forall\theta, r_1 \neq r_2)$

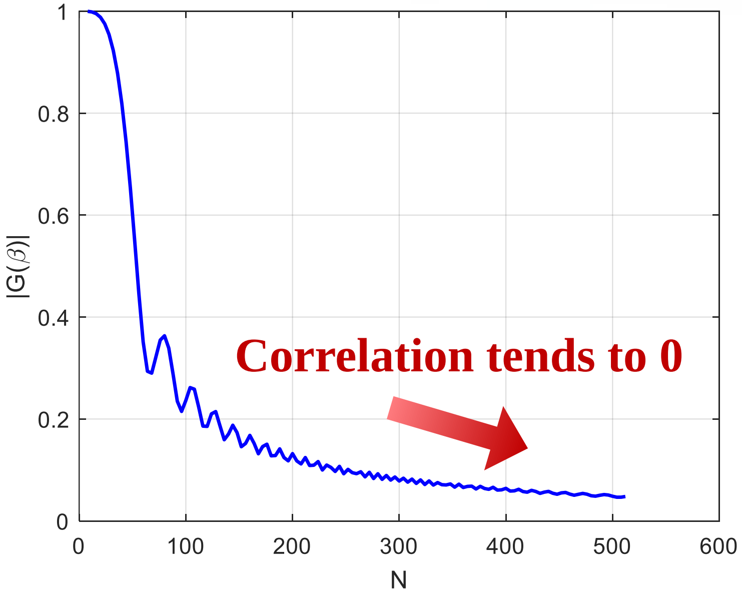

Correlation with increasing antennas

Simulation Results for LDMA

- **Scenario 1: Users are linearly distributed along the same direction**
- **Scenario 2: Users are uniformly distributed within a cell**

BS Antennas	UE Antennas	Frequency	UE Numbers	Elevation/ Azimuth Angle Range	Distance Range
256	1	30 GHz	20	$[-\pi/2, \pi/2]$	[4m, 100m]

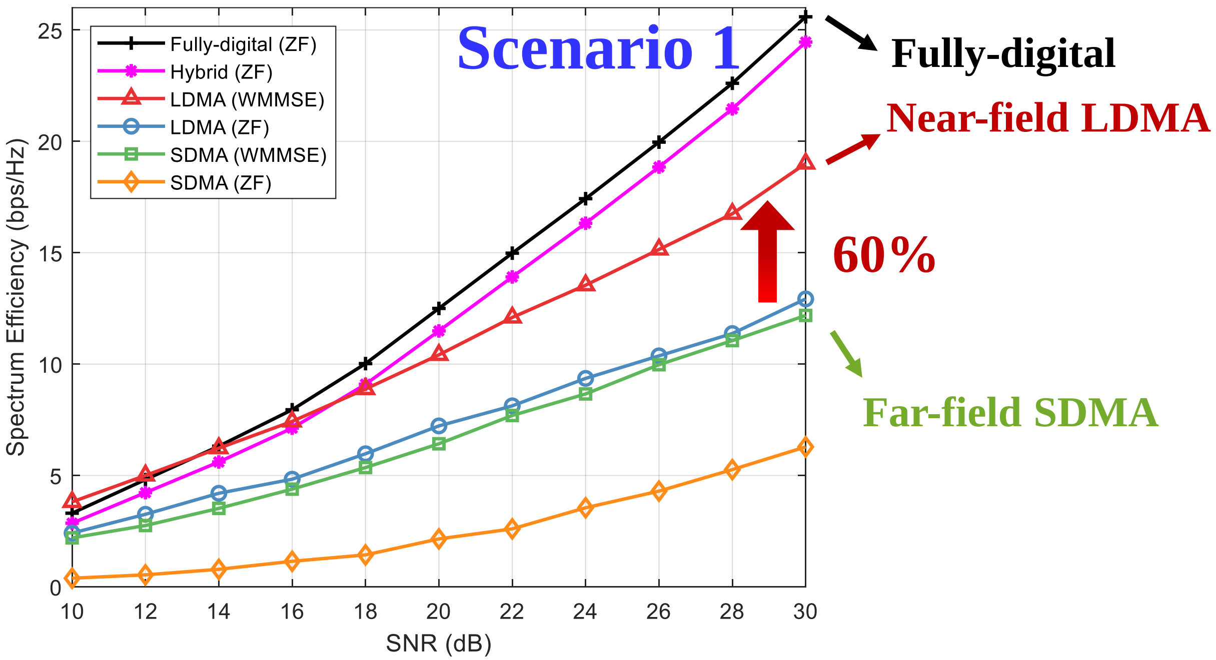

Fully-digital

Near-field LDMA

60%

Far-field SDMA

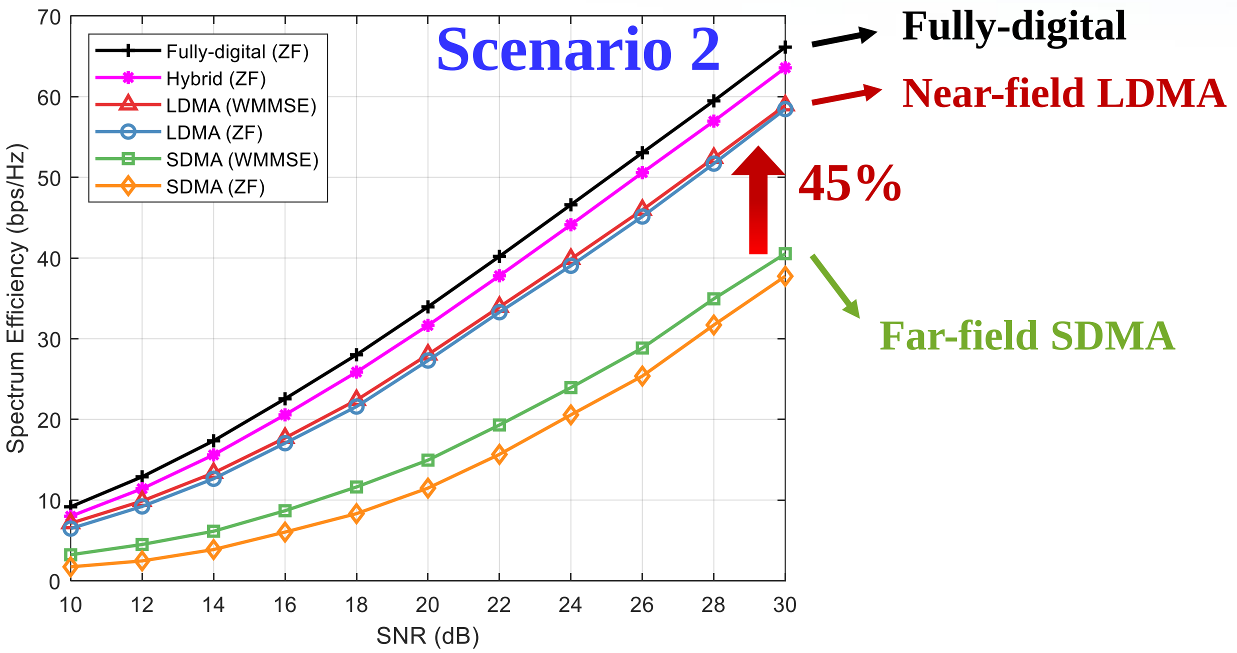

Fully-digital

Near-field LDMA

45%

Far-field SDMA

Z. Wu and L. Dai, “Multiple access for near-field communications: SDMA or LDMA? ” *IEEE J. Sel. Areas Commun.*, vol. 41, no. 6, pp. 1918-1935, Jun. 2023.

Outline of Part 3

- ☐ **Near-Field Single-User MIMO Capacity Enhancement**
- ☐ **Near-Field Location Division Multiple Access**
- ☐ **Near-Field Airy Beam for Blockage Mitigation**

Near-Field Airy Beam for Blockage Mitigation

- **LoS blockage can severely degrade high-frequency near-field links, and Airy beams offer a promising physical approach to blockage mitigation.**
- **Key properties of Airy beams:**
  - **Self-acceleration: Curved trajectory to bypass an obstacle**
  - **Non-diffraction: Fixed structure during propagation**
  - **Self-healing: Reconstruct the main lobe after blockage**

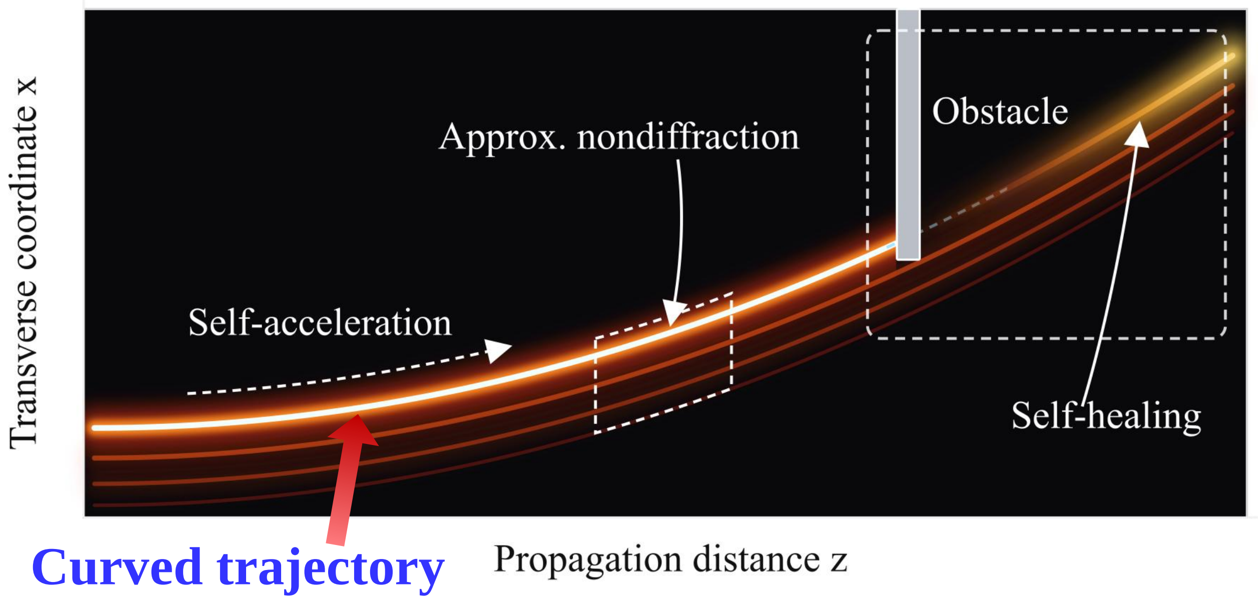

Curved trajectory

Fixed beam structure

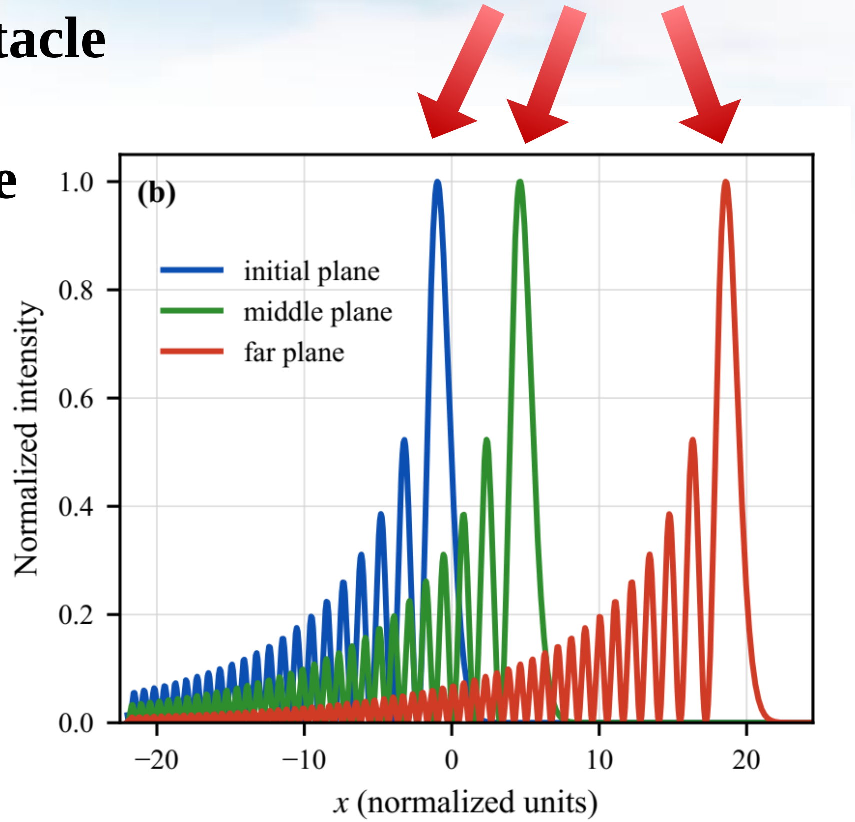

N. K. Efremidis, Z. Chen, M. Segev, and D. N. Christodoulides, "Airy beams and accelerating waves: An overview of recent advances," *Optica*, vol. 6, no. 5, pp. 686–701, May 2019.

Geometry Sensitivity of Airy Beam

- **Single-Airy beamforming is highly sensitive to Tx–obstacle–Rx geometry errors: A small mismatch can block the designed main lobe.**
- **This sensitivity stems from the single-trajectory structure: Most useful energy travels along one dominant curved trajectory.**

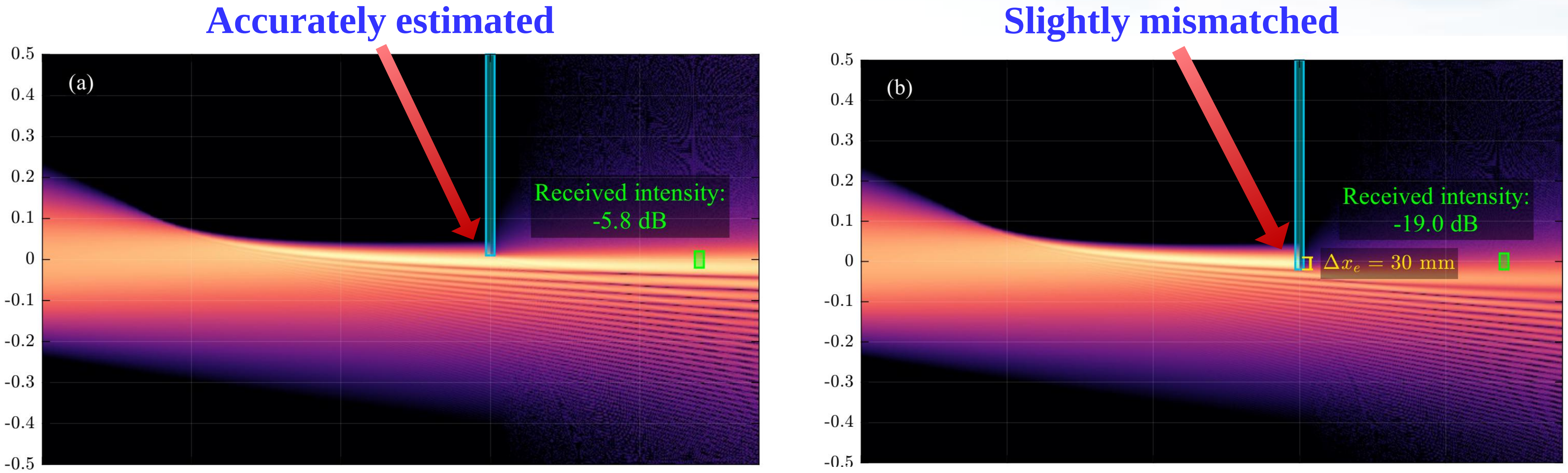
Accurately estimated

Slightly mismatched

A 30 mm error causes a 13dB loss in received energy

Y. Wang and **L. Dai**, "Blockage-robust beamforming for near-field communications: From single-Airy to multi-Airy," arXiv:2607.07278, Jul. 2026.

From Single-Airy to Coordinated Multi-Airy

- **Compared with Single-Airy, Multi-Airy creates multiple tailored trajectories to provide path diversity against blockage.**
- **Tailored phase offsets align the sub-array responses, allowing airy beams to be coherently combined at target user.**

Aperture field

$$\psi_0(x;\boldsymbol{\eta},\boldsymbol{\delta}) = \sum_{m=1}^{M} e^{\mathrm{j}\delta_m}\psi_{0,m}(x;\boldsymbol{\eta}_m)$$

Phase offsets

$$\delta_m^{(0)} = \phi_0 - \arg(g_m), \qquad m = 1,\ldots,M$$

Target field

$$\Psi_{\text{sum}}(x_0,z_0;\boldsymbol{\delta}) = \sum_{m=1}^{M} e^{\mathrm{j}\delta_m} g_m$$

Coherently combined

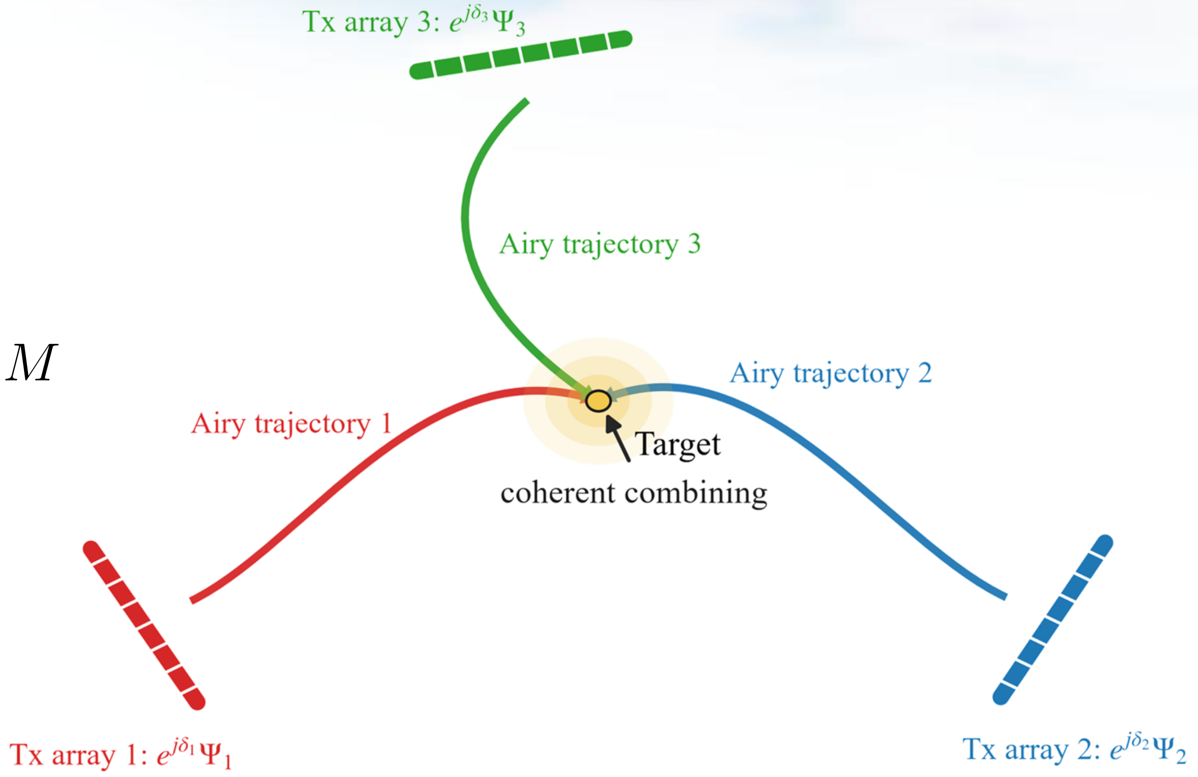

Y. Wang and **L. Dai**, "Blockage-robust beamforming for near-field communications: From single-Airy to multi-Airy," arXiv:2607.07278, Jul. 2026.

Robustness and Rate Gains

- **Under a 40-mm geometry error, Multi-Airy reduces the achievable-rate loss from 97.2% for Single-Airy to 33.3%.**
- **Even without geometry errors, Multi-Airy achieves up to 2.57× higher rates than Single-Airy under severe blockage.**

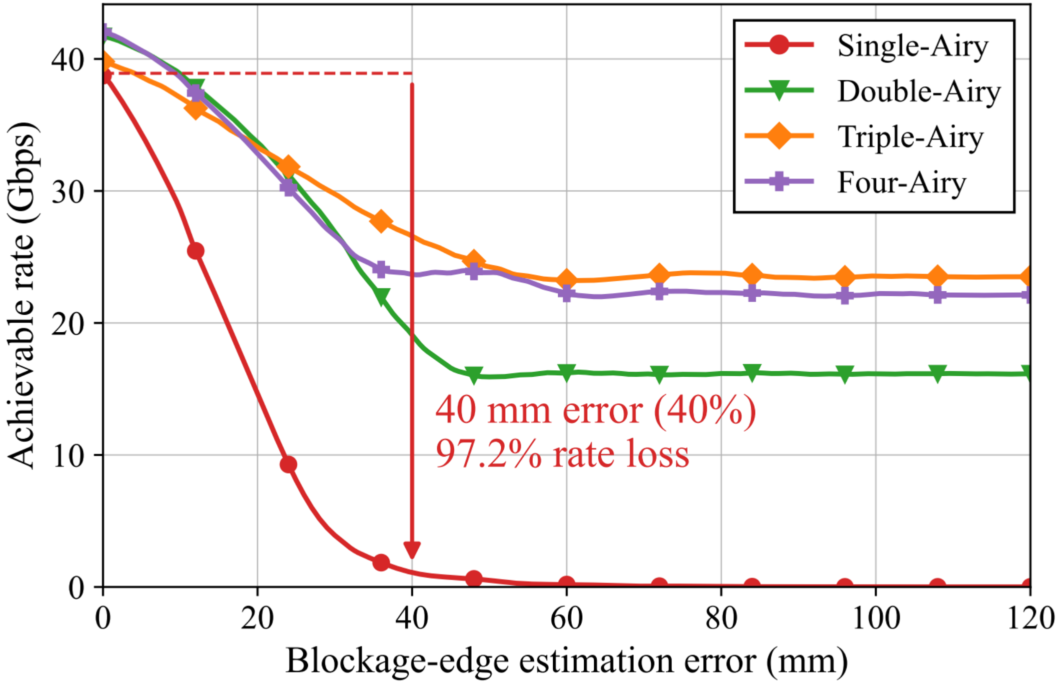

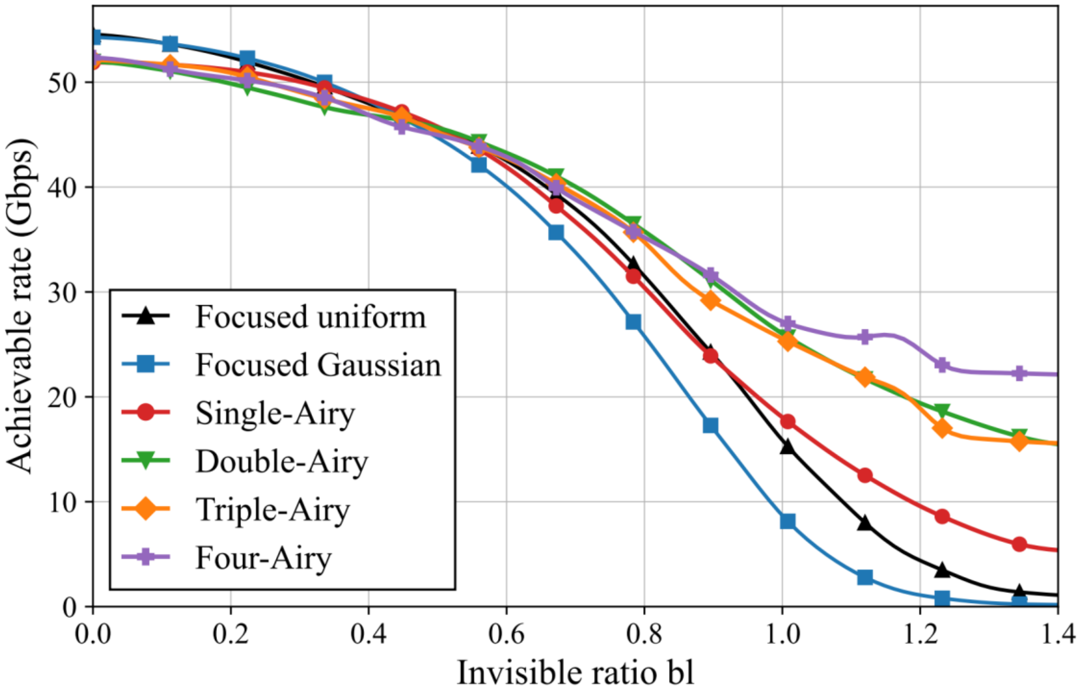

Y. Wang and **L. Dai**, "Blockage-robust beamforming for near-field communications: From single-Airy to multi-Airy," arXiv:2607.07278, Jul. 2026.

The Trajectory-Selection Problem of Airy Beam

- **Under blockage, existing methods rely on either costly beam training or black-box learning to navigate a vast continuous trajectory space. Neither provides a physically interpretable selection rule.**
- **The trajectory-edge coupling mechanism reveals the received-power balance between the unblocked contribution and edge-diffraction contribution, yielding an optimality condition for trajectory selection.**

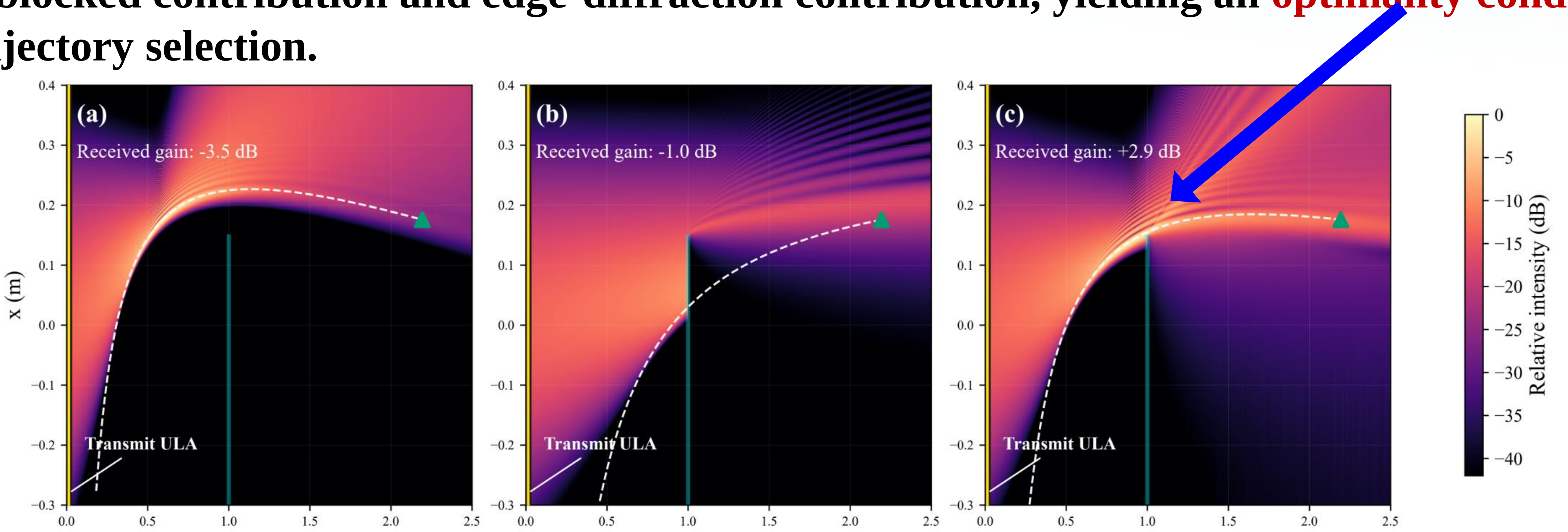

Y. Wang and **L. Dai**, "Physics-guided neural Airy beamforming for near-field blockage mitigation," *arxiv:2608.04388*, Aug. 2026.

Physics-Guided Trajectory Region

- **The trajectory-selection optimality condition defines a continuous trajectory structure, rather than isolated solutions.**
- **This structure yields a compact physics-defined region that effectively captures near-optimal trajectories.**

Optimality condition:

$$\nabla_{\mathbf{q}} P_{\text{rx}}(\mathbf{q}) = \mathbf{0} \quad \Longleftrightarrow \quad \nabla_{\mathbf{q}} P_{\text{free}}(\mathbf{q}) = -\nabla_{\mathbf{q}} \Delta P_{\text{e}}(\mathbf{q})$$

Continuous structure:

$$\mathcal{T}_{\text{br}}(\mathcal{I};\epsilon_{\text{dB}}) = \bigcup_{j} \{(\eta_w,\beta) : |\eta_w - \eta_j(\beta)| \le w_j(\beta;\epsilon_{\text{dB}})\}$$

Compact region:

$$\mathcal{T}_{\text{stat}}(\mathcal{I};\epsilon_{\text{dB}}) = \mathcal{T}_{\text{br}}(\mathcal{I};\epsilon_{\text{dB}}) \cup \mathcal{K}_{\partial\mathcal{F}_{\text{A}}}(\mathcal{I}) \subset \mathcal{Q} \quad \boxed{\frac{\text{Area}(\mathcal{T}_{\text{stat}})}{\text{Area}(\mathcal{Q})} \ll 1}$$

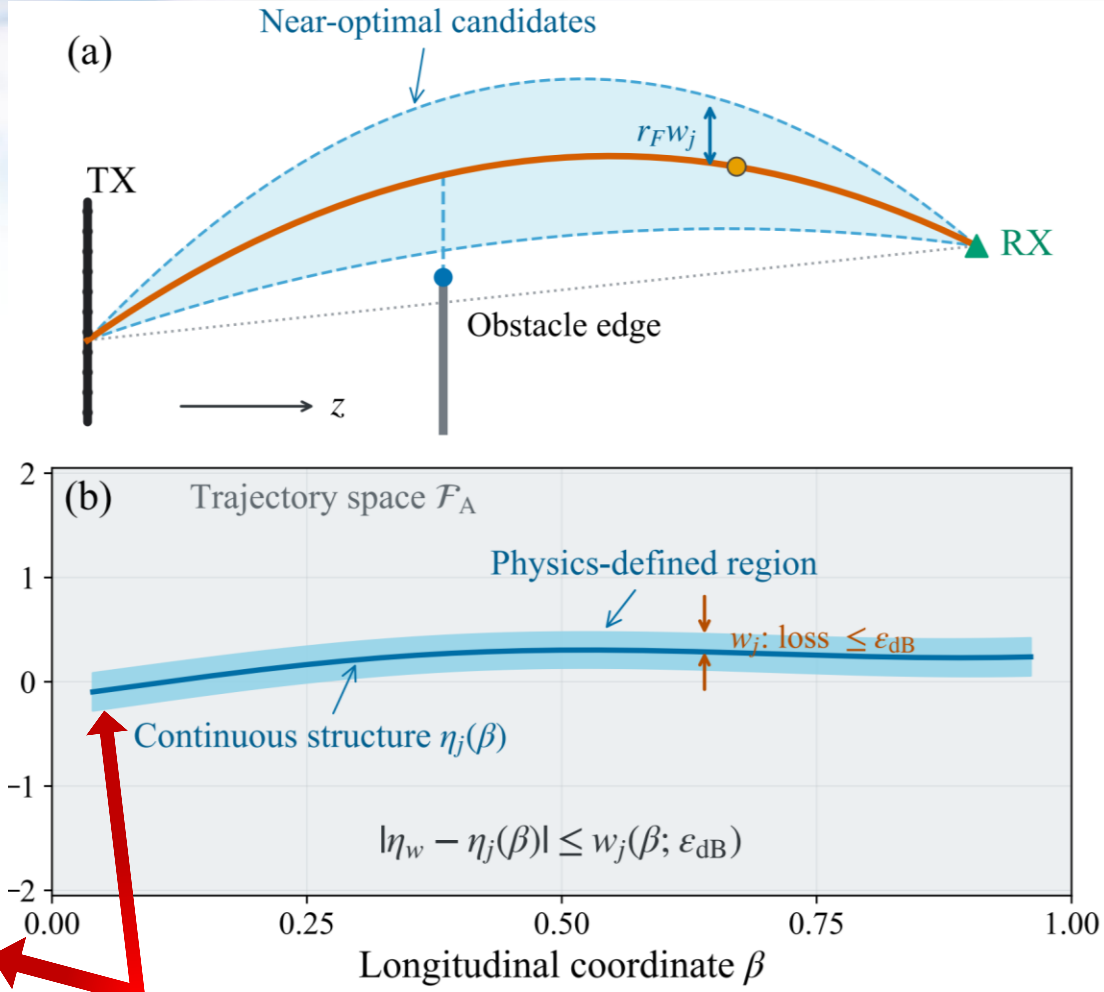

compact region

Y. Wang and **L. Dai**, "Physics-guided neural Airy beamforming for near-field blockage mitigation," *arxiv:2608.04388*, Aug. 2026.

Physics-Guided Trajectory Region

- **Guided by this compact physics-defined region, a lightweight Neural Airy Beamforming framework is designed to directly select a near-optimal trajectory without beam training.**

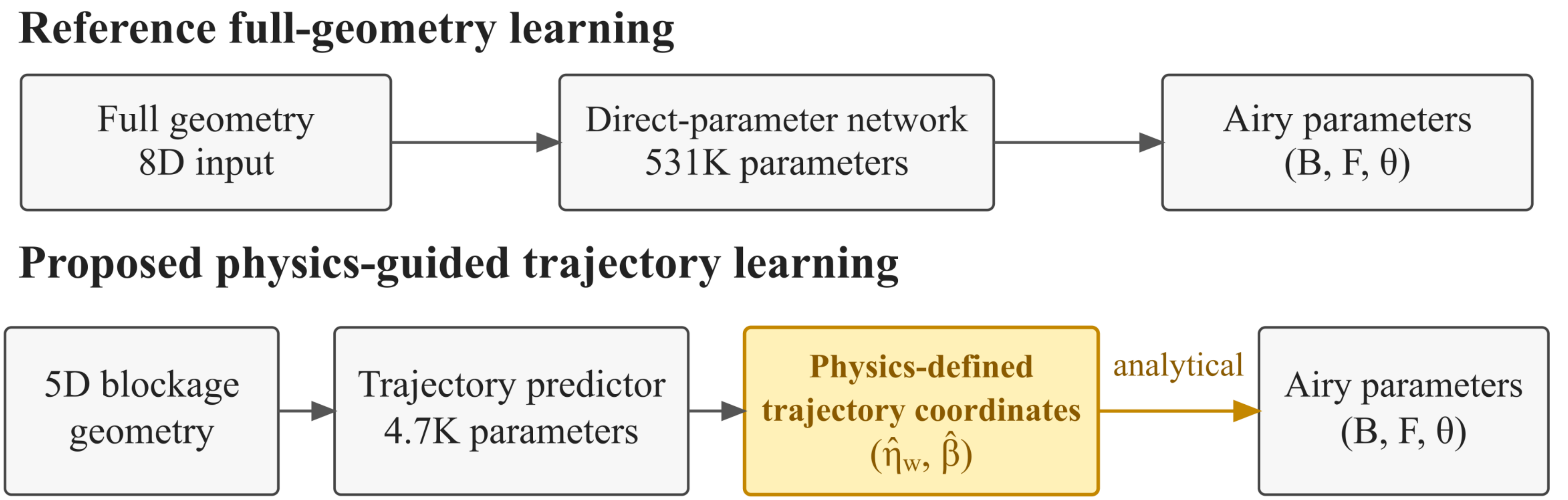

Reference full-geometry learning

Full geometry 8D input → Direct-parameter network 531K parameters → Airy parameters (B, F, θ)

Proposed physics-guided trajectory learning

5D blockage geometry → Trajectory predictor 4.7K parameters → **Physics-defined trajectory coordinates** $(\hat{\eta}_w, \hat{\beta})$ → analytical → Airy parameters (B, F, θ)

Y. Wang and **L. Dai**, "Physics-guided neural Airy beamforming for near-field blockage mitigation," *arxiv:2608.04388*, Aug. 2026.

Near-Optimal Performance in One Shot

- **The compact physics-defined region captures near-optimal trajectories while occupying only about 6% of the candidate-space area on average.**
- **The proposed framework retains 99.7% of the reference rate obtained through numerical optimization and nearly matches the data-driven method with approximately 112× fewer neural-network parameters.**

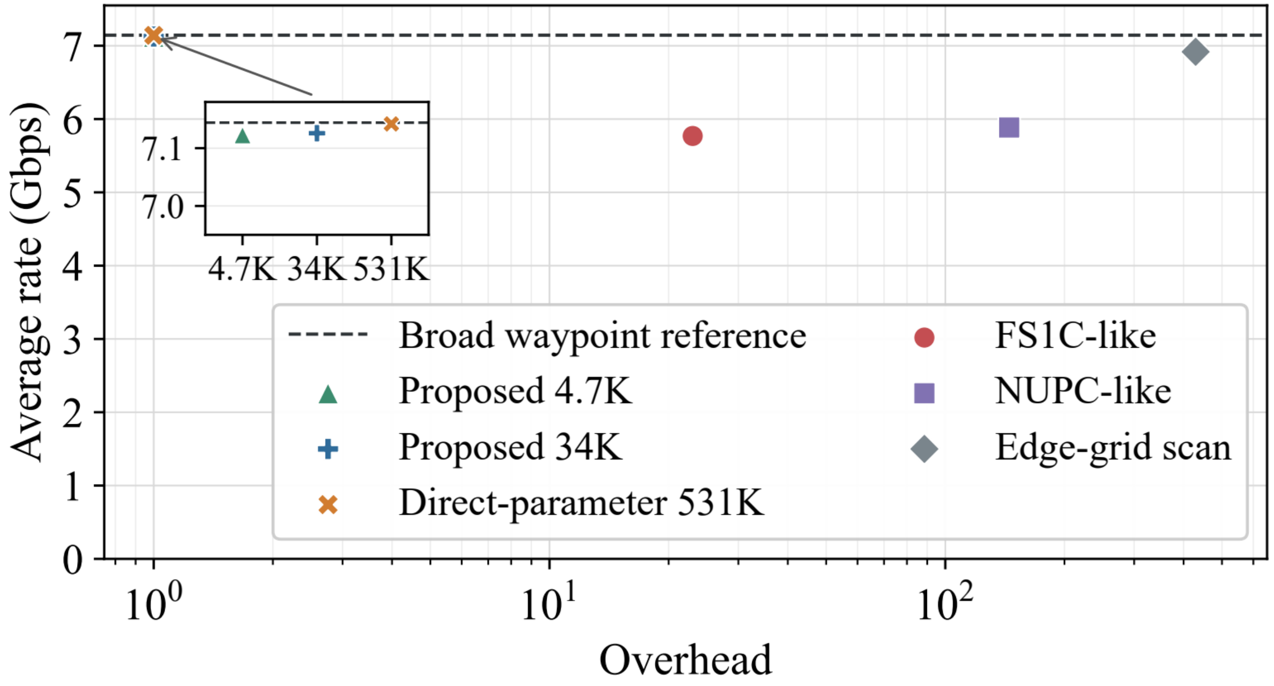

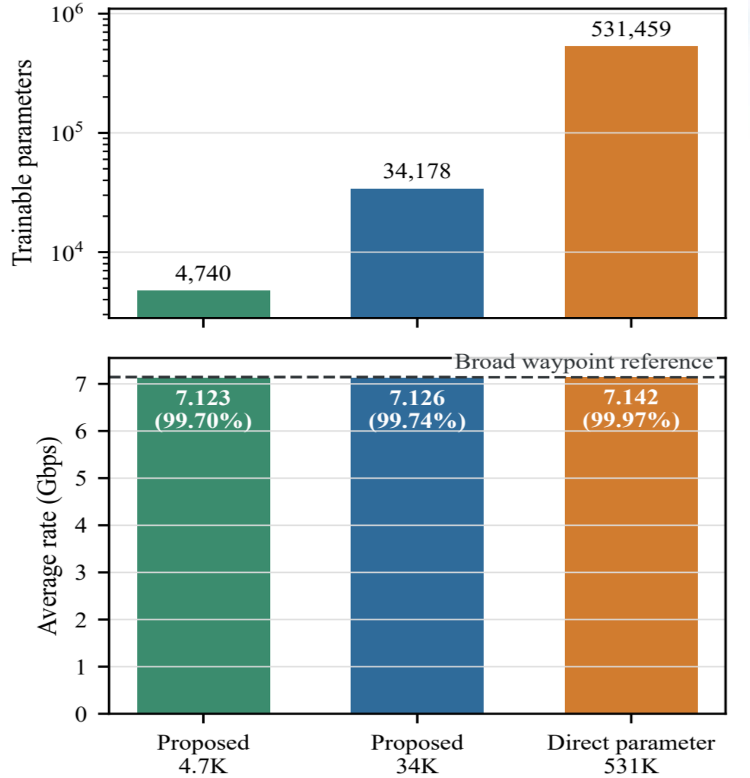

Y. Wang and **L. Dai**, “Physics-guided neural Airy beamforming for near-field blockage mitigation,” *arxiv:2608.04388*, Aug. 2026.

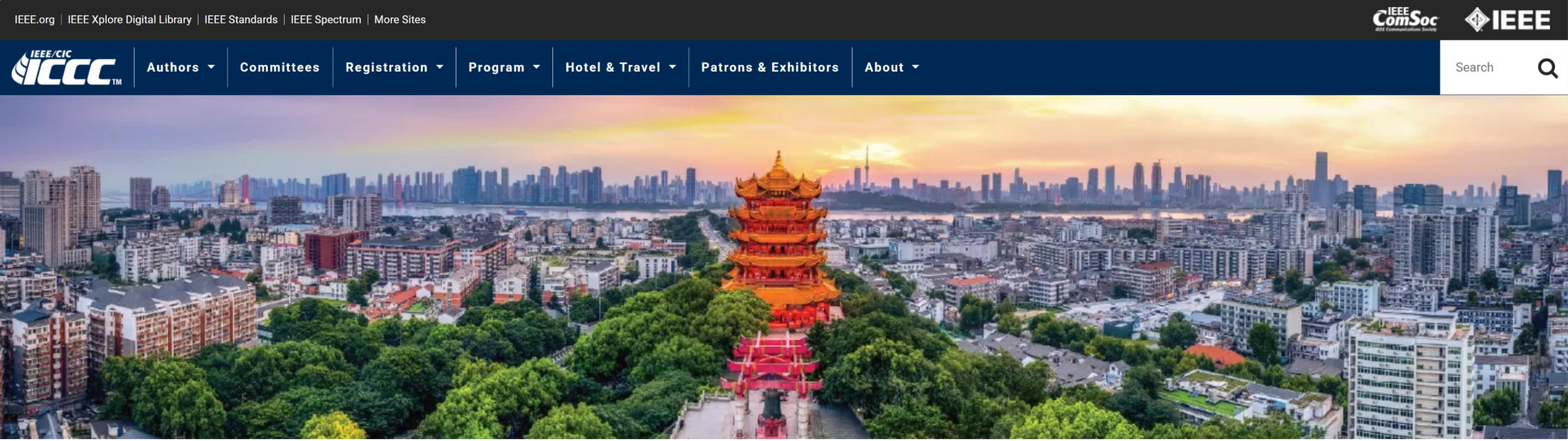

Part 4: Challenges of Near-Field Communications

Outline of Part 4

- ☐ **Near-Field Channel State Information Acquisition**
  - ➢ **Near-field MISO channel estimation**
  - ➢ **Near-field MIMO channel estimation**
  - ➢ **Near-field beam training**
- ☐ **Near-Field Beam Split**
  - ➢ **Phase-delay beam focusing**
  - ➢ **Near-field rainbow-based beam training**
  - ➢ **Distance-dependent beam split based beam training**
- ☐ **Near-field Grating Lobes Suppression**
  - ➢ **From modular ULA to modular MRA**

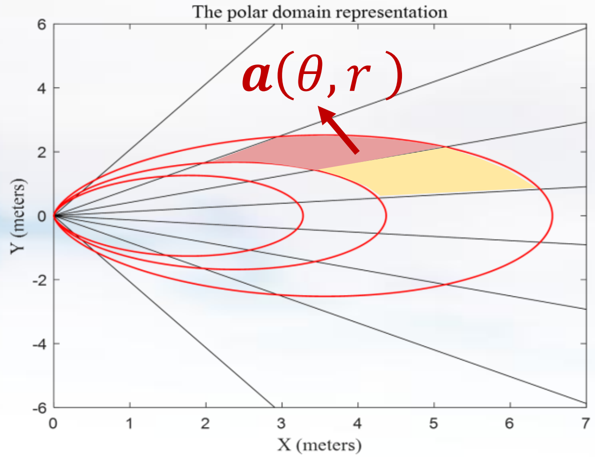

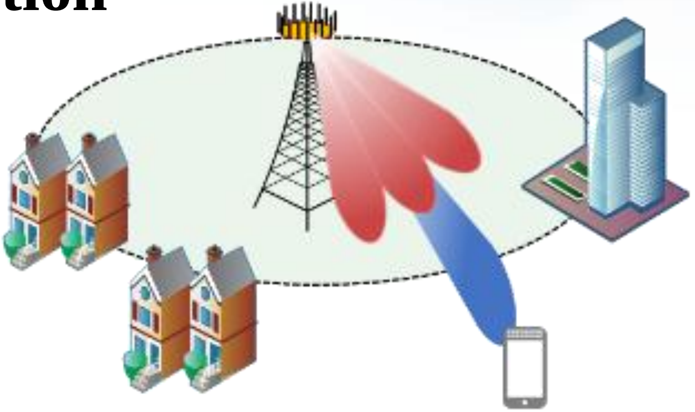

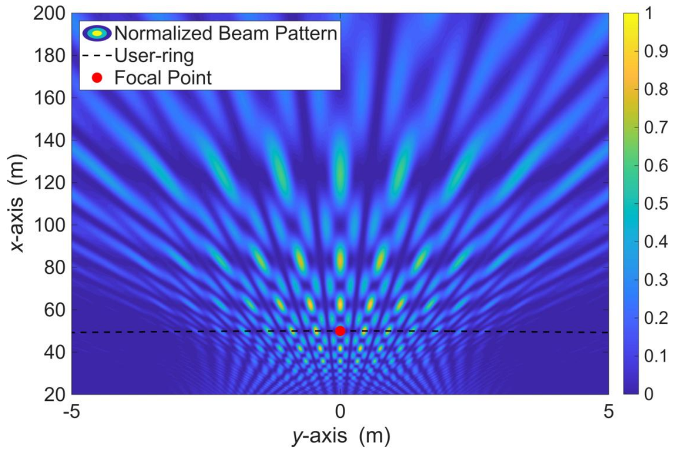

Challenge of Near-Field Channel Estimation

- **Existing far-field channel estimation relies on the angle-domain sparsity exploited by the orthogonal angle-domain codebook, i.e., the DFT codebook**
- **The near-field angle-domain channels suffer from a severe energy spreading problem**

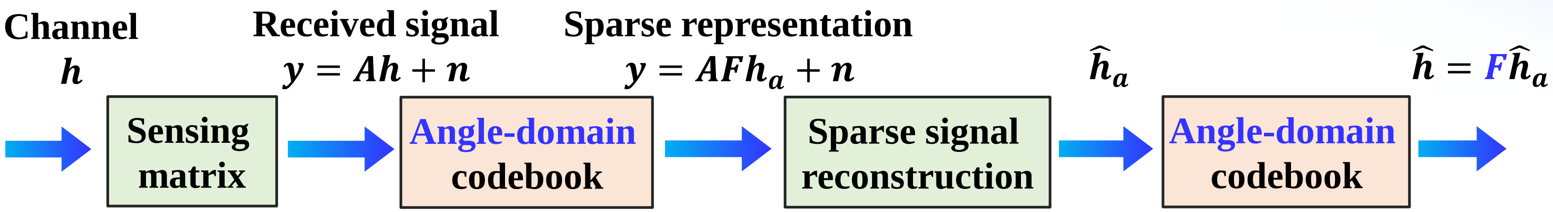

Channel h

Received signal $y = Ah + n$

Sparse representation $y = AF h_a + n$

$\hat{h}_a$

$\hat{h} = F\hat{h}_a$

Sensing matrix

Angle-domain codebook

Sparse signal reconstruction

Angle-domain codebook

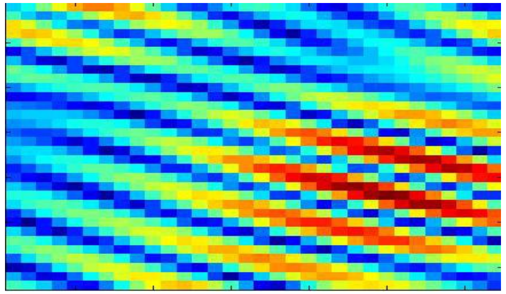

Far-field

antenna-domain

Angle-domain codebook

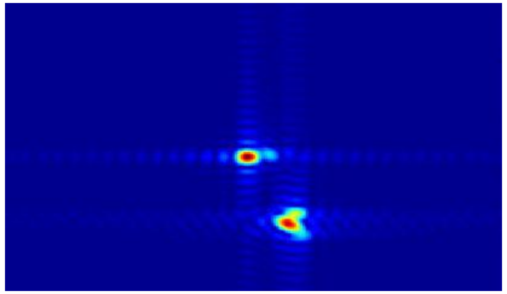

Far-field

angle-domain

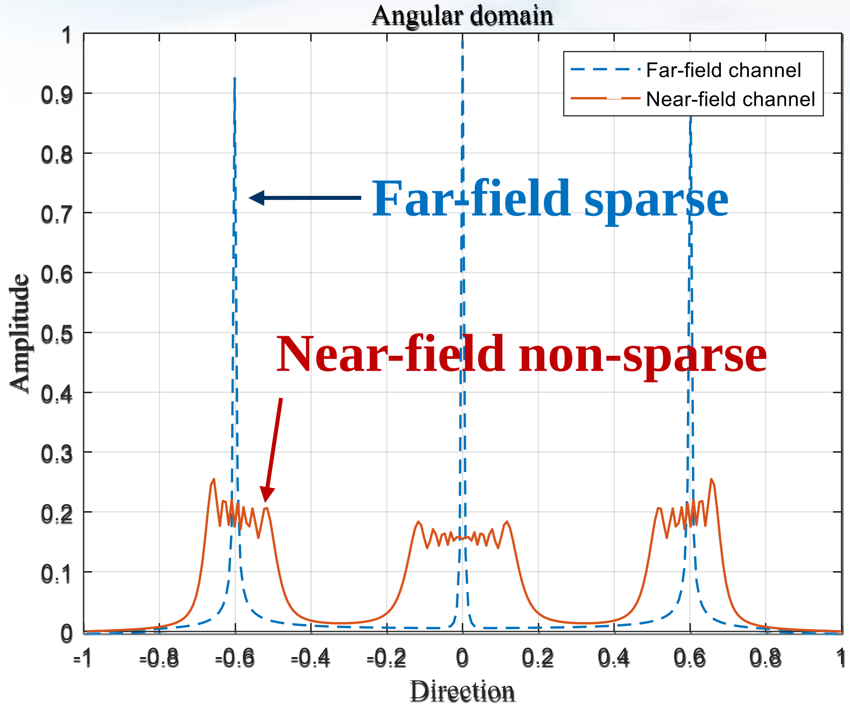

The angle-domain codebook is not appropriate for near-field channel estimation

Near-Field Codebook Design

- **Far-field codebook: samples multiple angle grids in the angle domain**
- **Near-field codebook: samples multiple “angle-distance” grids in the polar domain**

Angle-domain codeword $\boldsymbol{a}(\theta) = \left[e^{jn\pi\theta}\right]_{n=-N}^{N}$

Polar-domain codeword $\boldsymbol{a}(\theta, r) = \left[e^{jk\sqrt{r+n^2d^2-2rnd\theta}}\right]_{n=-N}^{N}$

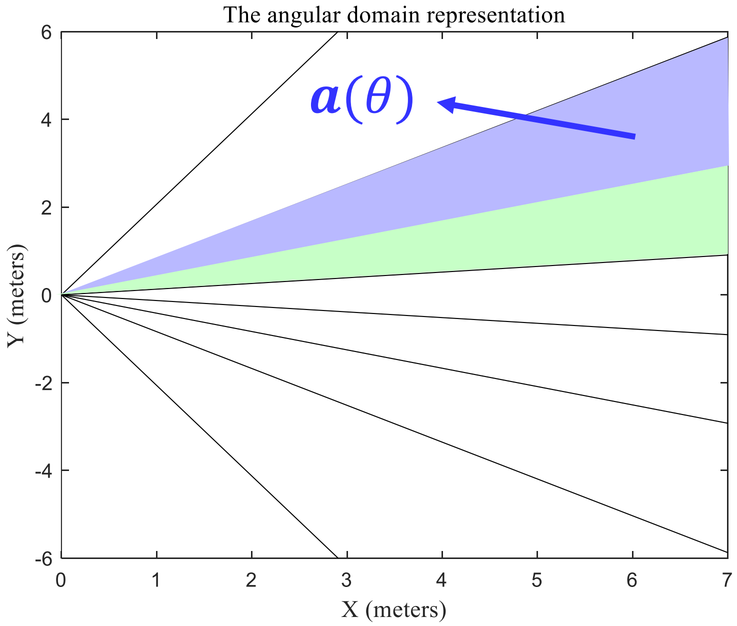

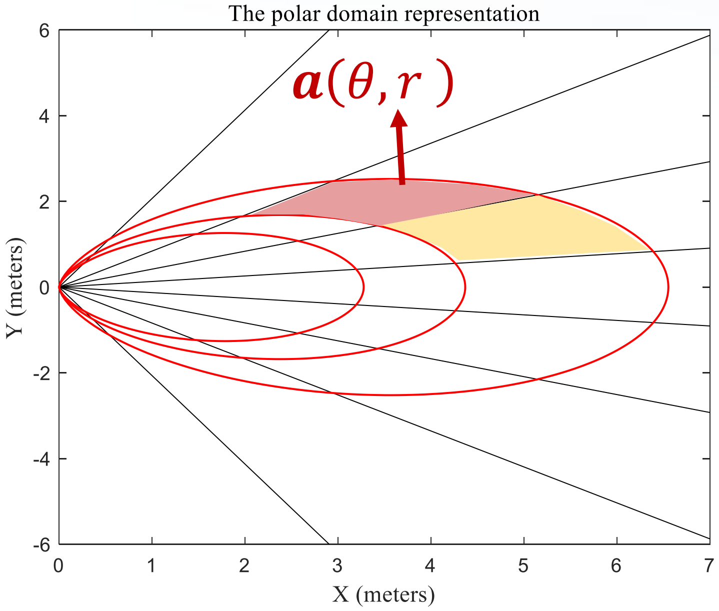

The near field codebook should sample in polar domain instead of angle domain

M. Cui and L. Dai, “Channel estimation for extremely large-scale MIMO: Far-field or near-field?,” *IEEE Trans. Commun.*, vol. 70, no. 4, pp. 2663-2677, Apr. 2022.

The Distance-Sampling Criterion

- **The grids can be sampled sparsely far away from ELAA, but densely near the ELAA**

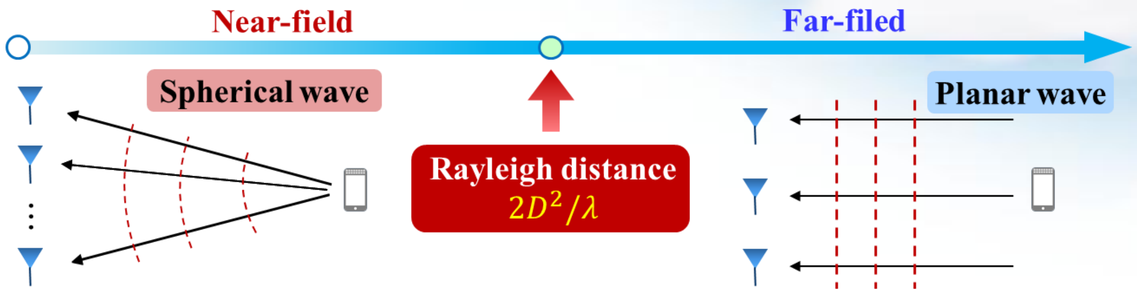

- **Codebook design method: Minimizing the maximum coherence of the polar-domain codebook**
- **Based on the Fresnel approximation, we prove the following sampling criteria**

Uniform angle sampling: $\theta_n = -1 + \frac{n+N+1}{2N+1}, \quad n = \{-N, \cdots, 0, \cdots, N\}$

Non-uniform distance sampling: $r_{n,s} = \frac{1}{s}\left(1 - \theta_n^2\right) Z_\Gamma, \ s = \{1,2,\cdots,S\}, \ Z_\Gamma = \frac{M^2 d^2}{2\lambda\beta_\Gamma^2}$

The number of sampled distances

Threshold

- **The polar-domain codebook can be constructed as**

$$\boldsymbol{P}_n = \left[\boldsymbol{a}\left(\theta_n, r_{n,1}\right), \boldsymbol{a}\left(\theta_n, r_{n,2}\right), \cdots, \boldsymbol{a}(\theta_n, r_{n,S})\right] \qquad \boldsymbol{P} = \left[\boldsymbol{P}_{-N}, \cdots, \boldsymbol{P}_0, \cdots, \boldsymbol{P}_N\right]$$

M. Cui and L. Dai, "Channel estimation for extremely large-scale MIMO: Far-field or near-field?," *IEEE Trans. Commun.*, vol. 70, no. 4, pp. 2663-2677, Apr. 2022.

Polar-Domain Codebook Based Channel Estimation

- **Angle-domain codebook is replaced by polar-domain codebook**
- **Other procedures are similar**

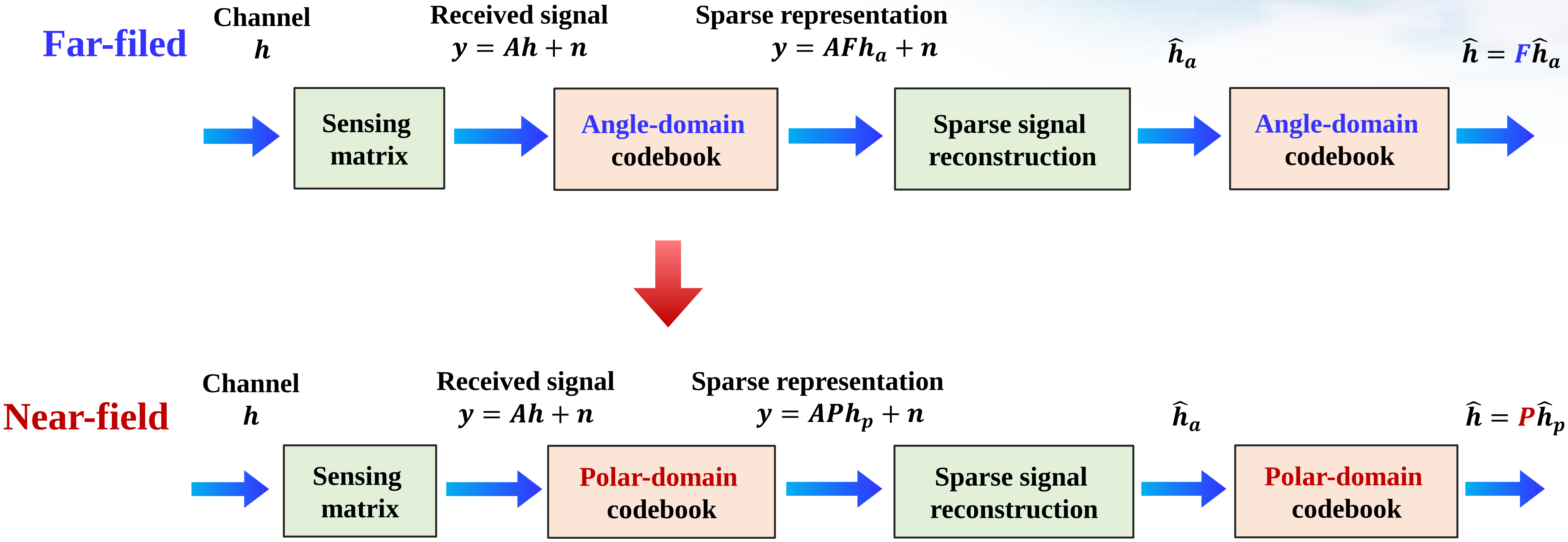

Far-filed

Channel $\boldsymbol{h}$

Received signal $\boldsymbol{y} = \boldsymbol{A}\boldsymbol{h} + \boldsymbol{n}$

Sparse representation $\boldsymbol{y} = \boldsymbol{A}\boldsymbol{F}\boldsymbol{h}_a + \boldsymbol{n}$

$\hat{\boldsymbol{h}}_a$

$\hat{\boldsymbol{h}} = \boldsymbol{F}\hat{\boldsymbol{h}}_a$

Sensing matrix → **Angle-domain codebook** → **Sparse signal reconstruction** → **Angle-domain codebook**

Near-field

Channel $\boldsymbol{h}$

Received signal $\boldsymbol{y} = \boldsymbol{A}\boldsymbol{h} + \boldsymbol{n}$

Sparse representation $\boldsymbol{y} = \boldsymbol{A}\boldsymbol{P}\boldsymbol{h}_p + \boldsymbol{n}$

$\hat{\boldsymbol{h}}_a$

$\hat{\boldsymbol{h}} = \boldsymbol{P}\hat{\boldsymbol{h}}_p$

Sensing matrix → **Polar-domain codebook** → **Sparse signal reconstruction** → **Polar-domain codebook**

M. Cui and L. Dai, "Channel estimation for extremely large-scale MIMO: Far-field or near-field?," *IEEE Trans. Commun.*, vol. 70, no. 4, pp. 2663-2677, Apr. 2022.

Simulation Results

- **The proposed schemes can accurately estimate the near-field channel**

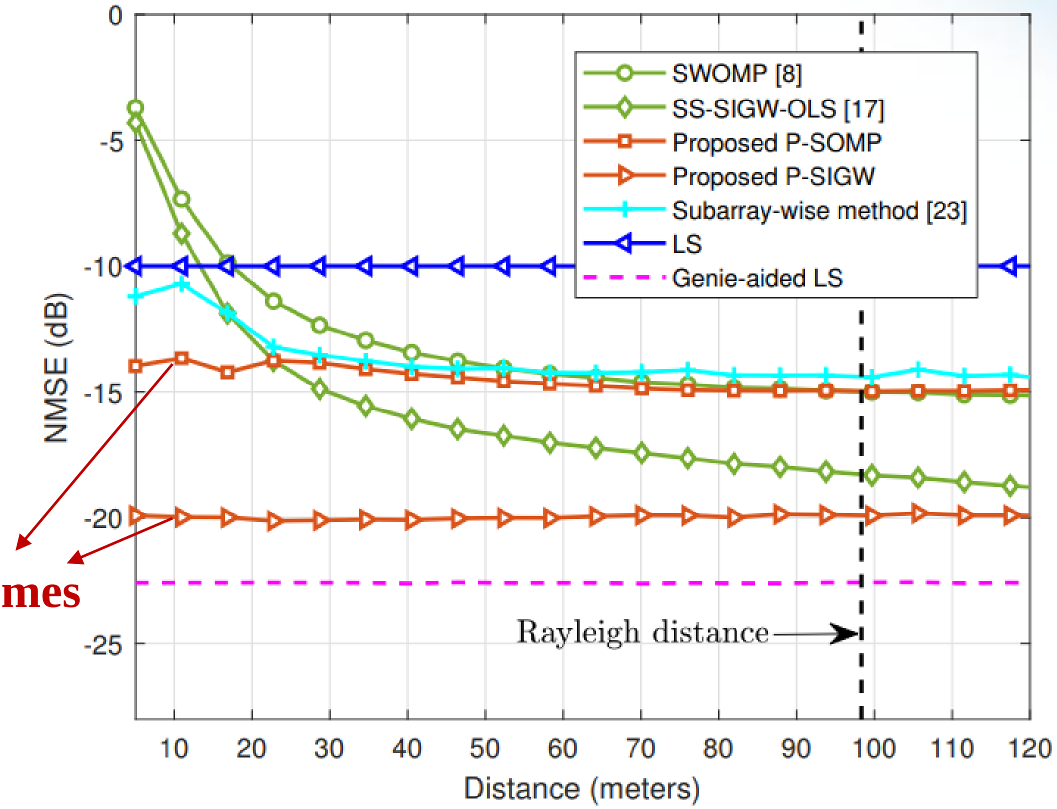

Proposed schemes

Parameters	Value
Carrier	100 GHz
Bandwidth	400 MHz
Number of carriers	1024
Array Aperture	0.4 m
SNR	10 dB
Pilot compression ratio	0.5

Polar-domain codebook naturally decay to the angle-domain codebook in far field

M. Cui and L. Dai, "Channel estimation for extremely large-scale MIMO: Far-field or near-field?," *IEEE Trans. Commun.*, vol. 70, no. 4, pp. 2663-2677, Apr. 2022.

Outline of Part 4

- ☐ **Near-Field Channel State Information Acquisition**
  - ➢ **Near-field MISO channel estimation**
  - ➢ **Near-field MIMO channel estimation**
  - ➢ **Near-field beam training**
- ☐ **Near-Field Beam Split**
  - ➢ **Phase-delay beam focusing**
  - ➢ **Near-field rainbow-based beam training**
  - ➢ **Distance-dependent beam split based beam training**
- ☐ **Near-field Grating Lobes Suppression**
  - ➢ **From modular ULA to modular MRA**

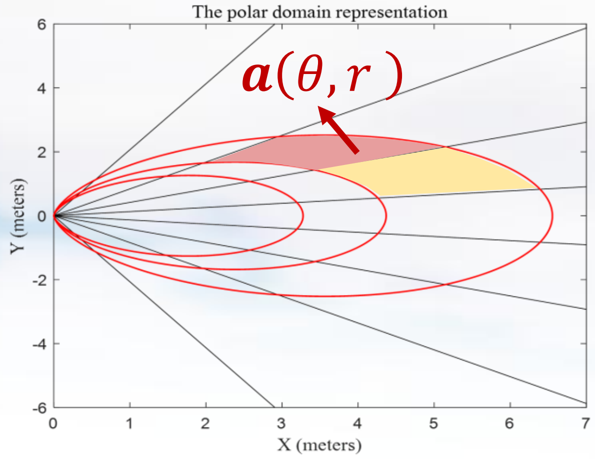

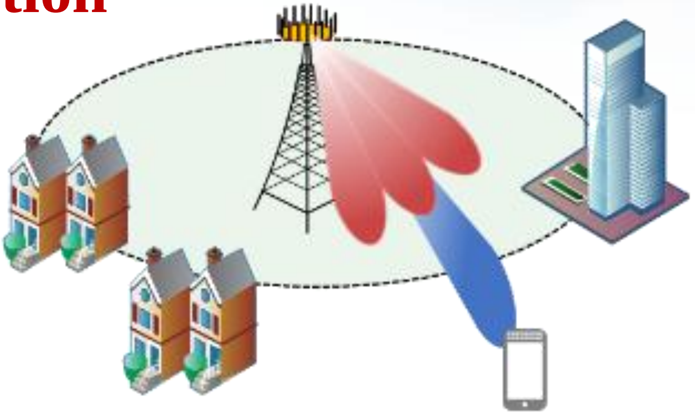

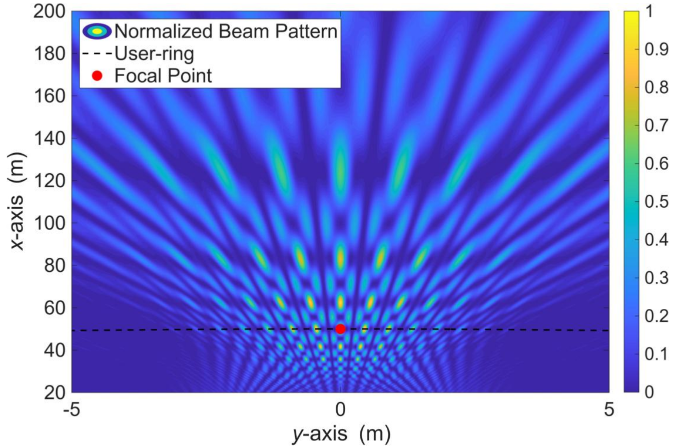

Near-Field Scenario: From MISO to MIMO

- **MISO: Only the BS is equipped with multiple antennas**
- **MIMO: The user is also equipped with multiple antennas**

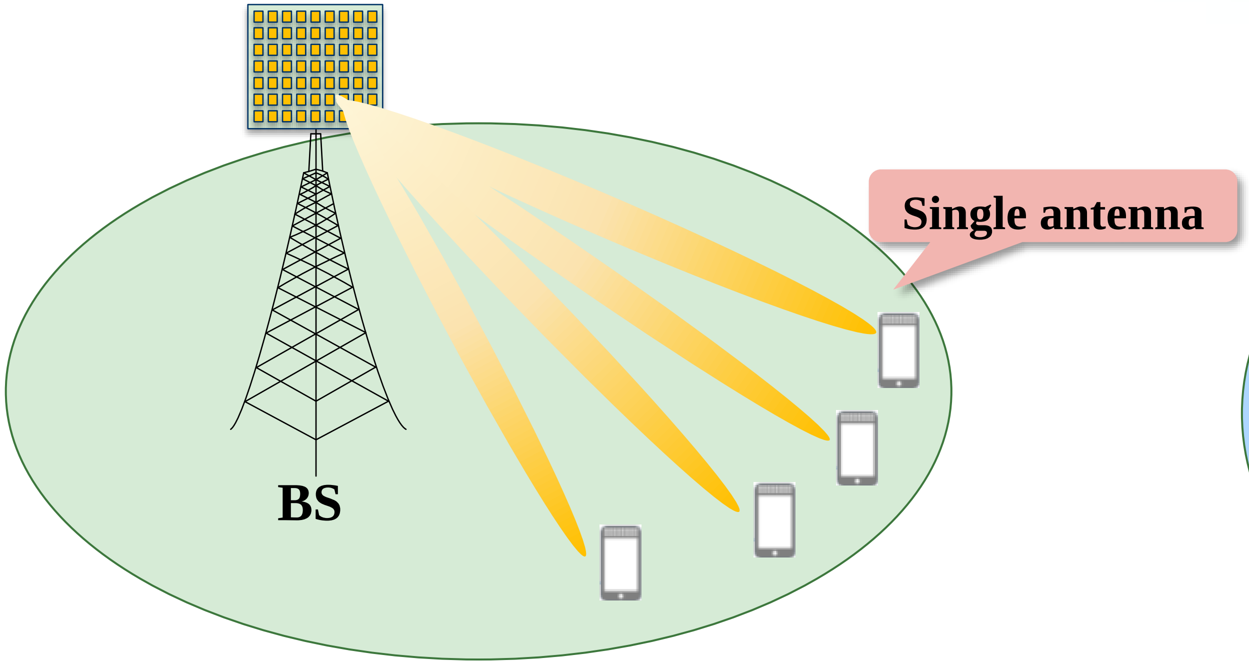

MISO

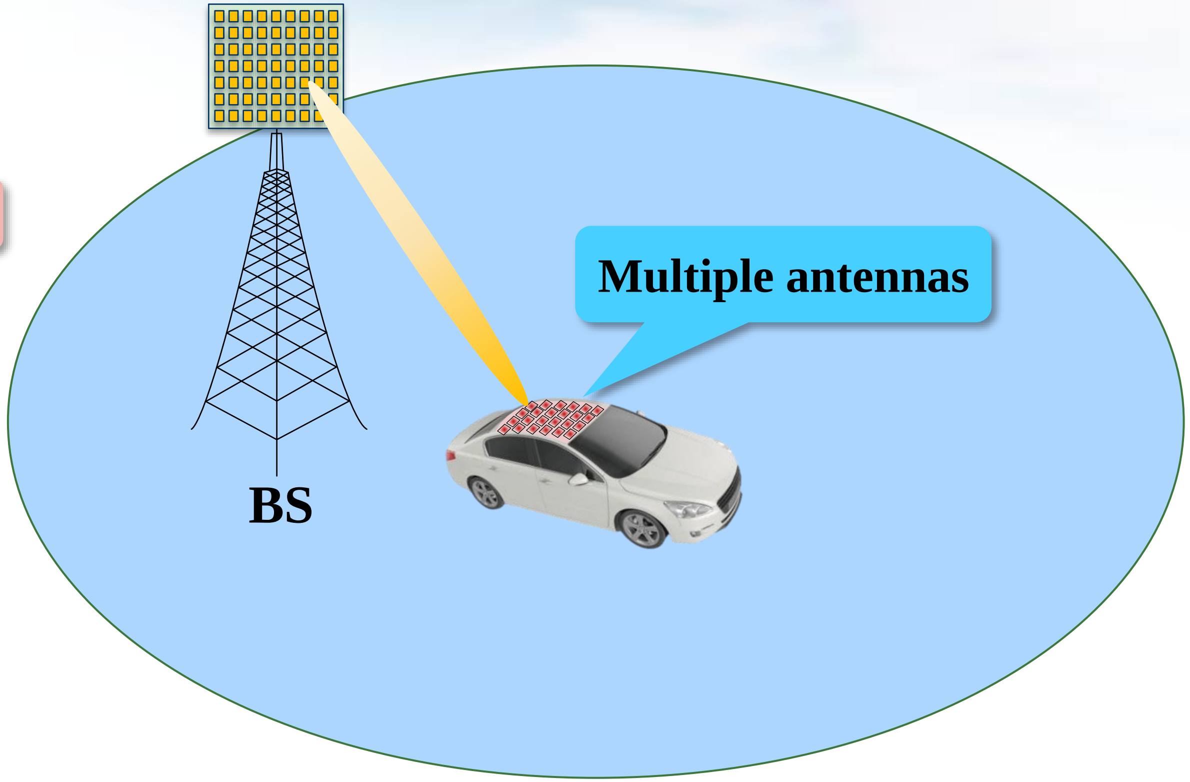

MIMO

Near-Field MIMO Channel Model

- **Similar to far-field MIMO channel model, the existing near-field MIMO channel model is based on the near-field steering vector**

$$\mathbf{H}_{\text{near-field}} = \sqrt{\frac{N_1 N_2}{L}} \sum_{l=1}^{L} g_l \mathbf{a}(\theta_r^l, d_r^l)\, \mathbf{b}^H(\theta_t^l, d_t^l)$$

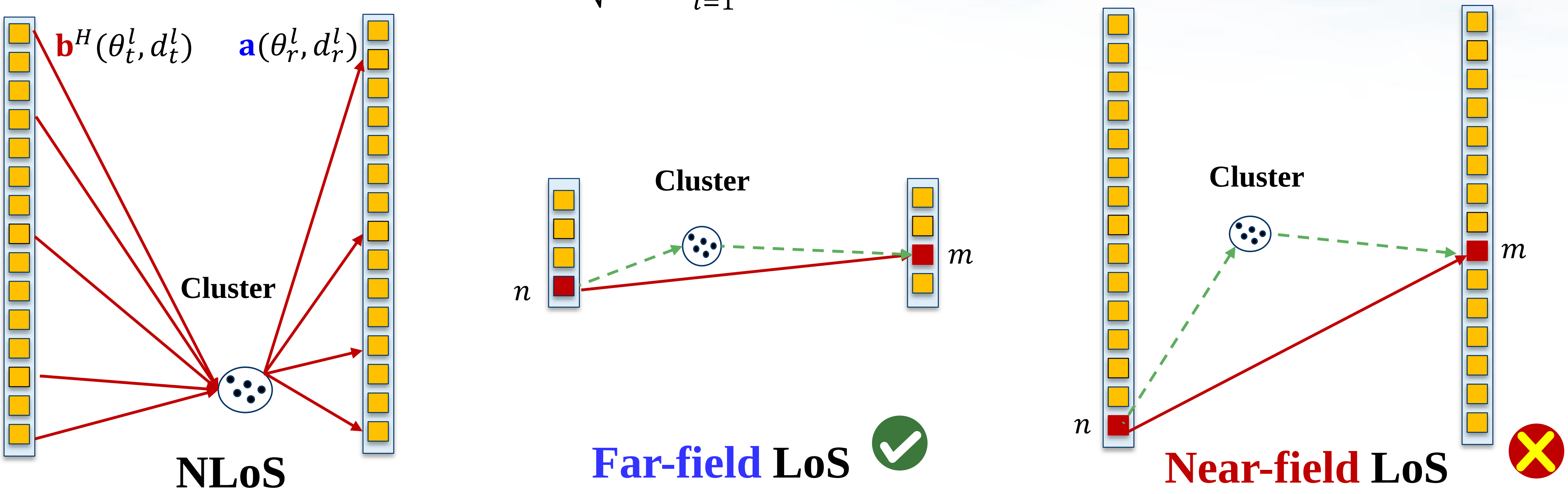

The existing model cannot accurately describe the characteristic of near-field LoS path

Proposed Near-Field MIMO Channel Model

- **The LoS and NLoS paths are modeled separately**

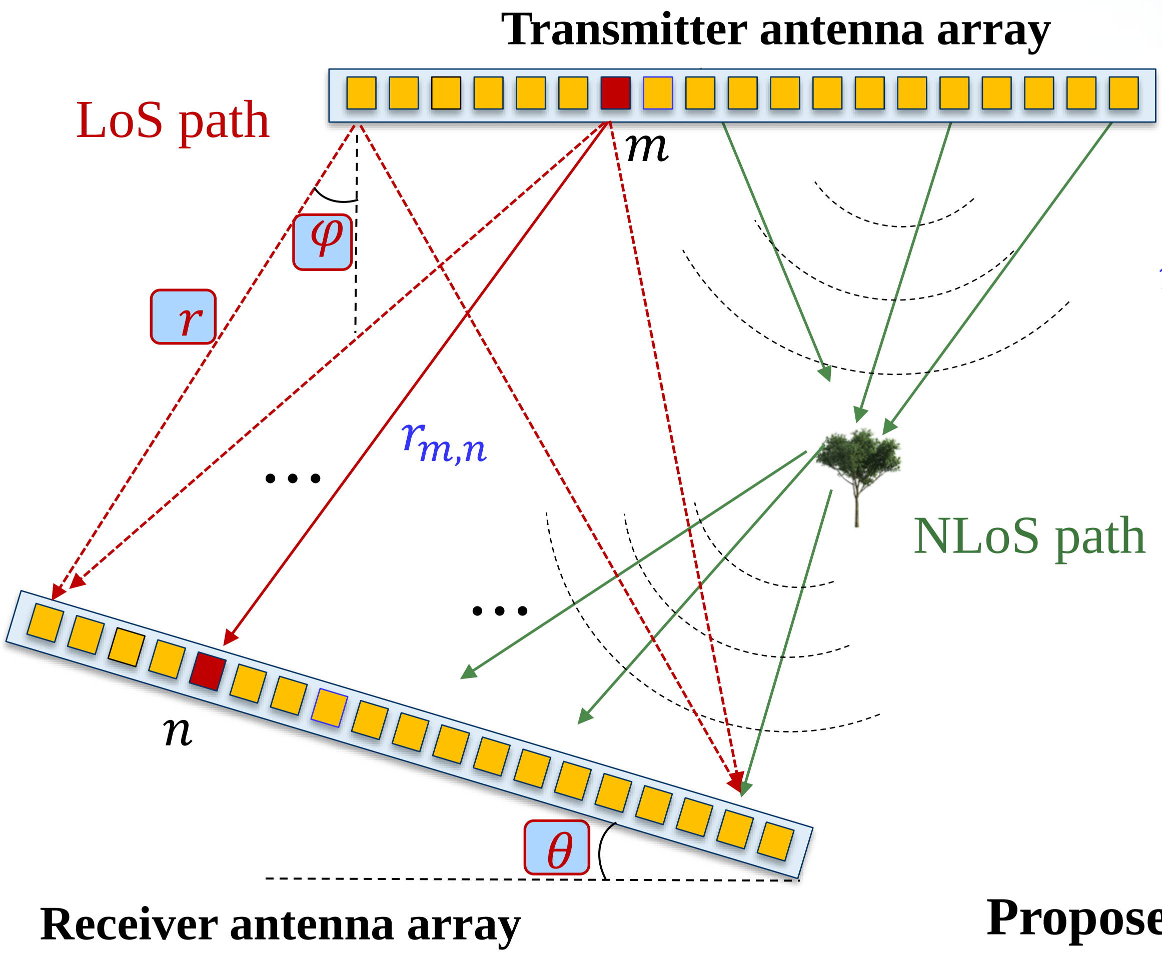

LoS: Free-space propagation

$$\mathbf{H}_{\mathrm{LoS},(m,n)} = \frac{e^{-j2\pi r_{m,n}/\lambda}}{r_{m,n}}$$

$$r_{m,n} = \sqrt{r^2 + (md)^2 + (nd)^2 - 2rmd\cos(\theta + \varphi) + 2rnd\cos(\theta) - 2mnr^2\cos(\varphi)}$$

$$\mathbf{H}_{\mathrm{LoS}}(r,\theta,\varphi) = \begin{bmatrix} \frac{e^{-j2\pi r_{1,1}/\lambda}}{r_{1,1}} & \cdots & \frac{e^{-j2\pi r_{1,N}/\lambda}}{r_{1,N}} \\ \vdots & \ddots & \vdots \\ \frac{e^{-j2\pi r_{M,1}/\lambda}}{r_{M,1}} & \cdots & \frac{e^{-j2\pi r_{M,N}/\lambda}}{r_{M,N}} \end{bmatrix}$$

NLoS: Based on near-field steering vector

$$\mathbf{H}_{\mathrm{NLoS}} = \sum_{l=1}^{L} g_l \boldsymbol{a}(\theta_r^l, r_r^l)\, \mathbf{b}^H(\theta_t^l, r_t^l)$$

Proposed near-field MIMO channel model: $\mathbf{H} = \mathbf{H}_{\mathrm{LoS}} + \mathbf{H}_{\mathrm{NLoS}}$

Y. Lu and L. Dai, "Near-field channel estimation in mixed LoS/NLoS environments for extremely large-scale MIMO systems," *IEEE Trans. Commun.*, vol. 71, no. 11, pp. 7748-7760, Jun. 2023.

Near-Field MIMO Rayleigh Distance

- **Rayleigh distance: The transceiver distance when the maximum phase discrepancy between spherical wave and plane wave is $\pi/8$**
  - **Classical MISO Rayleigh Distance:** $R_1 = 2D^2/\lambda$
  - **Proposed MIMO Rayleigh Distance:** $R_2 = 2(D_1 + D_2)^2/\lambda$

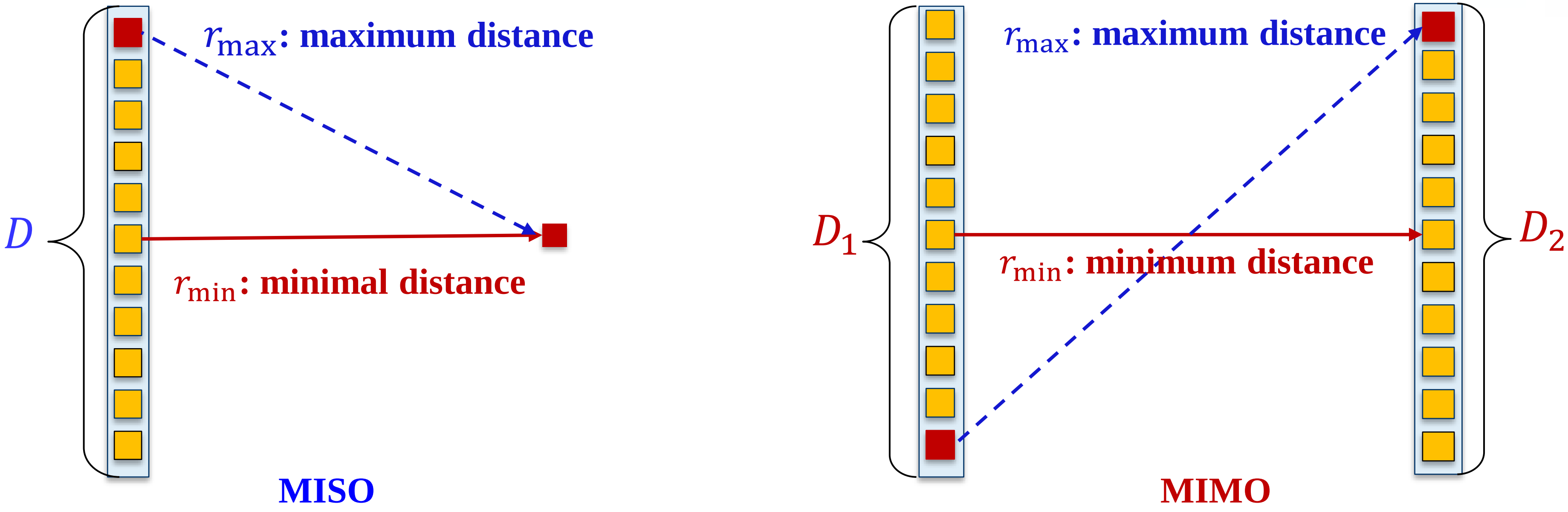

Y. Lu and L. Dai, "Near-field channel estimation in mixed LoS/NLoS environments for extremely large-scale MIMO systems," *IEEE Trans. Commun.*, vol. 71, no. 11, pp. 7748-7760, Jun. 2023.

Simulation Results

- **The proposed scheme can accurately estimate the near-field MIMO channel**

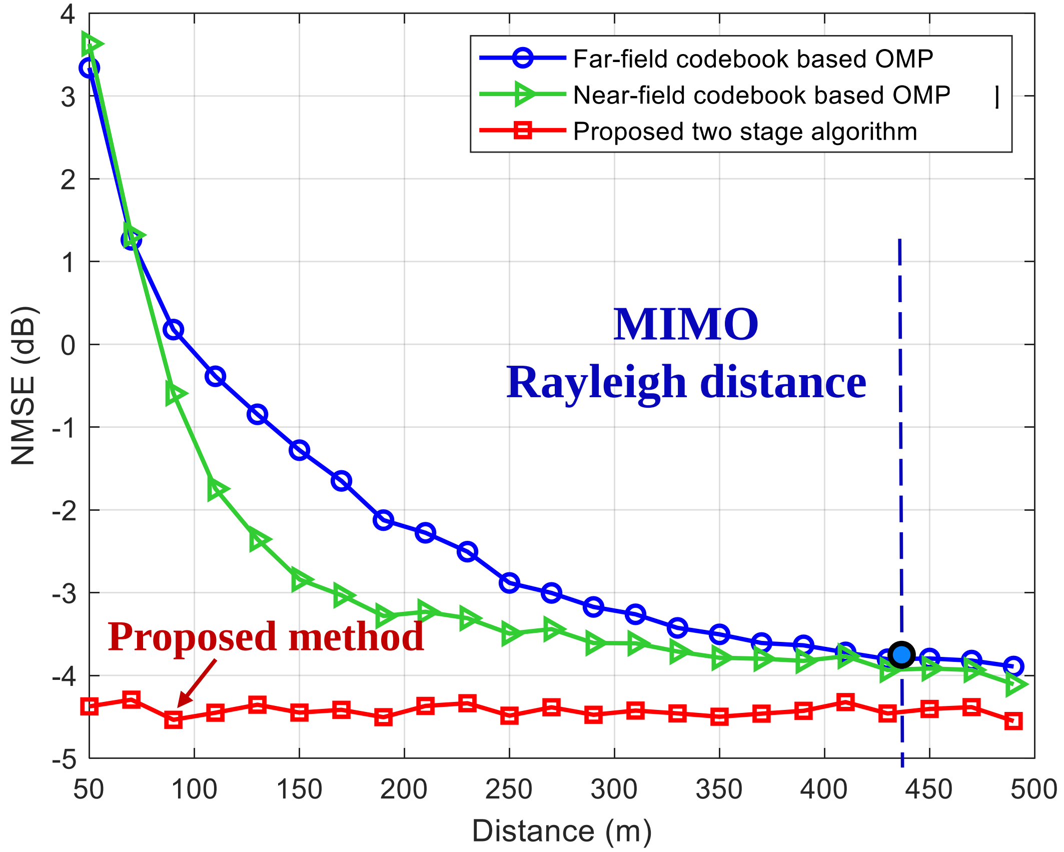

Parameters	**Value**
Carrier	**50 GHz**
Element number of transmit antenna array	**256**
Element number of transmit antenna array	**128**
Number of NLoS Paths	**5**
SNR	**5 dB**
Pilot compression ratio	**0.5**

Y. Lu and L. Dai, "Near-field channel estimation in mixed LoS/NLoS environments for extremely large-scale MIMO systems," *IEEE Trans. Commun.*, vol. 71, no. 11, pp. 7748-7760, Jun. 2023.

Outline of Part 4

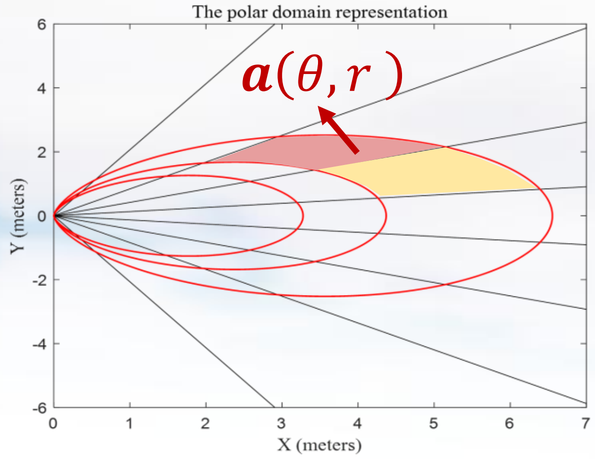

- ☐ **Near-Field Channel State Information Acquisition**
  - ➢ **Near-field MISO channel estimation**
  - ➢ **Near-field MIMO channel estimation**
  - ➢ **Near-field beam training**
- ☐ **Near-Field Beam Split**
  - ➢ **Phase-delay beam focusing**
  - ➢ **Near-field rainbow-based beam training**
  - ➢ **Distance-dependent beam split based beam training**
- ☐ **Near-field Grating Lobes Suppression**
  - ➢ **From modular ULA to modular MRA**

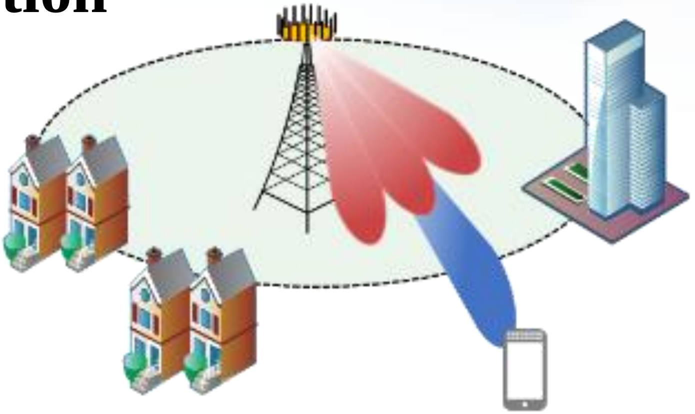

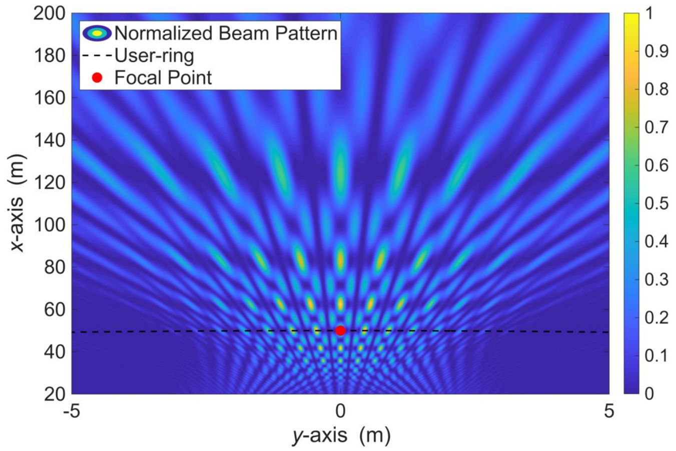

The Challenge of Near-Field Beam Training

- **Beam training is an essential method is acquire the channel state information (CSI)**
- **However, since the near-field codebook requires extra grids on the distance domain, its codebook size is much larger than that of the far-field codebook**

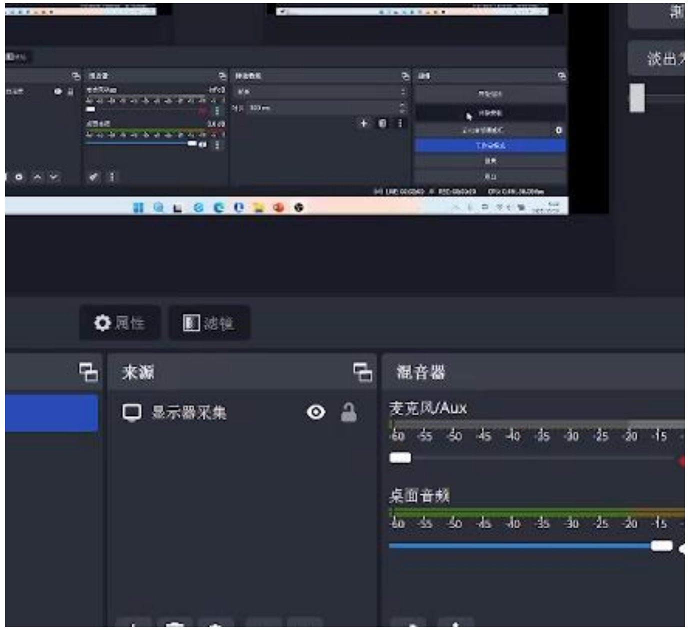

Exhaustive search

Parameters	Far-field codebook	Near-field codebook
Number of antennas	512	512
Carriers	100 GHz	100 GHz
Number of angle grids	512	512
Number of distance grids	1	20
Codebook size	512	10240

The overhead of near-field exhaustive beam training is unaffordable

Near-Field Hierarchical Beam Training

- **Low-resolution** beam covers a wider range of angle and distance, and each layer of codebook narrows the search range gradually
- Perform binary search on both angle and distance simultaneously

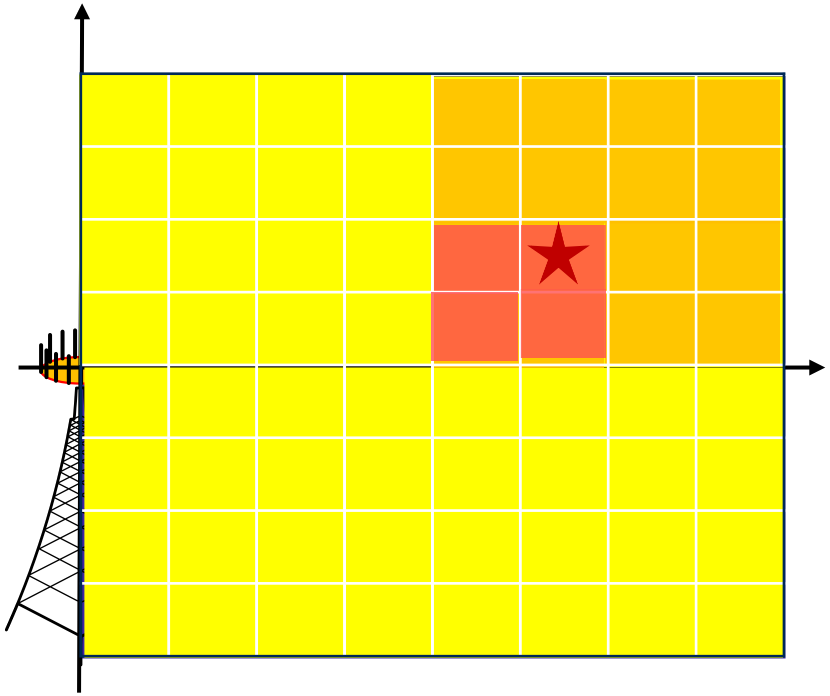

Near-Field Hierarchical Beam Training

N: number of angle grids
S: number of distance grids

Schemes	Complexity
far-field	$\mathcal{O}(NS)$
near-field	$\mathcal{O}(\log(N)+\log(S))$

Near-Field Multi-Resolution Codeword Design

- **The aim to design a codeword $\mathbf{v}$ is to approach the ideal beam pattern after beamforming with $\mathbf{v}$**

codeword needed to be designed

ideal beam pattern

$$\begin{aligned} \min_{\mathbf{v}, f(\theta,r)} \quad & \|\mathbf{A}^H \mathbf{v} - \mathbf{g}\|_2^2 \\ \text{s.t.} \quad & \|\mathbf{v}\|_2 = 1; \\ & [\mathbf{g}]_{\theta,r} = |G(\theta,r)|\, e^{jf(\theta,r)} \end{aligned}$$

$$\mathbf{A} \triangleq \sqrt{N}\left[\mathbf{a}(\theta_1, r_1), \cdots, \mathbf{a}\left(\theta_N, r_{S_N}\right)\right]$$

additional phase: increase design freedom

ideal beam pattern

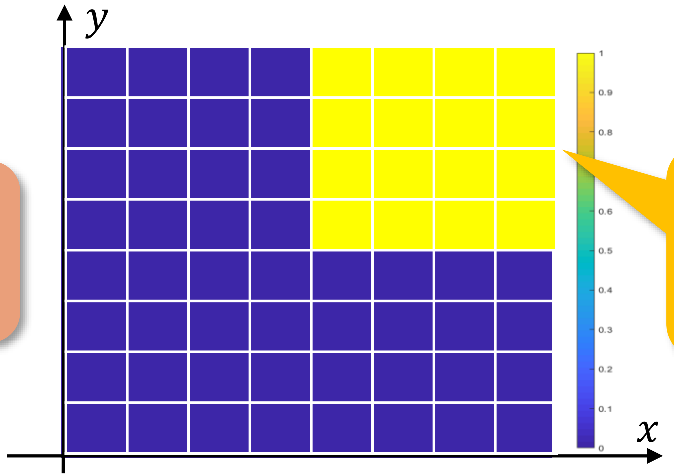

Target coverage $B_{\theta,r}$

$$|G(\theta,r)| = \begin{cases} \sqrt{C}, & (\theta,r) \in B_{\theta,r} \\ 0, & (\theta,r) \notin B_{\theta,r} \end{cases}$$

beamforming gains in target coverage are flattened

beamforming gains outside target coverage are zero

GS（Gerchberg-Saxton）Algorithm

- **Phase recovery in holographic imaging ≜ designing near-field multi-resolution codewords**

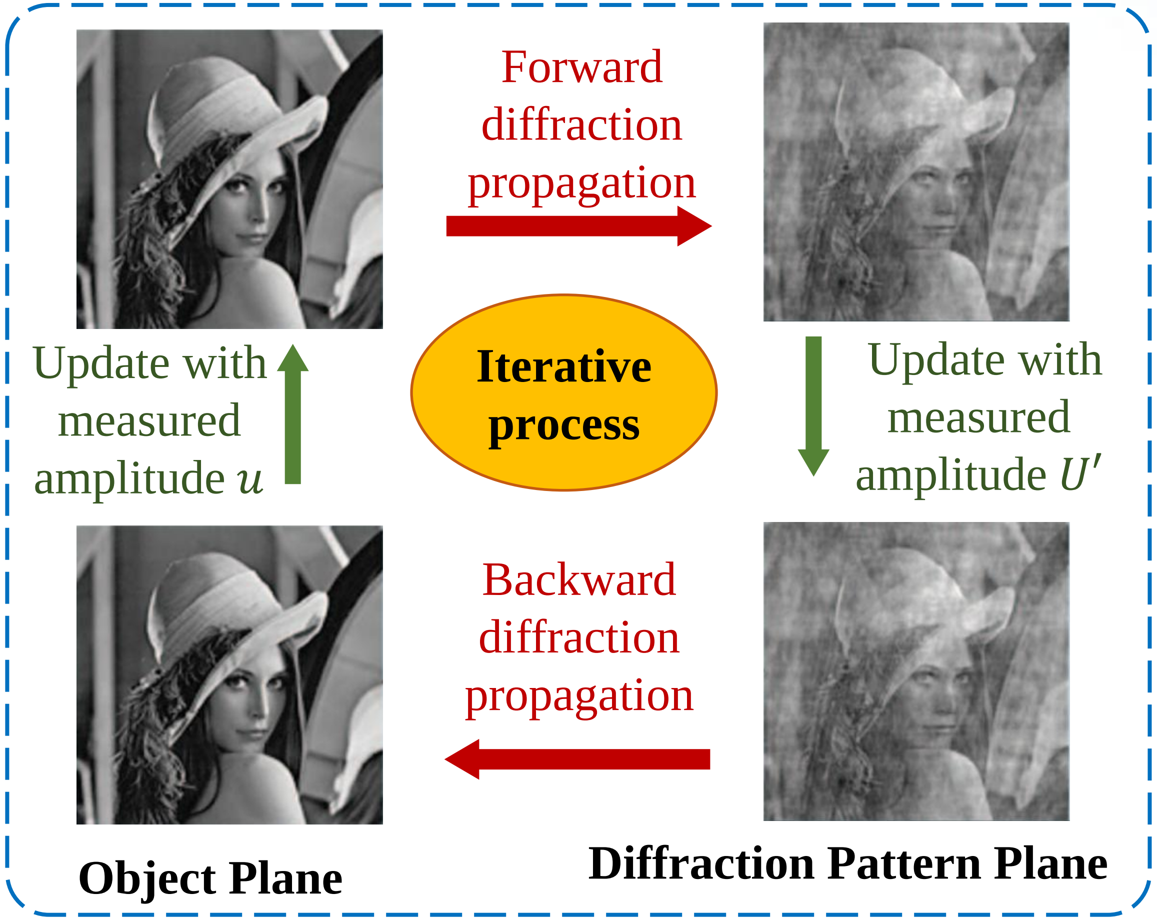

Forward diffraction propagation

Update with measured amplitude U'

Backward diffraction propagation

Update with measured amplitude u

Iterative process

Object Plane

Diffraction Pattern Plane

(a) GS algorithm in iterative phase retrieval problem.

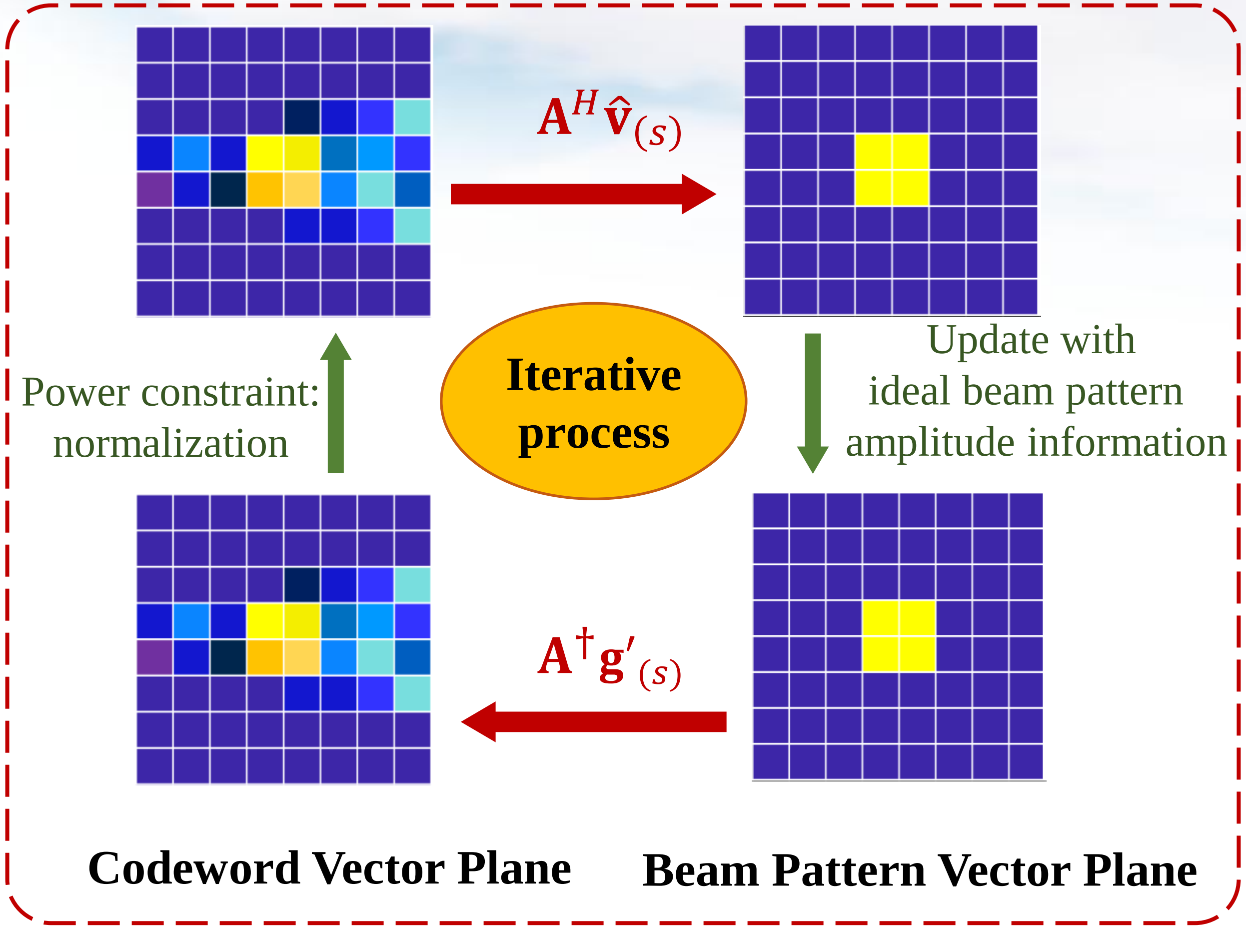

$\mathbf{A}^H\hat{\mathbf{v}}_{(s)}$

Update with ideal beam pattern amplitude information

$\mathbf{A}^{\dagger}\mathbf{g}'_{(s)}$

Power constraint: normalization

Iterative process

Codeword Vector Plane

Beam Pattern Vector Plane

(b) GS algorithm in codeword design.

Simulation Results

- **The proposed scheme provides a tradeoff between the performance and overhead**

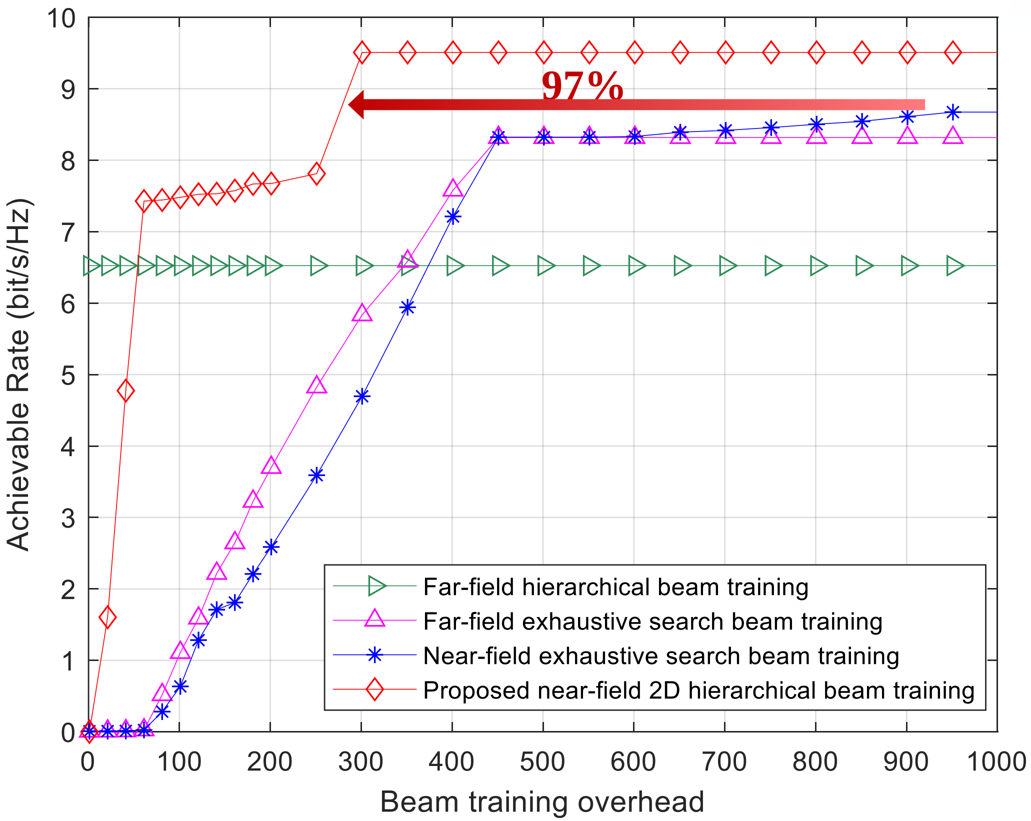

Scheme	Overhead
Near-field exhaustive search beam training	8192
Proposed near-field 2D hierarchical beam training	268

Parameters	Value
Number of antennas	512
Carrier	60GHz
Number of angle grids	512
Number of distance grids	16

Y. Lu and L. Dai, "Hierarchical beam training for extremely large-scale MIMO: from far-field to near-field ," *IEEE Trans. Commun.*, vol. 72, no. 5, pp. 3064-3078, May 2024.

Outline of Part 4

- **Near-Field Channel State Information Acquisition**
  - **Near-field MISO channel estimation**
  - **Near-field MIMO channel estimation**
  - **Near-field beam training**
- **Near-Field Beam Split**
  - **Phase-delay beam focusing**
  - **Near-field rainbow-based beam training**
  - **Distance-dependent beam split based beam training**
- **Near-field Grating Lobes Suppression**
  - **From modular ULA to modular MRA**

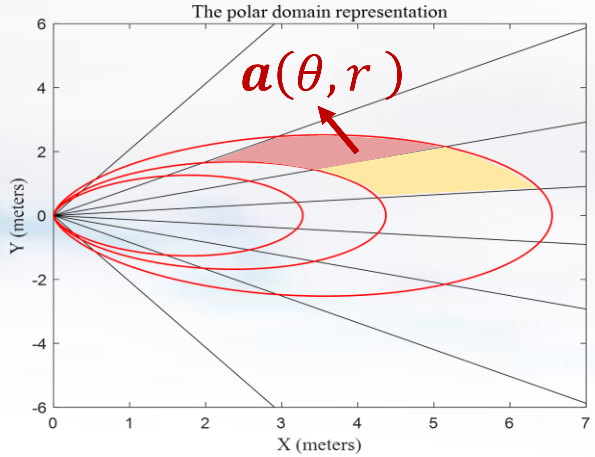

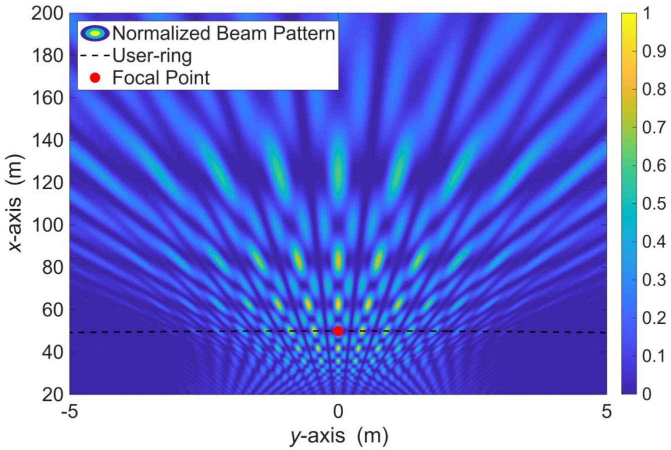

Far-Field Beam Split Effect

- **Beam split effect induced in wideband ELAA systems**
  - **For narrowband, beamforming is generally designed according to the central carrier f_c**
  - **In wideband systems, the beams at different frequencies will split towards different angles, where $f_c \sin \theta_0 = f \sin \theta$**

Prism

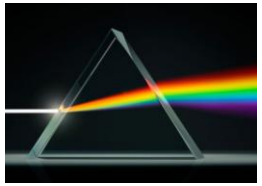

dispersion of light

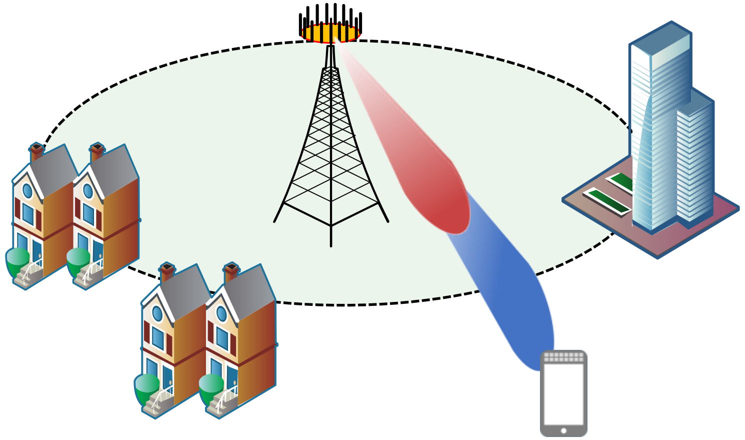

Beam squint[1] → Beam split[2]

System parameters	Beam width	Beam split	Relative split
Carrier 30 GHz, bandwidth 2 GHz, Antenna array 16×16	11.25°	3°	26%
Carrier 30 GHz, bandwidth 2 GHz, Antenna array 60×60	3°	3°	100%
Carrier 100 GHz, bandwidth 20 GHz, antenna array 16×16	11.25°	9°	80%
Carrier 100 GHz, bandwidth 20 GHz, antenna array 60×60	3°	9°	300%

ELAA introduces a severe beam split effect in far field

[1] X. Gao, L. Dai, S. Zhou, A. Sayeed, and L. Hanzo, "Beamspace channel estimation for wideband millimeter-wave MIMO with lens antenna array," in *Proc. IEEE Int. Conf. Commun. (IEEE ICC'18)*, Kansas, US, May 2018. (**IEEE ICC 2018 Best Paper Award**)

[2] L. Dai, J. Tan, Z. Chen, and H. Vincent Poor, "Delay-phase precoding for wideband THz massive MIMO," *IEEE Trans. Wireless Commun.* vol. 21, no. 9, pp. 7271-7286, Sep. 2022.

Near-Field Beam Split Effect

- In the near-field region, the near-field beam split effect induces the beams at different frequencies will split towards different locations

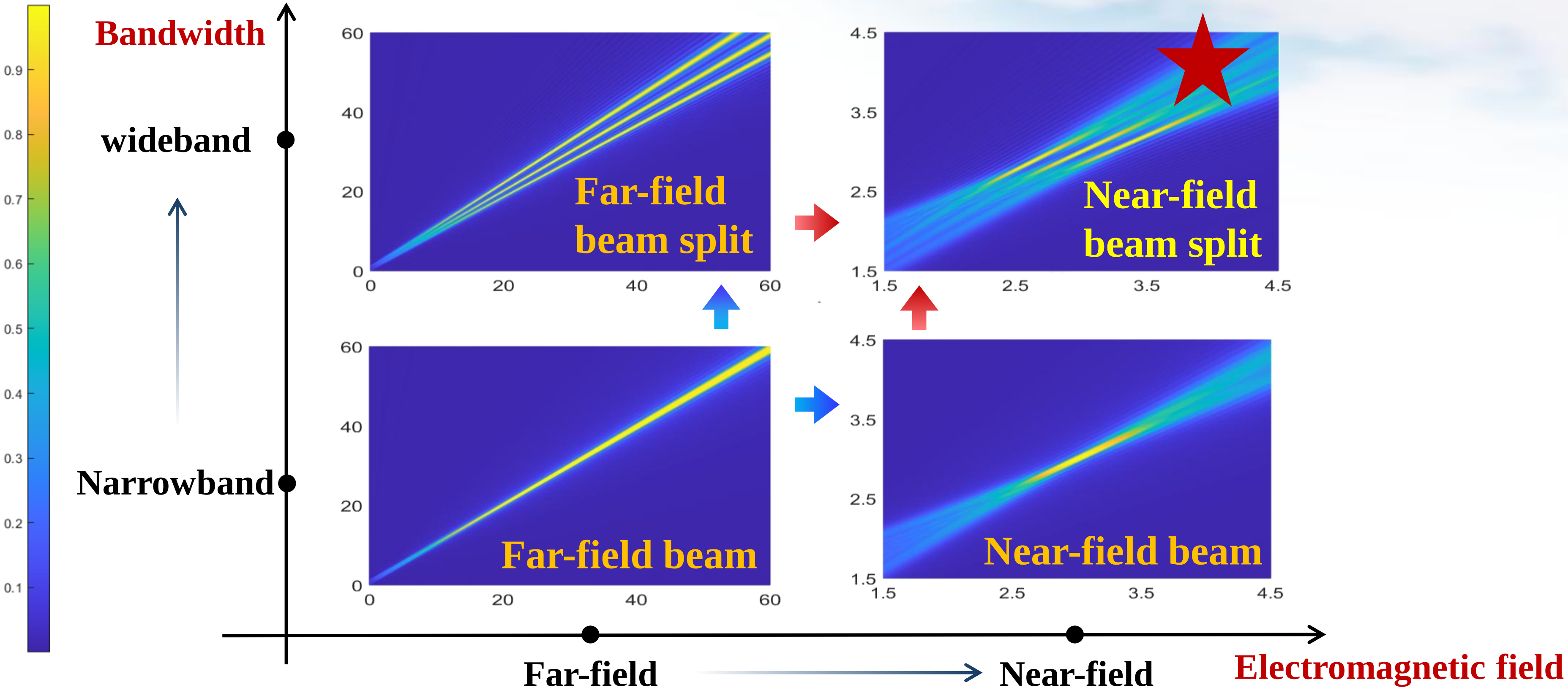

The near-field beam split effect has not been well studied

Challenge in Near-field Wideband Systems

- **Existing transmission technologies suffer from a severe performance loss in near-field wideband systems due to the near-field beam split effect**

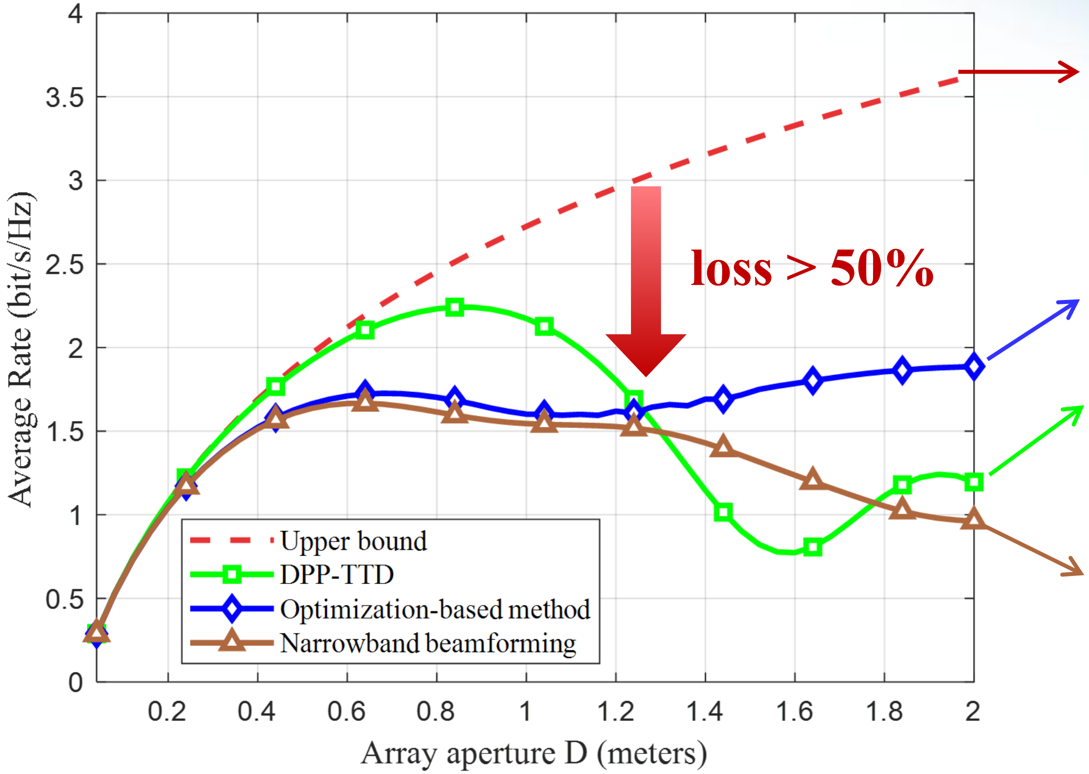

Upper bound

Near-field narrowband method[1]

Far-field wideband method[2]

Far-field narrowband method[3]

[1] N. J. Myers and R. W. Heath, "InFocus: A spatial coding technique to mitigate misfocus in near-field LoS beamforming," *IEEE Trans. Wireless Commun.*, vol. 21, no. 4, pp. 2193-2209, Apr, 2022.

[2] X. Yu, J. Shen, J. Zhang, and K. B. Letaief, "Alternating minimization algorithms for hybrid precoding in millimeter wave MIMO systems," *IEEE J. Sel. Topics Signal Process.*, vol. 10, no. 3, pp. 485-500, Mar. 2016.

[3] L. Dai, J. Tan, Z. Chen, and H. Vincent Poor, "Delay-phase precoding for wideband THz massive MIMO," *IEEE Trans. Wireless Commun.* vol. 21, no. 9, pp. 7271-7286, Sep. 2022.

Phase-Delay Focusing (PDF)

- **The partitioned-far-field approximation of the near-field channel**
  - ➢ **The entire large array is partitioned into Q small sub-arrays**

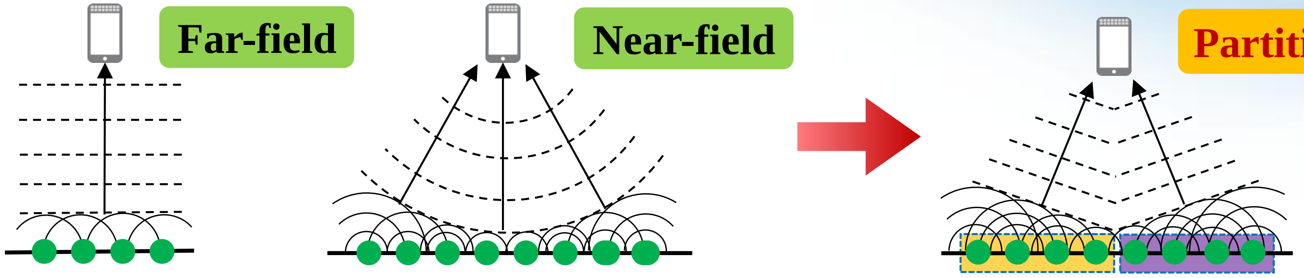

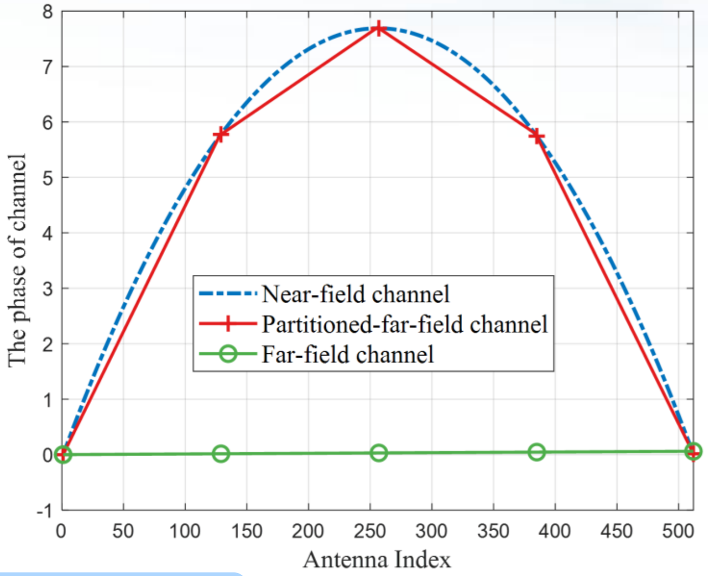

  - ➢ **The user is located in the far-field region of each small subarray**
    - **For the p-th antenna of the q-th subarray**

Distance: $$r_q^{(p)} \approx r_q + pd\theta_q$$

Phase: $$\phi_q^{(p)} = \frac{2\pi}{\lambda} r_q^{(p)} = \boxed{\frac{2\pi}{\lambda} r_q} + \boxed{\frac{2\pi}{\lambda} pd\theta_q}$$

Subarray-wise near-field phase

Antenna-wise far-field phase

The complicated near-field channel is decoupled to multiple far-field channels across different subarrays

Phase-Delay Focusing (PDF)

- A **very large phase-shift network** to compensate the antenna-wise phase
- A **small time-delay layer** to compensate the subarray-wise phase

$$\phi_q^{(p)} = \boxed{\frac{2\pi}{\lambda} r_q} + \boxed{\frac{2\pi}{\lambda} p d \theta_q}$$

Subarray-wise phase variation

Compensated by **time-delay**

Antenna-wise phase variation

Compensated by **phase-shift**

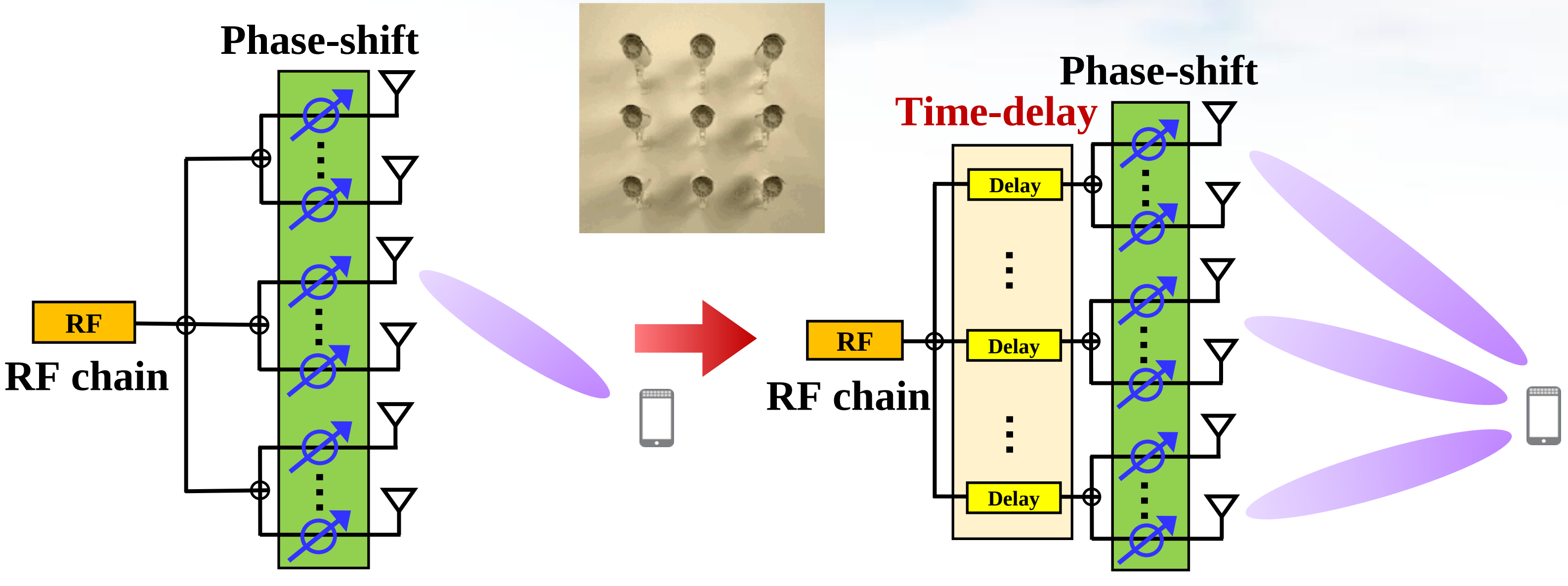

（a） Beamsteering

（b） Phase-delay focusing

Overcome the near-field beam split effect with much reduced time-delay elements

Simulation Results (1)

- **Achievable average rate vs. distance**
  - ➢ **Near-optimal average rate is realized**

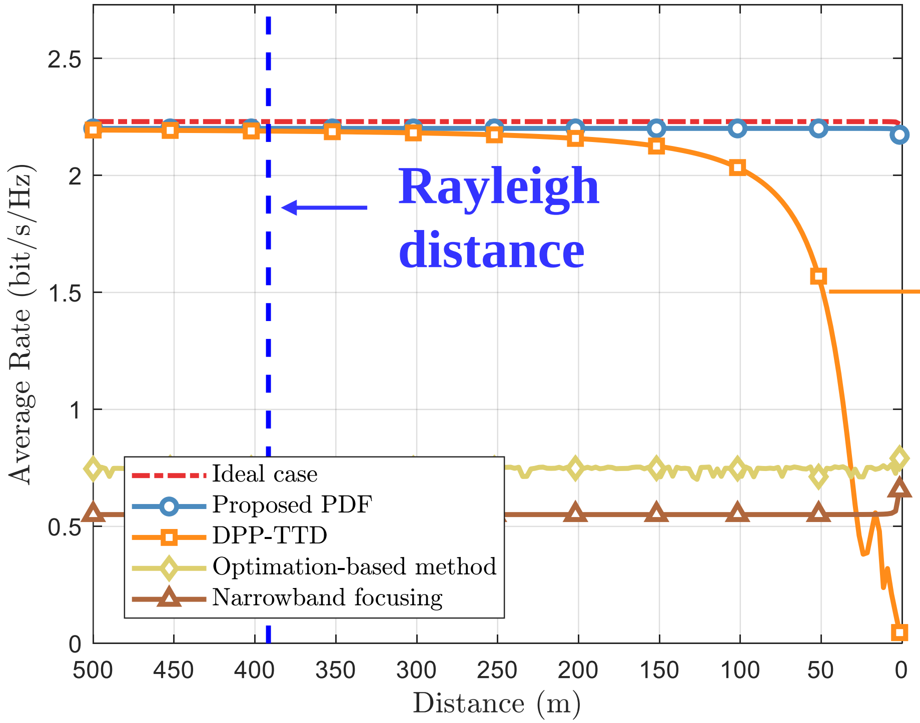

Rayleigh distance

→ **Proposed method**

→ **Far-field method**

Parameters	Values
Carrier	100 GHz
Bandwidth	5 GHz
Number of subcarriers	1024
Number of antennas	512
Rayleigh distance	400 meters
SNR	20 dB

An unusual discovery: Rayleigh distance overestimates the near-field range

M. Cui and L. Dai, "Near-field wideband beamforming for extremely large antenna array," *IEEE Trans. Wireless Commun.*, vol. 23, no. 10, pp. 13110-13124, Oct. 2024.

Outline of Part 4

- ☐ **Near-Field Channel State Information Acquisition**
  - ➢ **Near-field MISO channel estimation**
  - ➢ **Near-field MIMO channel estimation**
  - ➢ **Near-field beam training**
- ☐ **Near-Field Beam Split**
  - ➢ **Phase-delay beam focusing**
  - ➢ **Near-field rainbow-based beam training**
  - ➢ **Distance-dependent beam split based beam training**
- ☐ **Near-field Grating Lobes Suppression**
  - ➢ **From modular ULA to modular MRA**

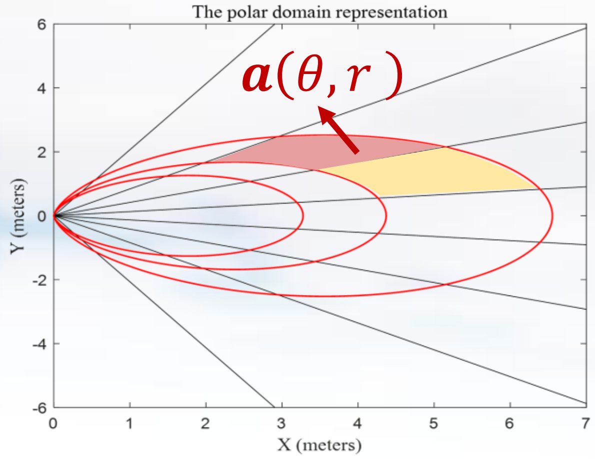

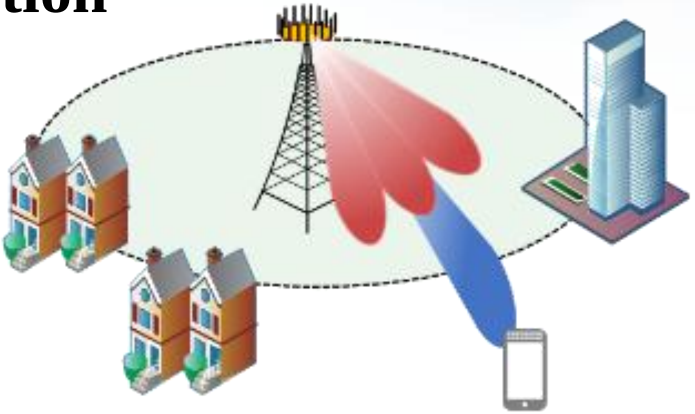

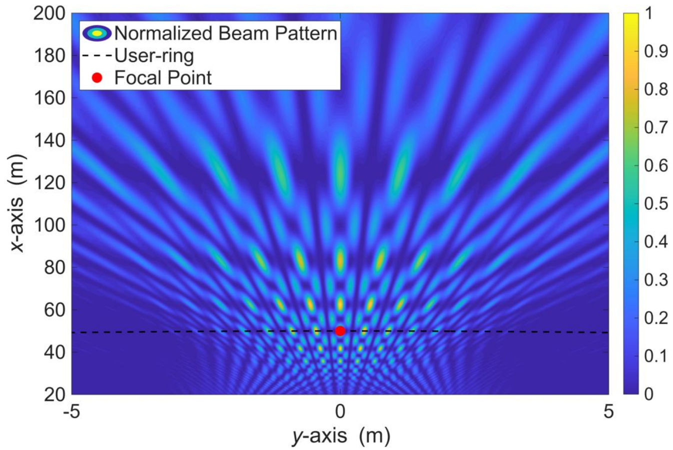

The Challenge of Near-Field Beam Training

- **Beam training is an essential method is acquire the channel state information (CSI)**
- **However, since the near-field codebook requires extra grids on the distance domain, its codebook size is much larger than that of the far-field codebook**

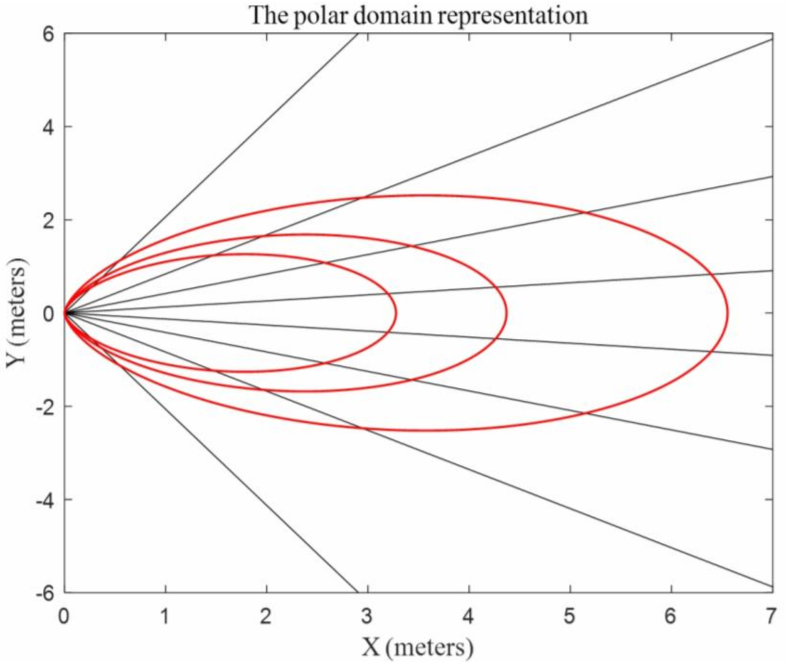

Exhaustive search

Parameters	Far-field codebook	Near-field codebook
Number of antennas	512	512
Carriers	100 GHz	100 GHz
Number of angle grids	512	512
Number of distance grids	1	20
Codebook size	512	10240

The overhead of near-field exhaustive beam training is unaffordable

Near-field Rainbow based Beam Training

- **Time-delay circuits are able to control the degree of the near-field beam split effect**
  - **The optimal distance is searched in a time division manner**
  - **The optimal angle is searched in a frequency division manner**

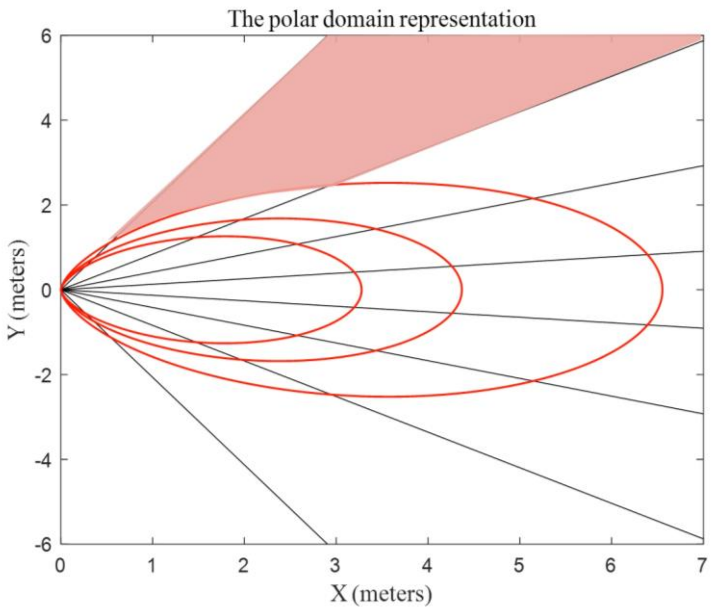

Exhaustive search

Prism

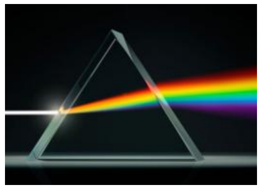

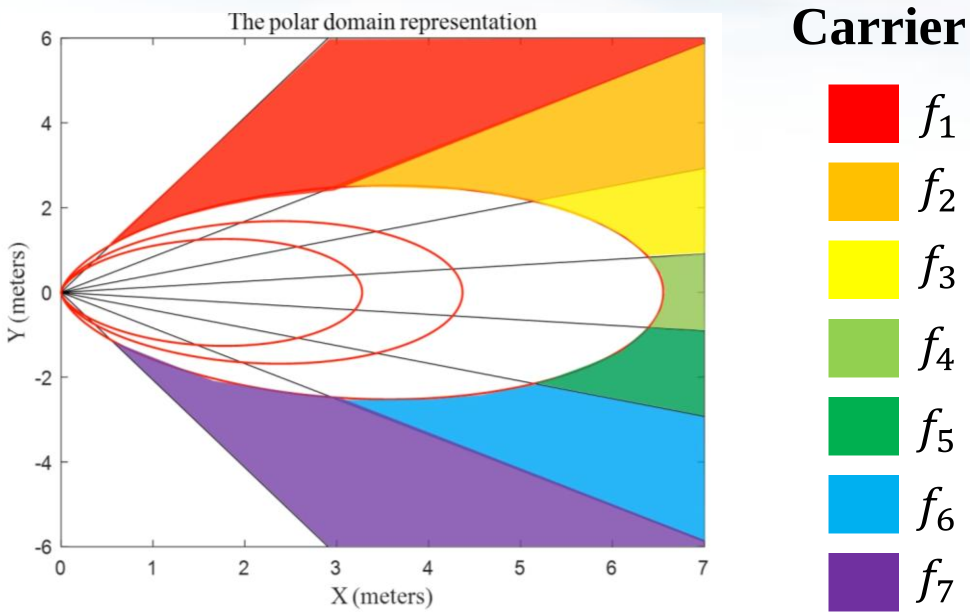

Near-field rainbow based search

The pilot overhead is determined by the search of distance

Simulation Results

- **The proposed scheme is able to achieve the near-optimal average rate performance with a very low training overhead**

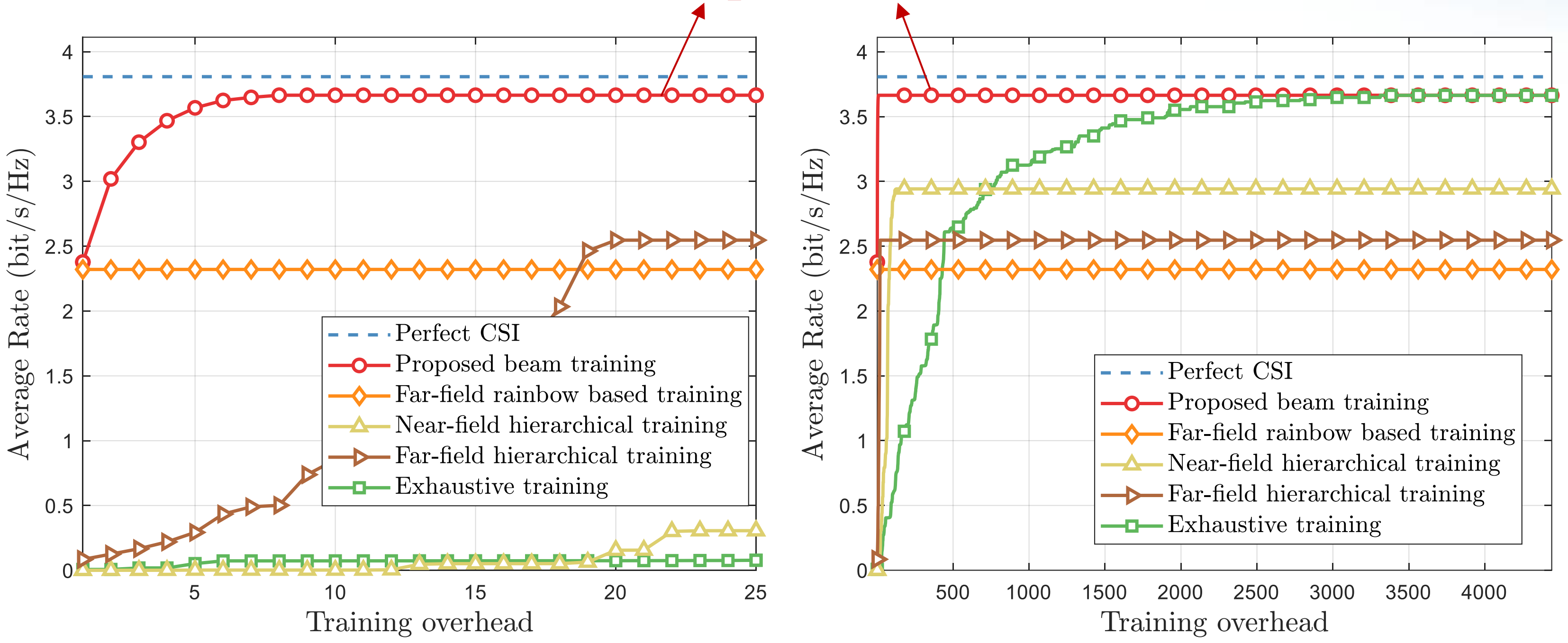

Parameter	Value
Carrier	60 GHz
Bandwidth	3 GHz
Subcarrier number	4096
Antenna number	256
SNR	20 dB
Distance	$U(3\text{ m},\ 40\text{ m})$
Angle	$U(-\sin\frac{\pi}{3},\sin\frac{\pi}{3})$

M. Cui, L. Dai, Z. Wang, S. Zhou, and N. Ge, "Near-field rainbow: Wideband beam training for XL-MIMO," *IEEE Trans. Wireless Commun.*, vol. 22, no. 6, pp. 3899-3912, Jun. 2023.

Outline of Part 4

- ☐ **Near-Field Channel State Information Acquisition**
  - ➢ **Near-field MISO channel estimation**
  - ➢ **Near-field MIMO channel estimation**
  - ➢ **Near-field beam training**
- ☐ **Near-Field Beam Split**
  - ➢ **Phase-delay beam focusing**
  - ➢ **Near-field rainbow-based beam training**
  - ➢ **Distance-dependent beam split based beam training**
- ☐ **Near-field Grating Lobes Suppression**
  - ➢ **From modular ULA to modular MRA**

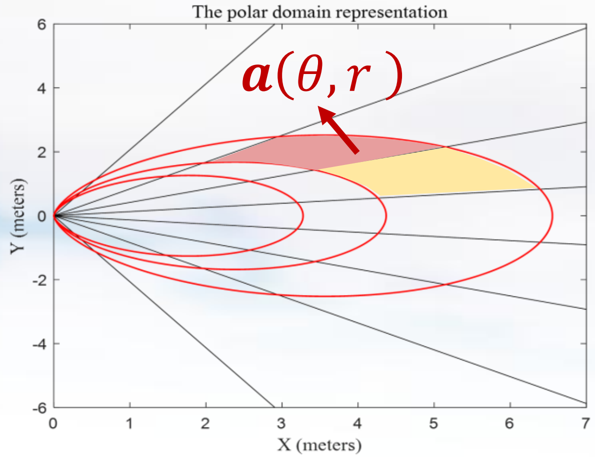

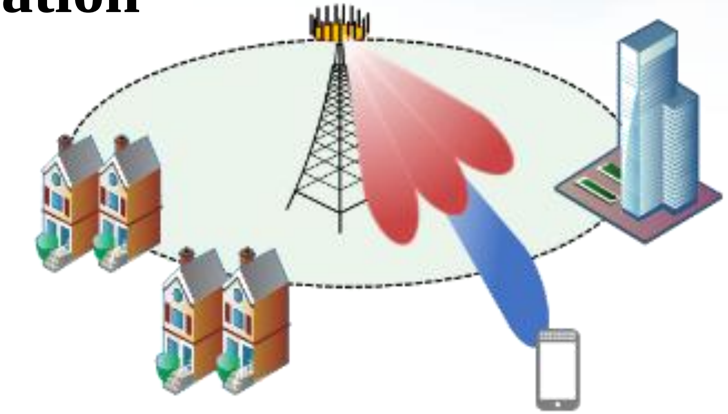

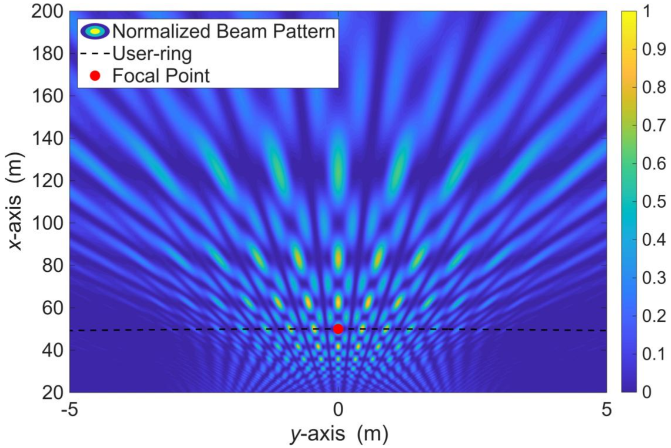

Limitations of Near-Field Rainbow

- **Beam split in near-field rainbow is essentially distance-independent beam split, which only involves beam split in angle domain**
- **The optimal distance is obtained by sequentially testing different distance rings**

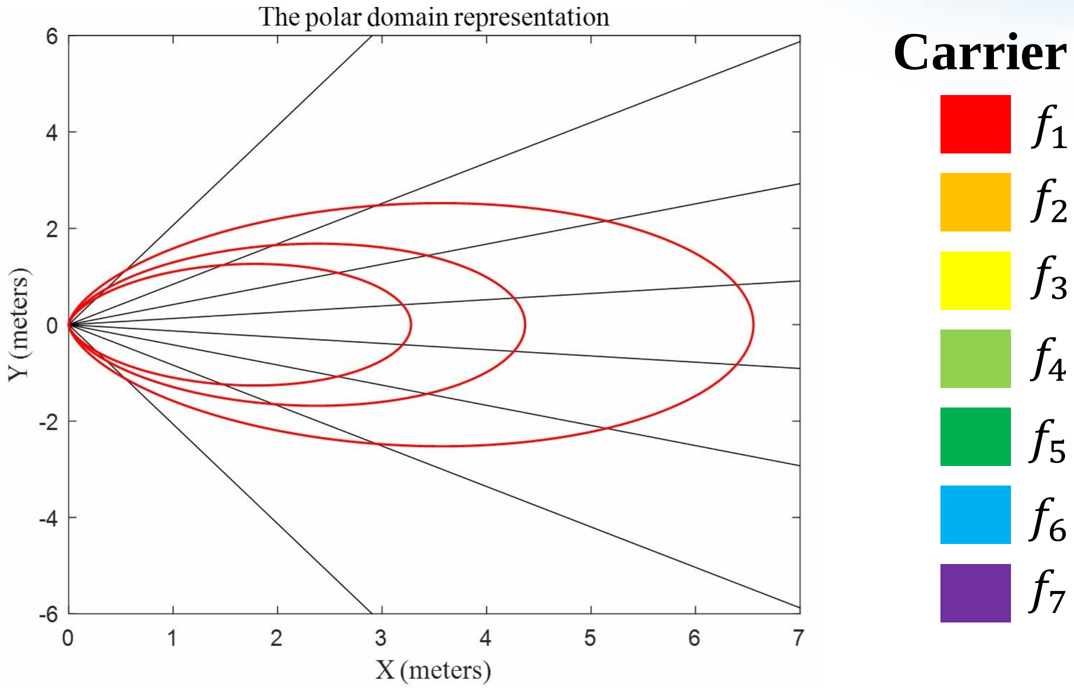

Can we design distance-dependent beam split to simultaneously search angles and distances

Distance-Dependent Beam Split Based Beam Training

- **Spread the focused points of beams on different angles of multi-distance-rings**
  - **The focused direction of the multi-frequency beams fluctuate periodically between the angular range while the focused distance ring increases monotonically with the frequency**
  - **Both different angles and distances can be search with a single pilot simultaneously in one time slot**

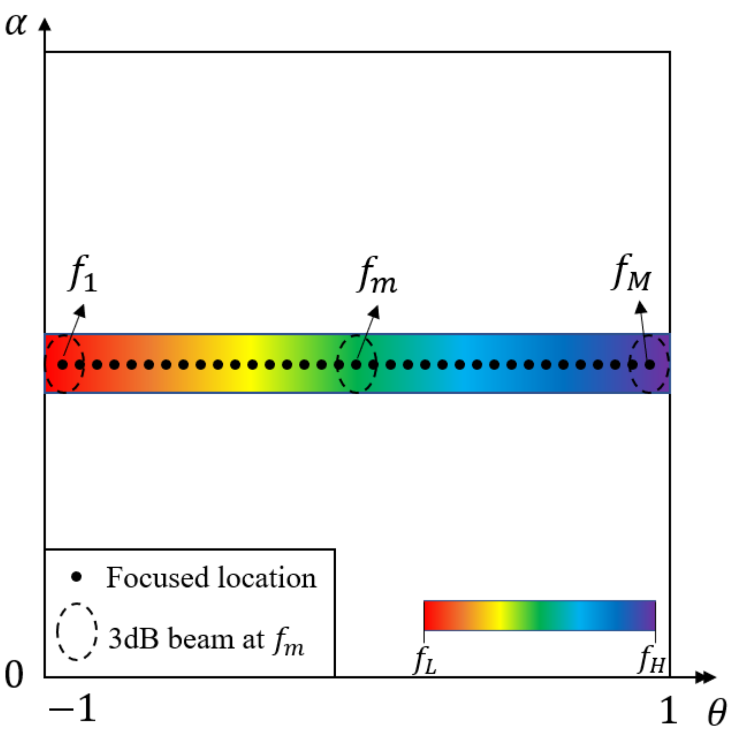

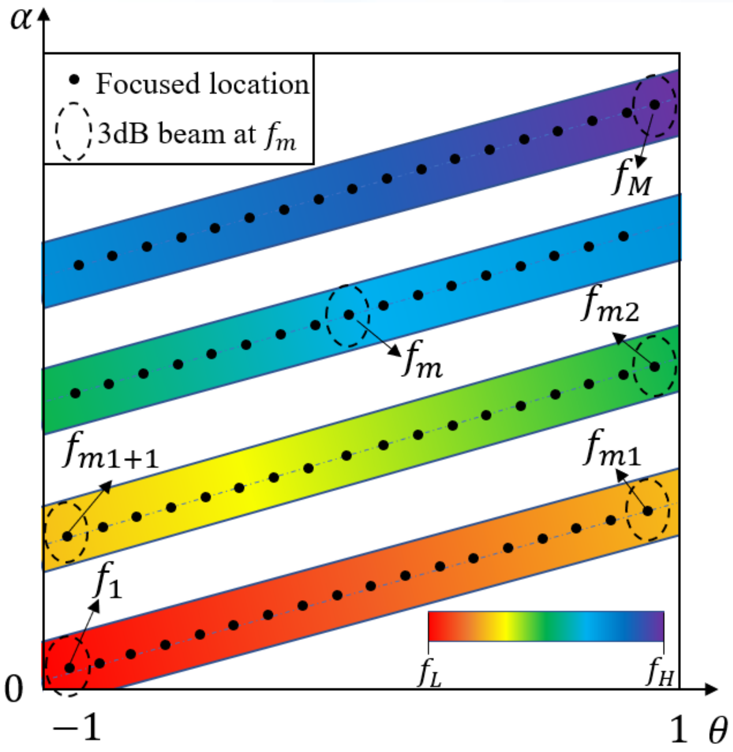

T. Zheng and L. Dai, "Near-field beam training based on distance-dependent beam split for XL-MIMO," submitted to *IEEE Trans. Wireless Commun.*, 2024.

Simulation Results

- **The proposed scheme can achieve the near-optimal average rate performance with extremely low training overhead (only 3 pilots)**

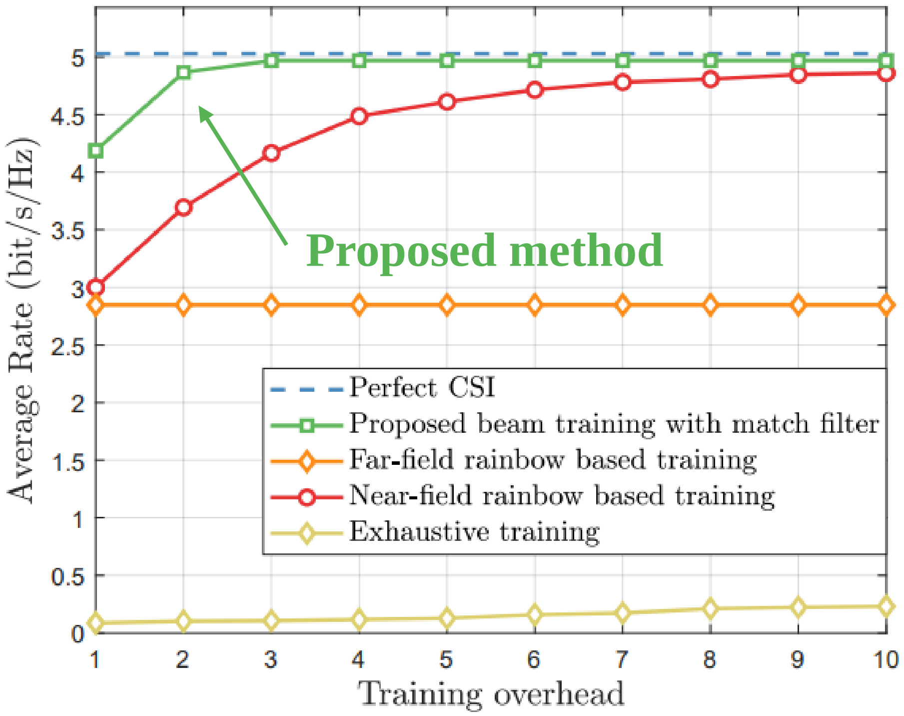

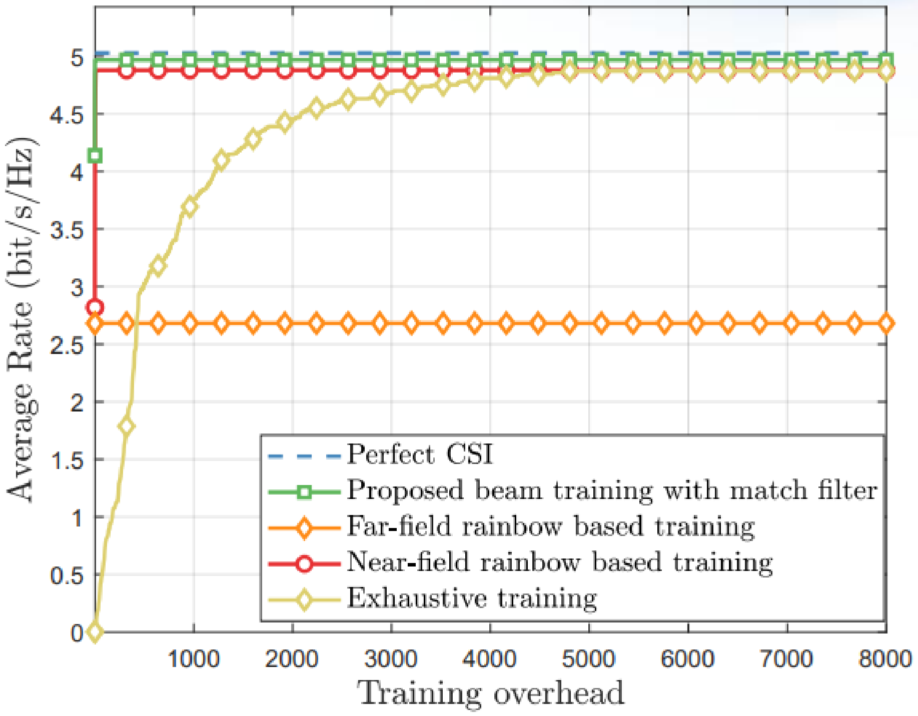

Parameter	**Value**
Carrier	**30 GHz**
Bandwidth	**3 GHz**
Subcarrier number	**1024**
Antenna number	**256**
Distance	**[5m,200m]**
Angle	$U(-\sin\frac{\pi}{3},\sin\frac{\pi}{3})$
SNR	**15 dB**

T. Zheng and L. Dai, “Near-field beam training based on distance-dependent beam split for XL-MIMO,” *IEEE Trans. Wireless Commun*., vol. 24, no. 2, pp. 1278-1292, Feb. 2025..

Outline of Part 4

- ☐ **Near-Field Channel State Information Acquisition**
  - ➢ **Near-field MISO channel estimation**
  - ➢ **Near-field MIMO channel estimation**
  - ➢ **Near-field beam training**
- ☐ **Near-Field Beam Split**
  - ➢ **Phase-delay beam focusing**
  - ➢ **Near-field rainbow-based beam training**
  - ➢ **Distance-dependent beam split based beam training**
- ☐ **Near-field Grating Lobes Suppression**
  - ➢ **From modular ULA to modular URA**

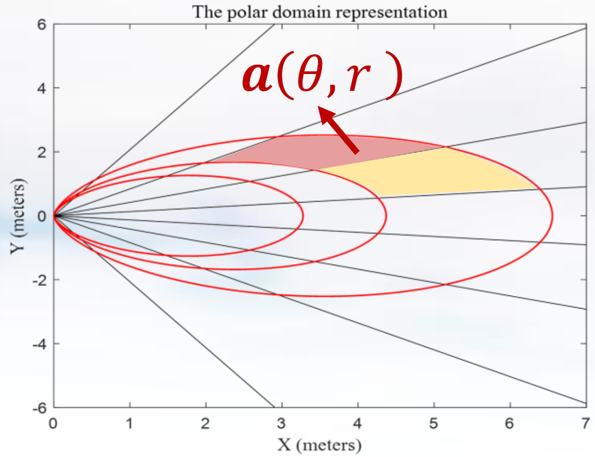

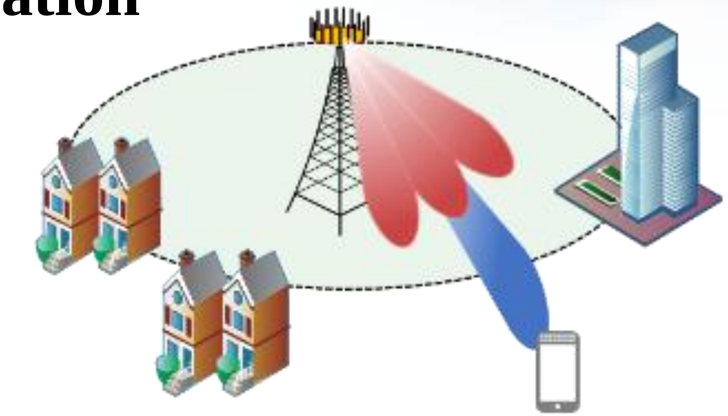

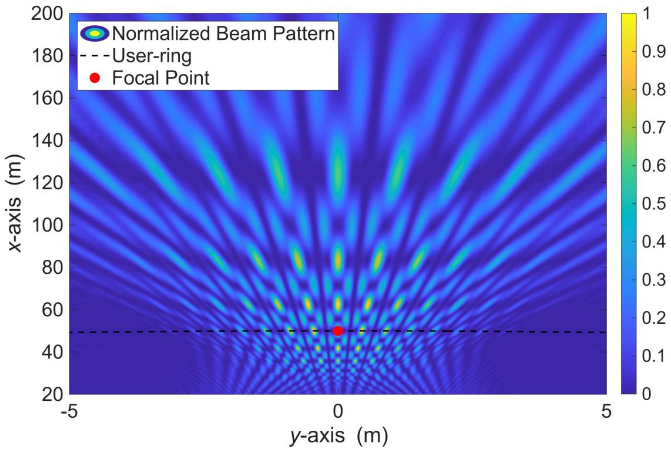

Quasi-Distributed Array

- **As a compromise between the collocated and distributed arrays, the quasi-distributed array spatially separates multiple antenna panels or subarrays within one base station.**
- **Extending the near-field range while retaining the benefits of centralized baseband processing.**

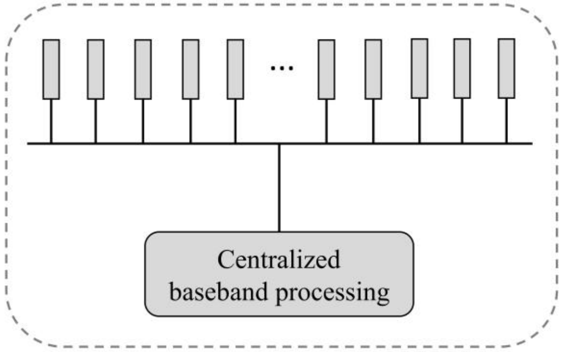

Collocated Array

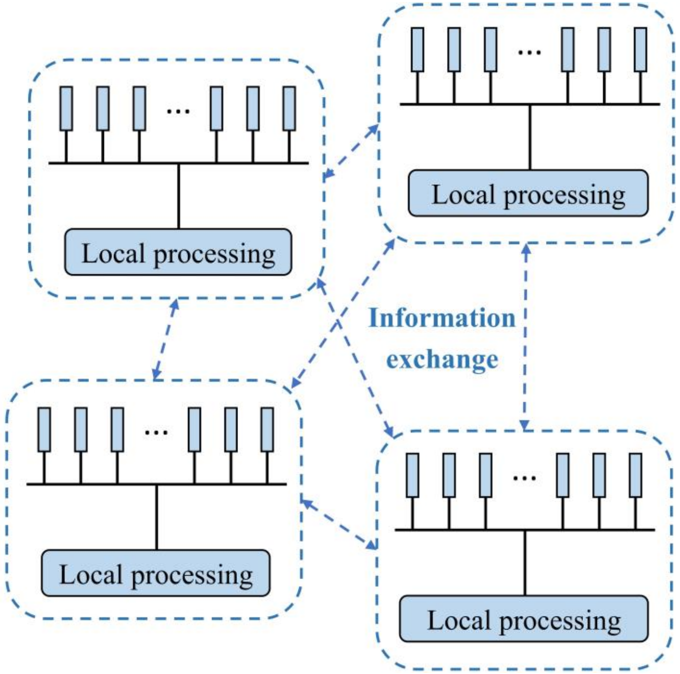

Distributed Array

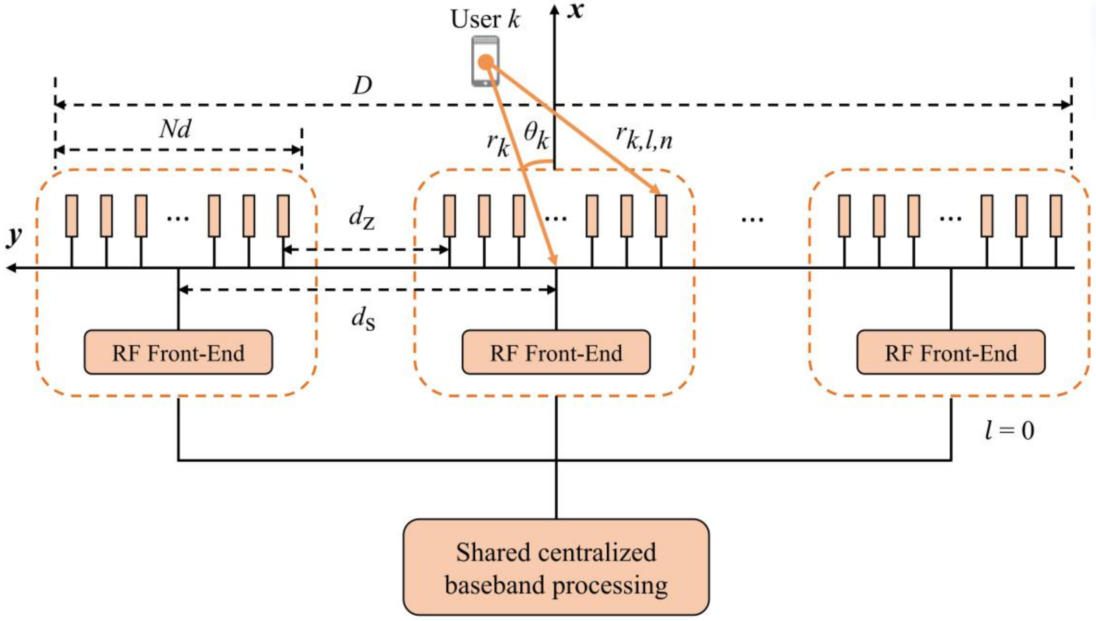

Modular array

(one of the typical implementation forms of quasi-distributed arrays)

M. Zhou, Z. Xu, and **L. Dai**, "Near-field communications with grating lobes for quasi-distributed arrays: From ULA to MRA," *arxiv:2607.29341*, Jul. 2026.

Challenge of Suppressing Grating Lobes For Modular Arrays

- **Existing software-based methods for grating lobe suppression rely on full CSI and fail in general non-static scenarios [1].**
- **Existing hardware-based methods suppress grating lobes by changing the position of each module [2], [3]. Thus, their suppression effect is almost negligible when the number of modules is limited, which is a practical scenario defined by 3GPP.**

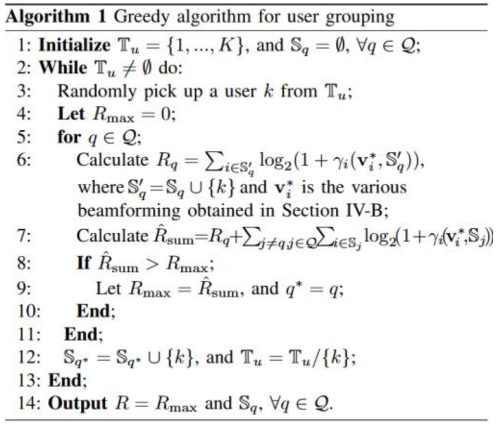

Algorithm 1 Greedy algorithm for user grouping

```
Initialize $\mathbb{T}_u = \{1, ..., K\}$, and $\mathbb{S}_q = \emptyset, \forall q \in \mathcal{Q}$;
While $\mathbb{T}_u \neq \emptyset$ do:
    Randomly pick up a user $k$ from $\mathbb{T}_u$;
    Let $R_{\max} = 0$;
    for $q \in \mathcal{Q}$;
        Calculate $R_q = \sum_{i \in \mathbb{S}'_q} \log_2(1 + \gamma_i(\mathbf{v}_i^*, \mathbb{S}'_q))$,
        where $\mathbb{S}'_q = \mathbb{S}_q \cup \{k\}$ and $\mathbf{v}_i^*$ is the various
        beamforming obtained in Section IV-B;
        Calculate $\hat{R}_{\text{sum}} = R_q + \sum_{j \neq q, j \in \mathcal{Q}} \sum_{i \in \mathbb{S}_j} \log_2(1 + \gamma_i(\mathbf{v}_i^*, \mathbb{S}_j))$
        If $\hat{R}_{\text{sum}} > R_{\max}$;
            Let $R_{\max} = \hat{R}_{\text{sum}}$, and $q^* = q$;
        End;
    End;
    $\mathbb{S}_{q^*} = \mathbb{S}_{q^*} \cup \{k\}$, and $\mathbb{T}_u = \mathbb{T}_u / \{k\}$;
End;
Output $R = R_{\max}$ and $\mathbb{S}_q, \forall q \in \mathcal{Q}$.
```

User-grouping algorithm [1]

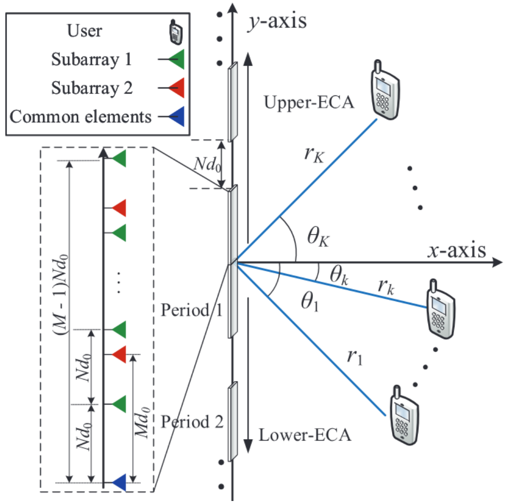

Extended coprime array [2]

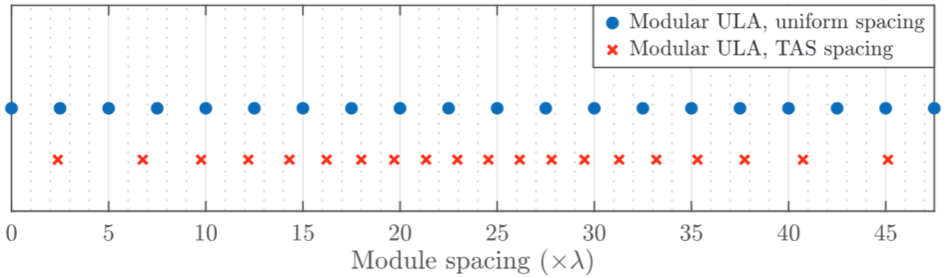

Tapered aperture sampling [3]
(nonuniform distribution)

[1] X. Li, Z. Dong, Y. Zeng, S. Jin and R. Zhang, "Multi-user modular XL-MIMO communications: Near-field beam focusing pattern and user grouping," *IEEE Transactions on Wireless Communications*., vol. 23, no. 10, pp. 13766-13781, Oct. 2024.

[2] C. Zhou, C. You, H. Zhang, L. Chen, and S. Shi, "Sparse array enabled near-field communications: Beam pattern analysis and hybrid beamforming design," *IEEE Trans. Wireless Commun*., vol. 24, no. 12, pp. 10261–10277, Dec. 2025.

[3] M. Parvini, B. Banerjee, M. Q. Khan, et al, "Angular spectrum shaping in modular XL-arrays via tapered aperture sampling," *IEEE Wireless Communications Letters*., vol. 15, pp.2070-2074, Mar. 2026.

Analysis of Near-Field Grating Lobe Location

- Contrary to the common belief that grating lobes only exist in the angle domain, we reveal that **near-field grating lobes may also occur in the distance domain**.

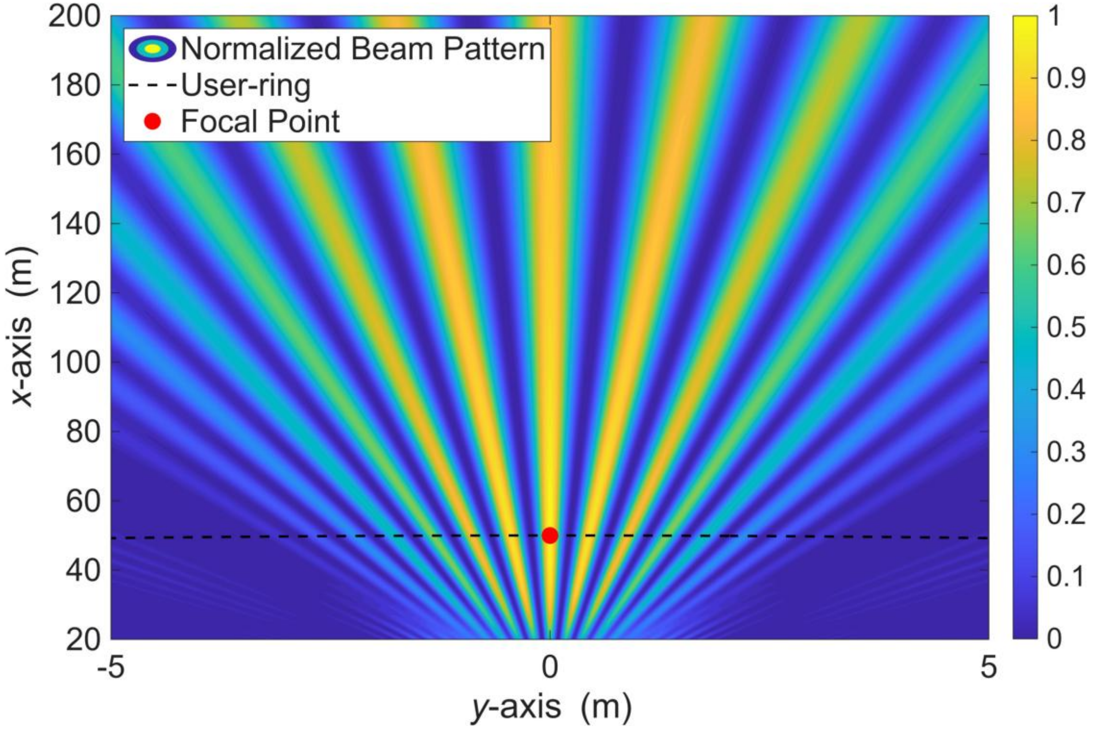

Modular uniform linear array (M-ULA) with 2 subarrays

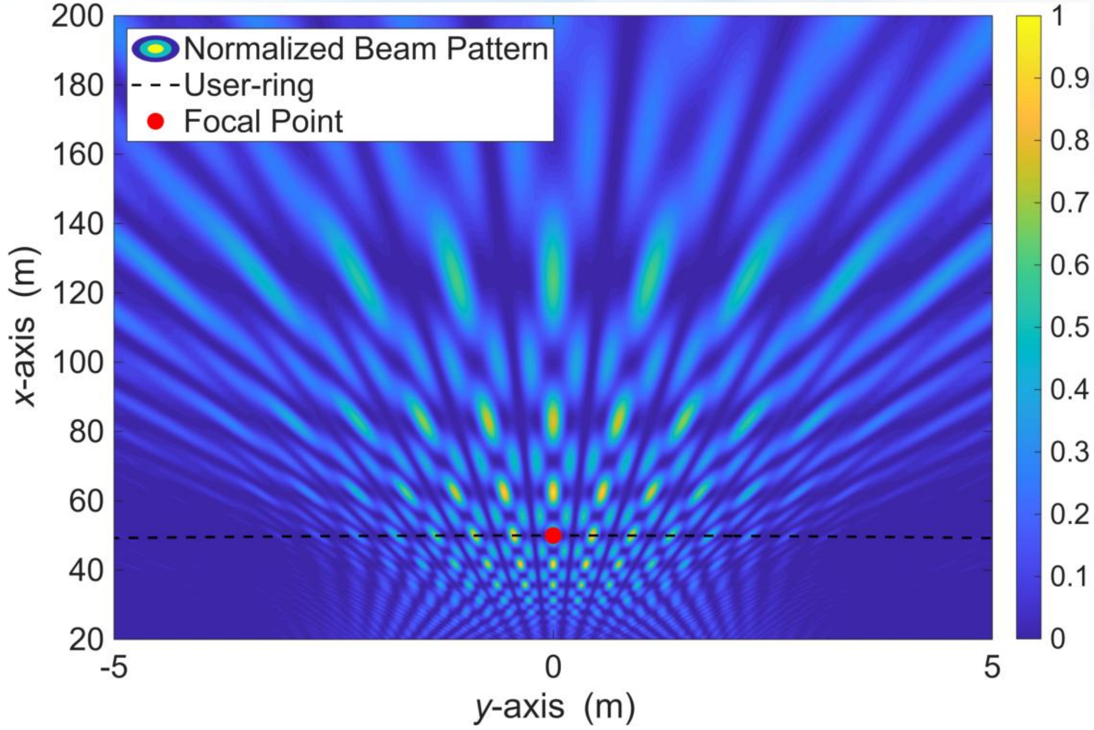

M-ULA with 4 subarrays

M. Zhou, Z. Xu, and **L. Dai**, "Near-field communications with grating lobes for quasi-distributed arrays: From ULA to MRA," *arxiv:2607.29341*, Jul. 2026.

Near-Field Grating Lobe Suppression for M-ULA

- **The envelope of array gain is mainly determined by the subarray structure, which inspires us to redesign the subarray structure to suppress near-field grating lobes.**

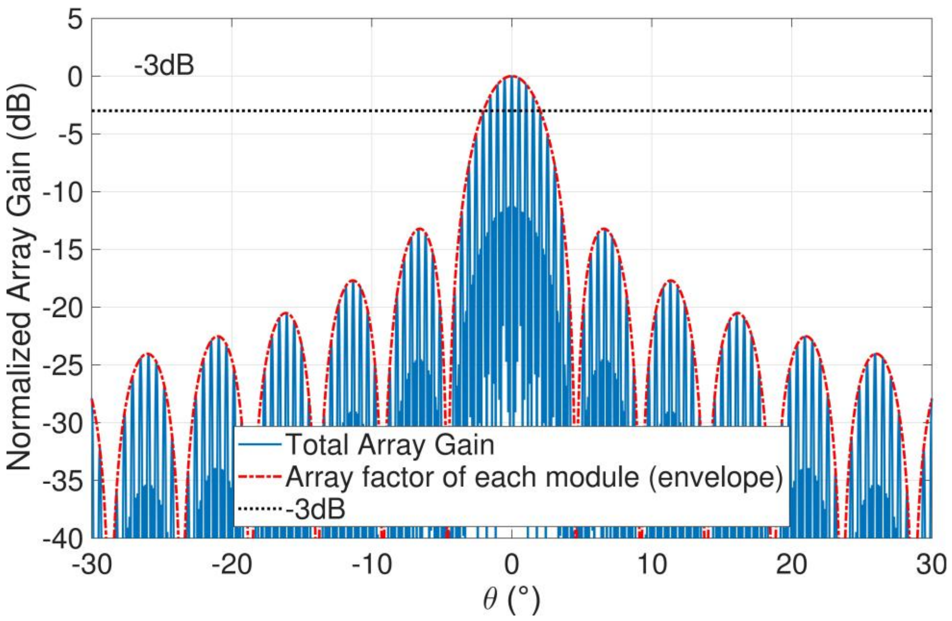

Increasing the number of antennas within each subarray (*N*)

can make the envelope narrower

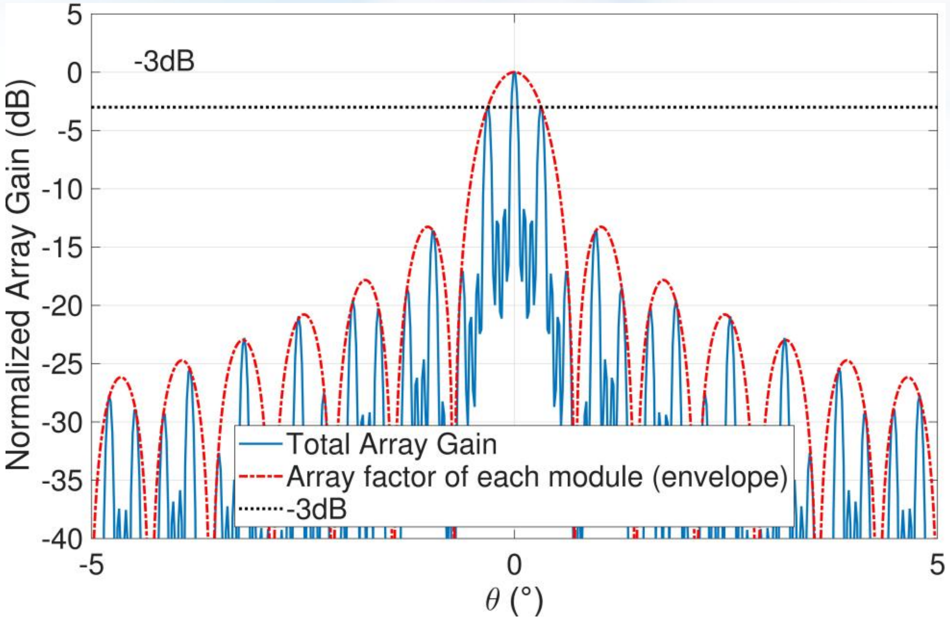

How to suppress near-field grating lobes without the limitation on the number of antennas?

M. Zhou, Z. Xu, and **L. Dai**, "Near-field communications with grating lobes for quasi-distributed arrays: From ULA to MRA," *arxiv:2607.29341*, Jul. 2026.

Proposed M-MRA

- **Minimum-redundancy array (MRA) provides narrower envelope under the same *N*.**
- **By utilizing the narrow envelope characteristic and combining it with modular arrays, we propose the Modular MRA (M-MRA) to suppress near-field grating lobes.**

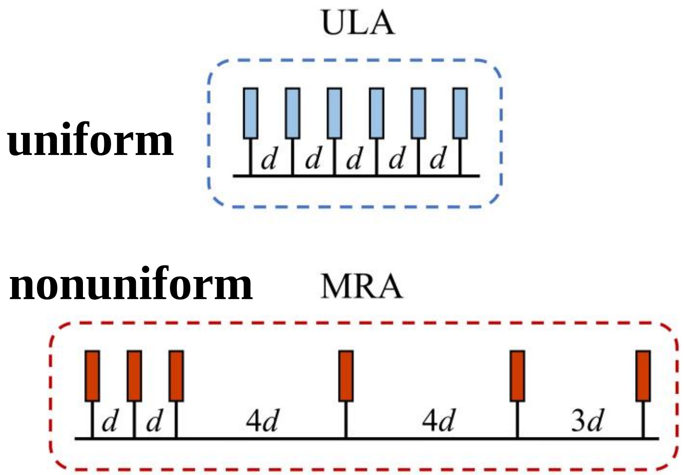

Subarray structure comparison ($N = 6$)

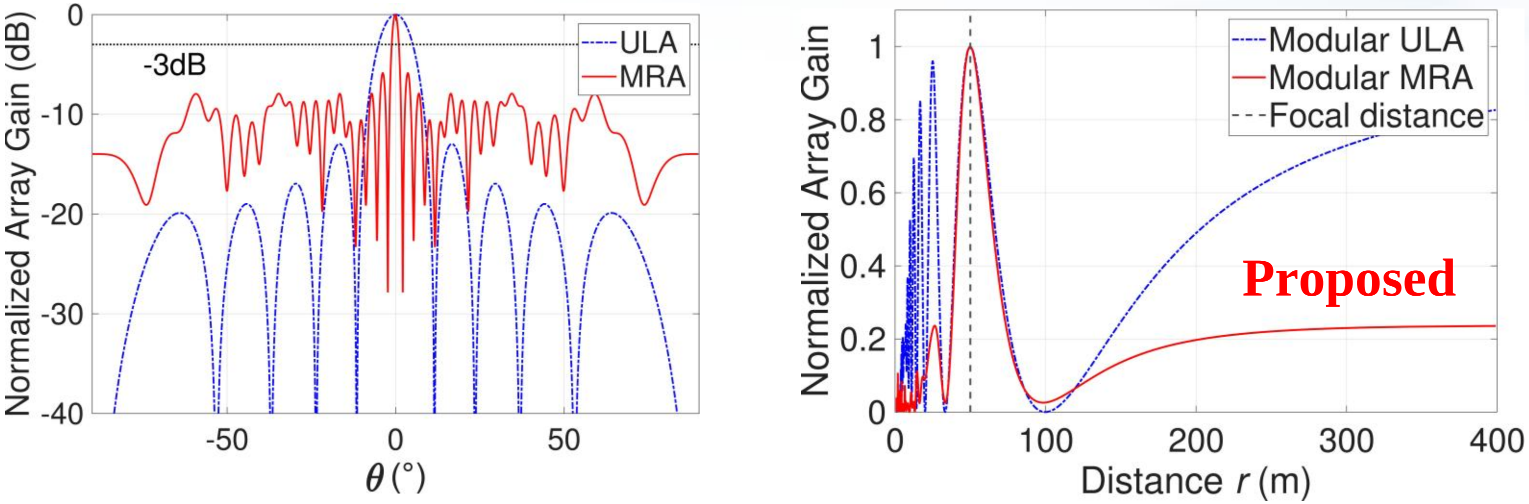

Suppression performance in the angle domain and the distance domain

Proposed M-MRA can suppress grating lobes in both angle and distance domains

M. Zhou, Z. Xu, and **L. Dai**, "Near-field communications with grating lobes for quasi-distributed arrays: From ULA to MRA," *arxiv:2607.29341*, Jul. 2026.

Simulation Results

- **Multi-user near-field beam pattern**

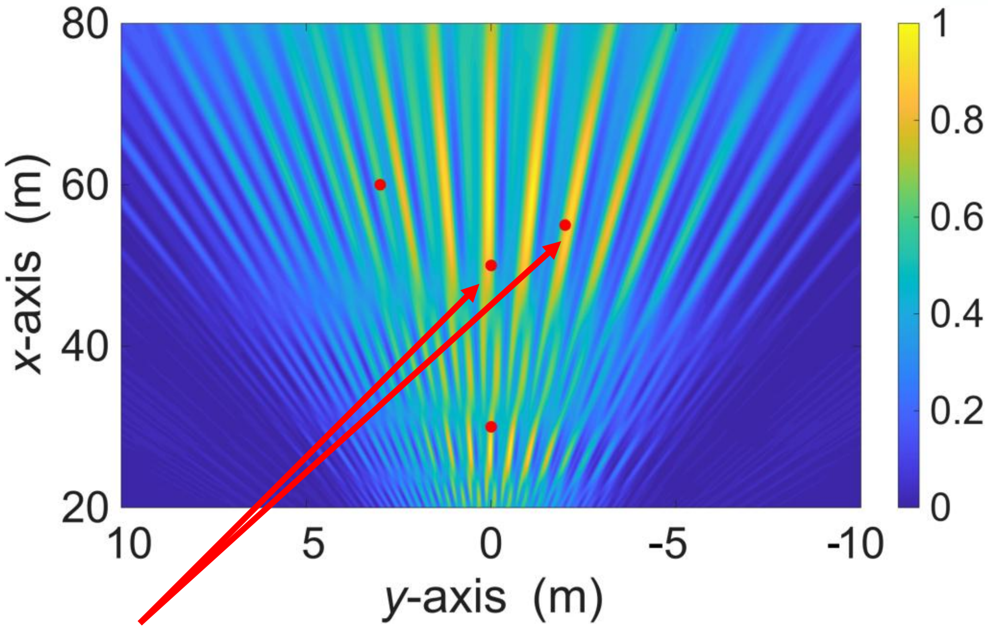

Conventional M-ULA

located in the grating lobe region of each other

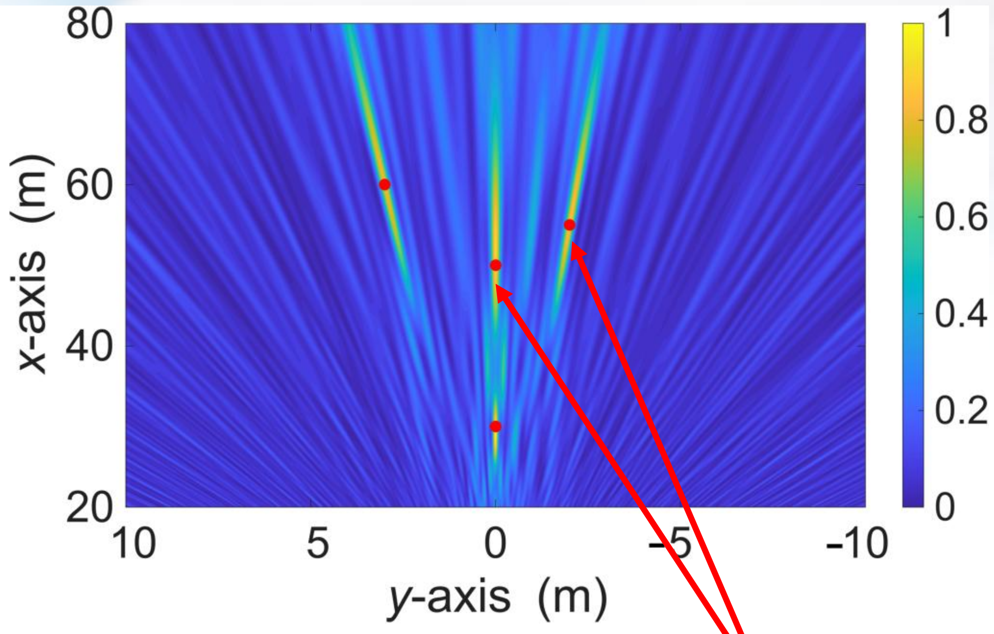

Proposed M-MRA

Effectively suppress grating lobes, thus reducing IUI

Proposed M-MRA can effectively reduce the inter-user interference caused by near-field grating lobes!

M. Zhou, Z. Xu, and **L. Dai**, "Near-field communications with grating lobes for quasi-distributed arrays: From ULA to MRA," *arxiv:2607.29341*, Jul. 2026.

Simulation Results

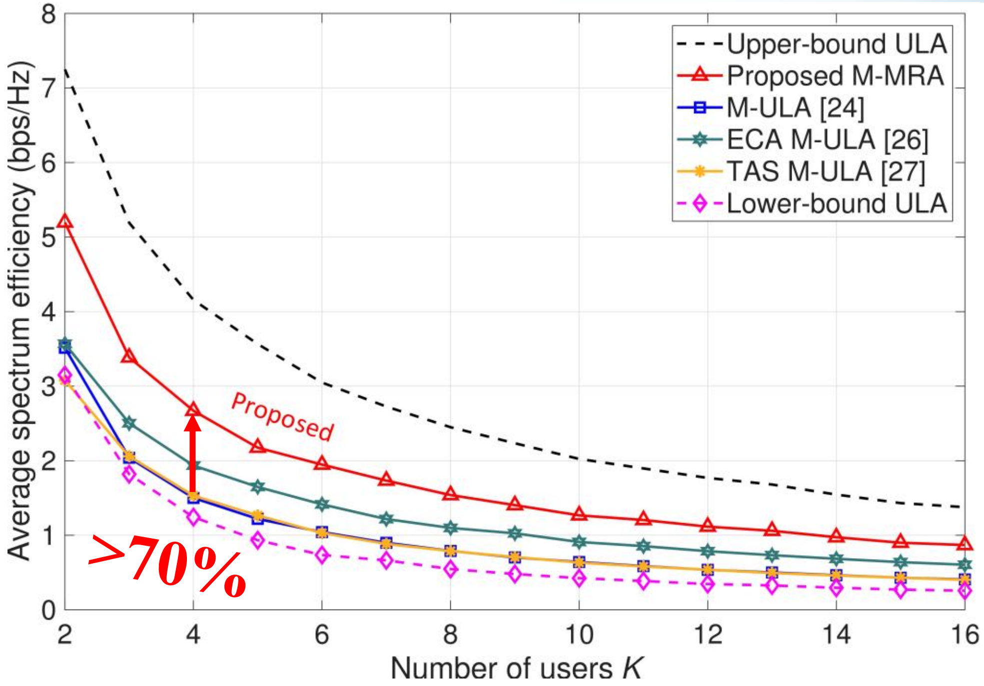

Fig. Average spectrum efficiency of six types of arrays versus different numbers of users

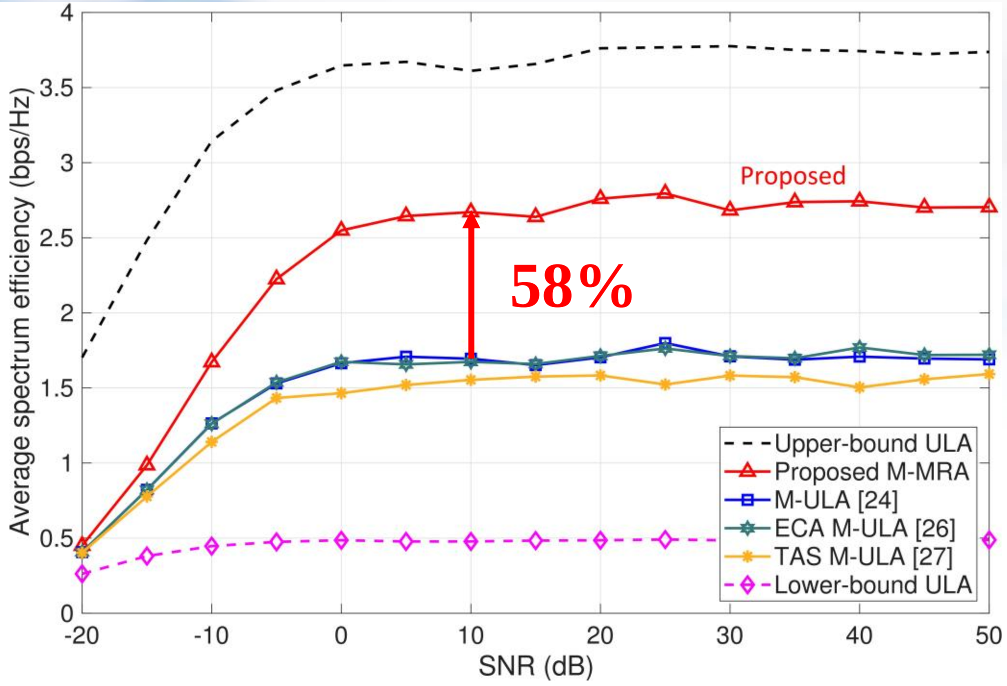

Fig. Average spectrum efficiency of six types of arrays versus different SNRs.

Proposed M-MRA can significantly improve the spectrum efficiency for multi-user near-field communications!

M. Zhou, Z. Xu, and **L. Dai**, "Near-field communications with grating lobes for quasi-distributed arrays: From ULA to MRA," *arxiv:2607.29341*, Jul. 2026.

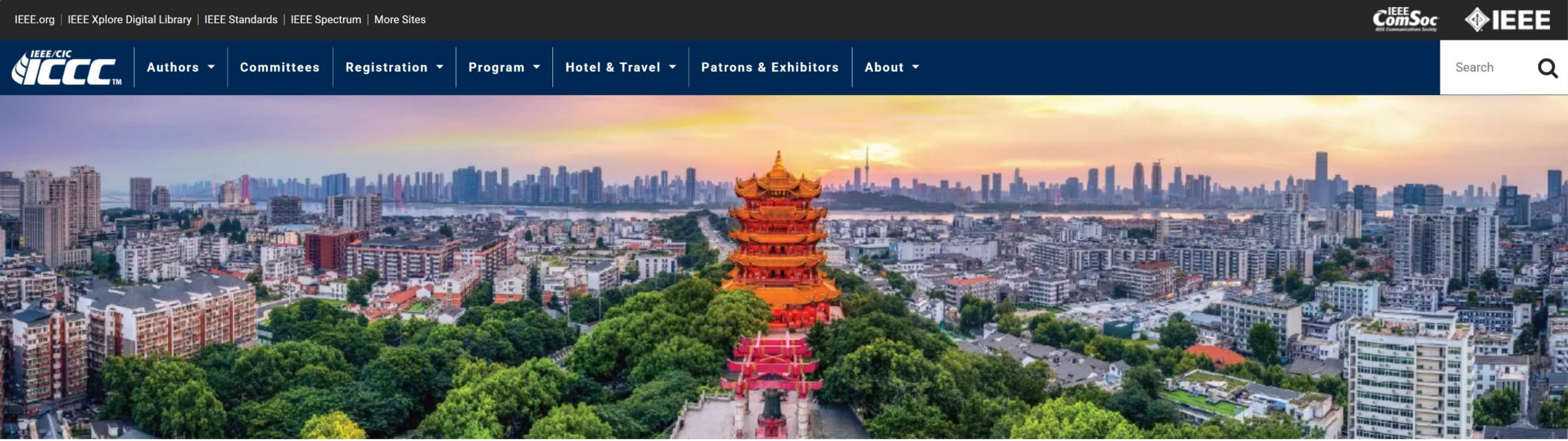

Part 5: Future Research Directions

1. Electromagnetic Information Theory (EIT)

- **Generalized near-field capacity analysis based on EIT**
  - **Existing near-field analysis on the DoFs assumes the uniform parallel array or LoS scenarios**
  - **DoFs analysis for generalized scenarios, such as RIS, cell-free, or NLoS scenarios, is required**

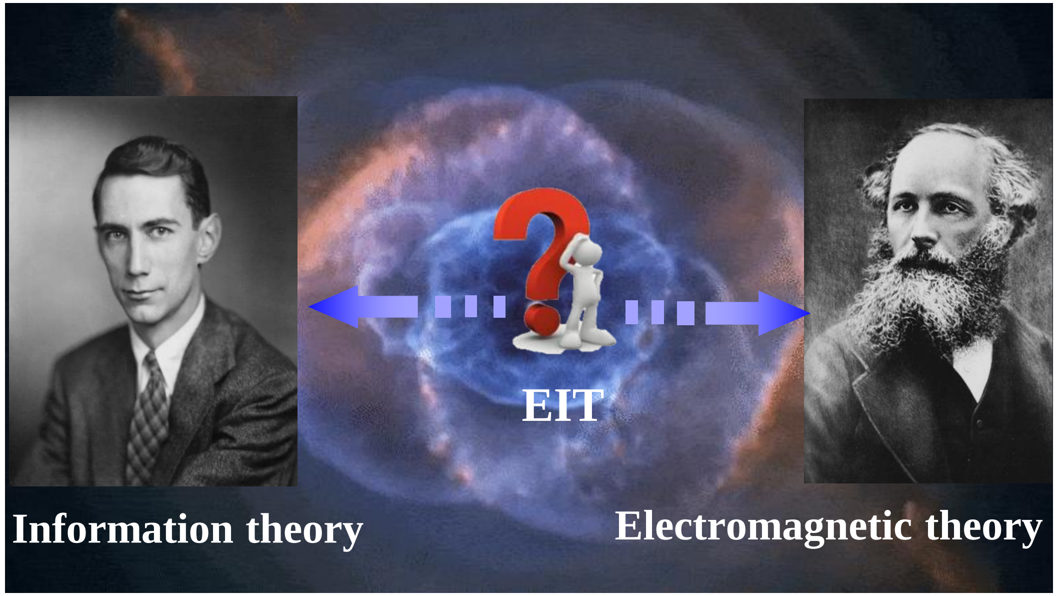

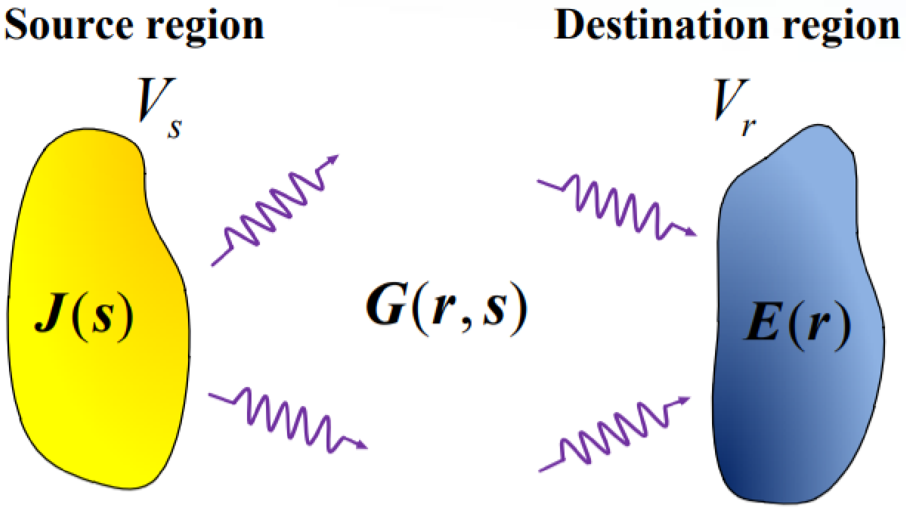

J. Zhu, Z. Wan, L. Dai, M. Debbah, and H. V. Poor, "Electromagnetic information theory: Fundamentals, modeling, applications, and open problems," *IEEE Wireless Commun.*, vol. 31, no. 3, pp. 156-162, Jun. 2024..

2. Near-Field Chanel Modeling

- **Near-field channel modeling faces high complexity issues**
- **The problem of spatial non-stationary can affect near-field channel modeling**

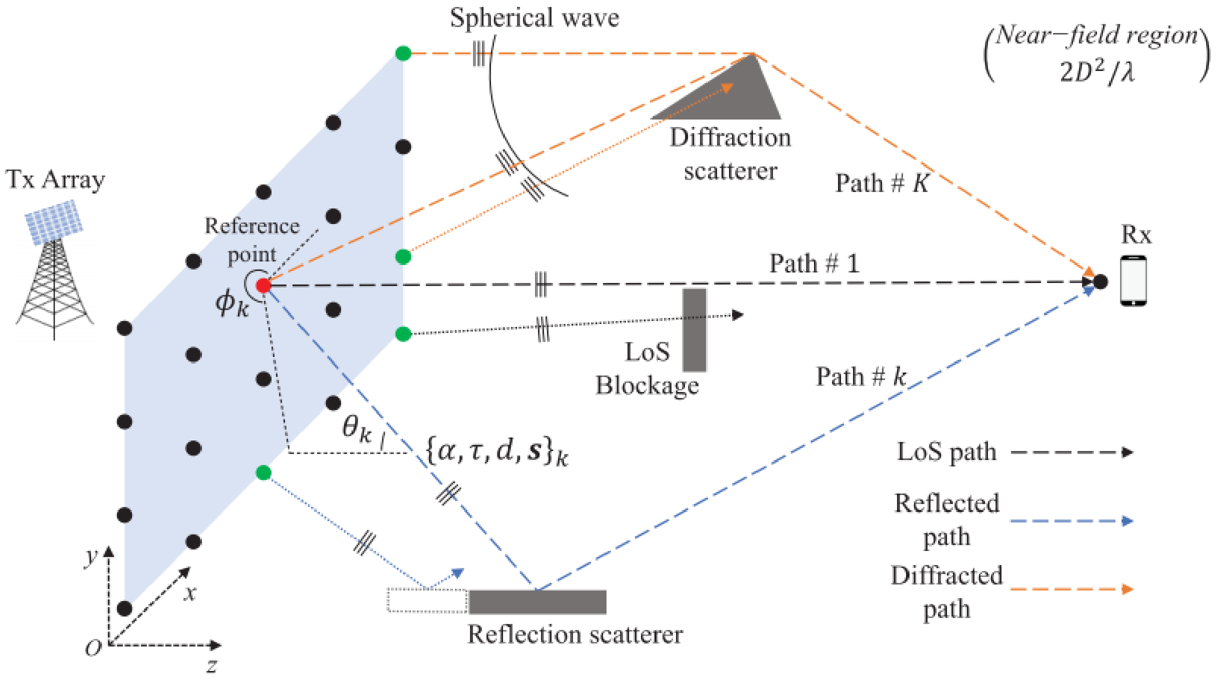

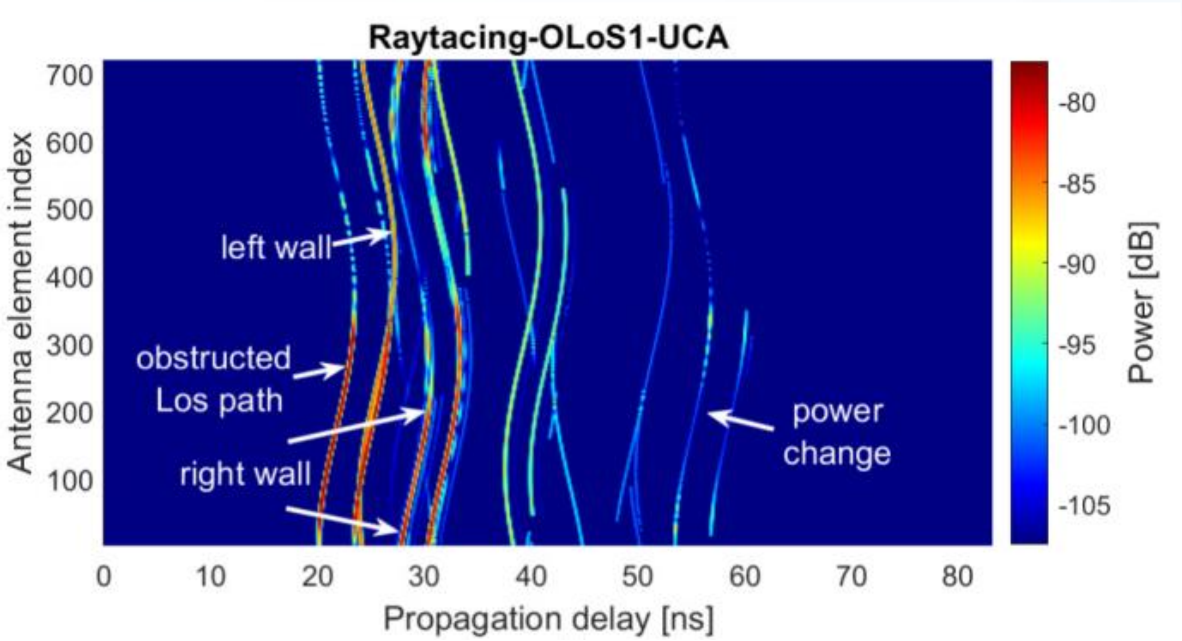

Z. Yuan, J. Zhang, Y. Ji, G. F. Pedersen and W. Fan, "Spatial non-stationary near-field channel modeling and validation for Massive MIMO systems," *IEEE Trans. Antennas Propag.*, vol. 71, no. 1, pp. 921-933, Jan. 2023.

3. Near-Field Curved Beams

- **Realize THz near-field curved beams curving around obstacles**
- **New possibilities of wave front manipulation for mmWave/THz communications**

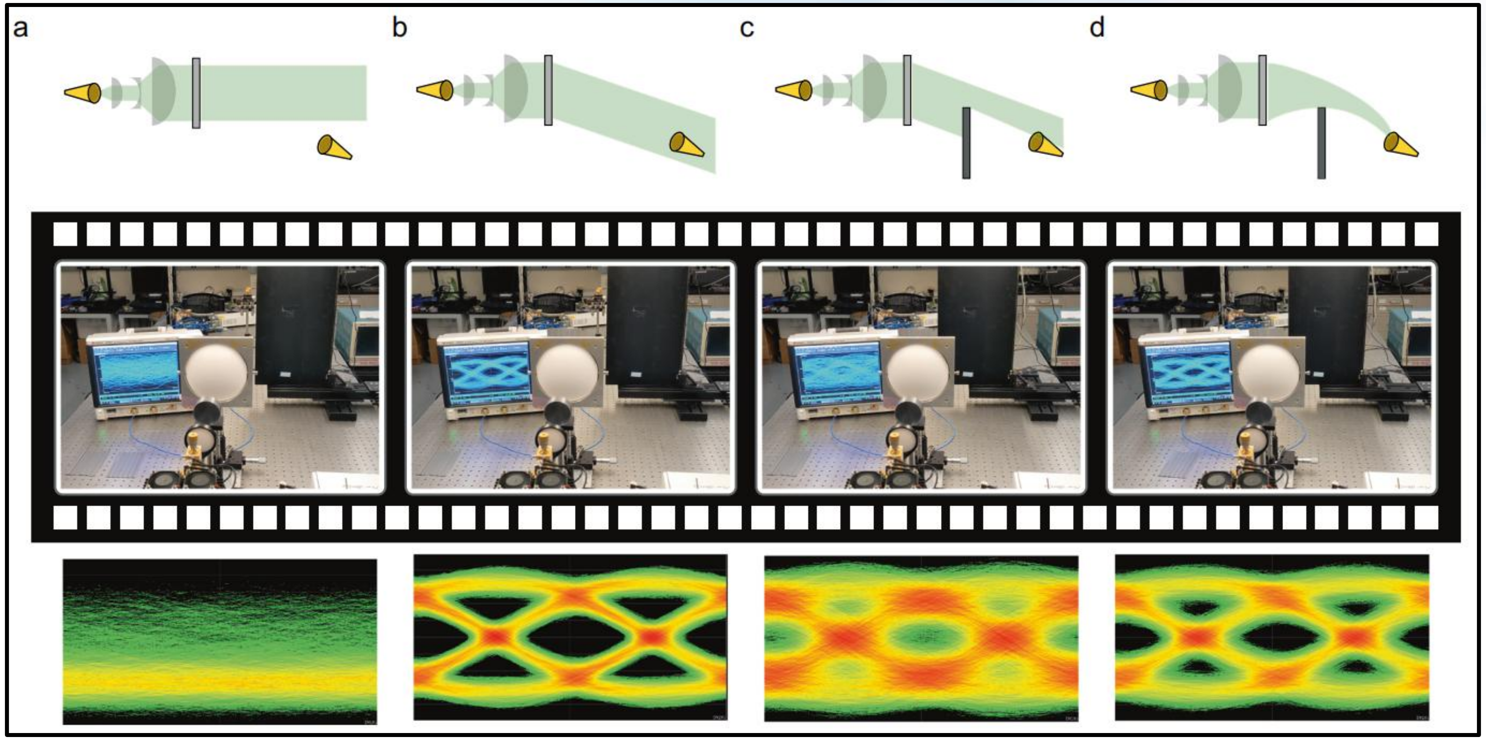

H. Chen, A. Kludze, and Y. Ghasempour, "A physics-informed Airy beam learning framework for blockage avoidance in sub-terahertz wireless networks," *Nature Communications*, 16: 4923, 2025.

4. Distributed Near-Field MIMO

- **Distributed MIMO with multiple BSs has larger virtual ELAA than cellular system**
  - **The near-field range will become larger in a distributed/cell-free MIMO systems**
  - **The near-field effect can improve the capacity of distributed/cell-free MIMO systems**

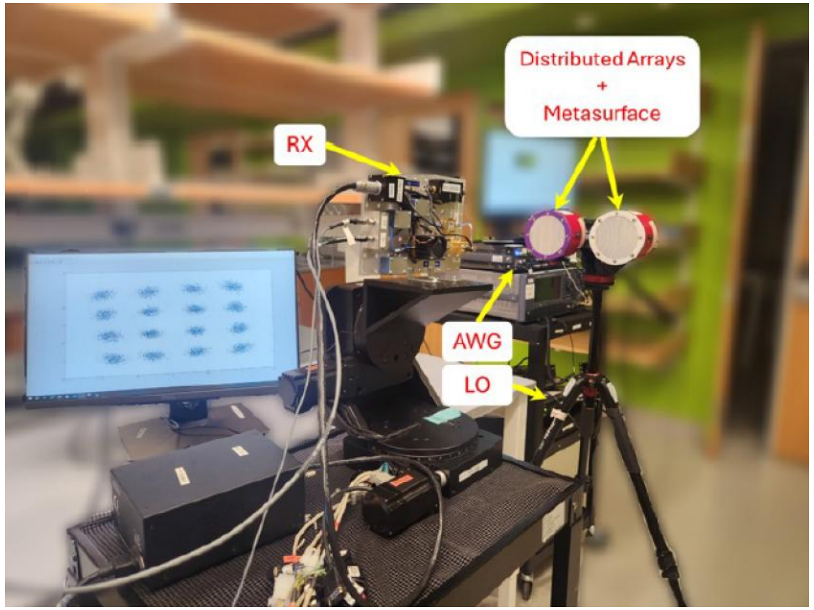

Distributed MIMO

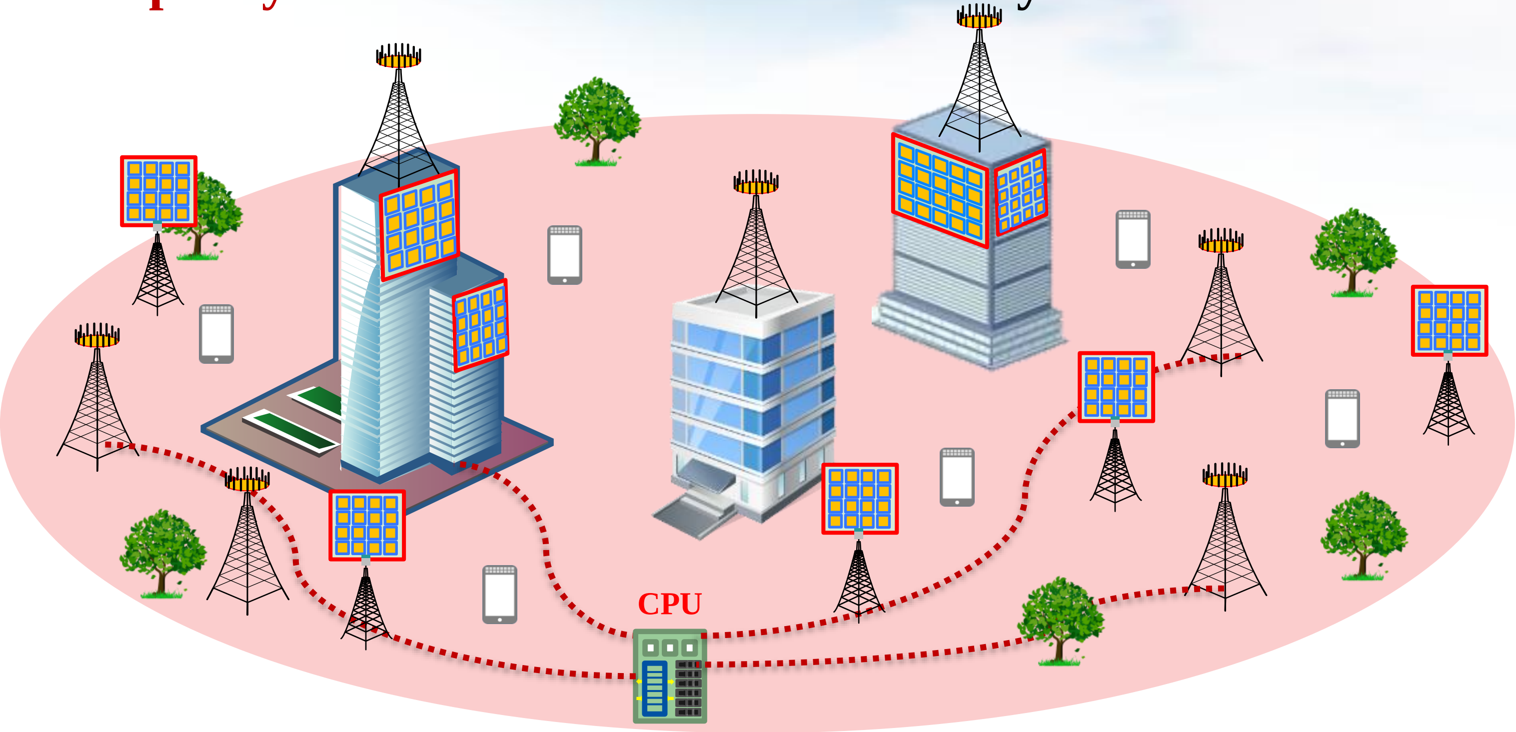

Cell-free MIMO

A. Kludze, D. Bodet, J. M.Jornet, and Y. Ghasempour, "Distributed wavefront shaping in radiative near-field sub-terahertz wireless networks," *Nature Communications*, 17, 5595, 2026.

5. RIS-Aided Near-Field Communications

- **Compared with MIMO, near-field becomes more dominant in RIS-aided systems**

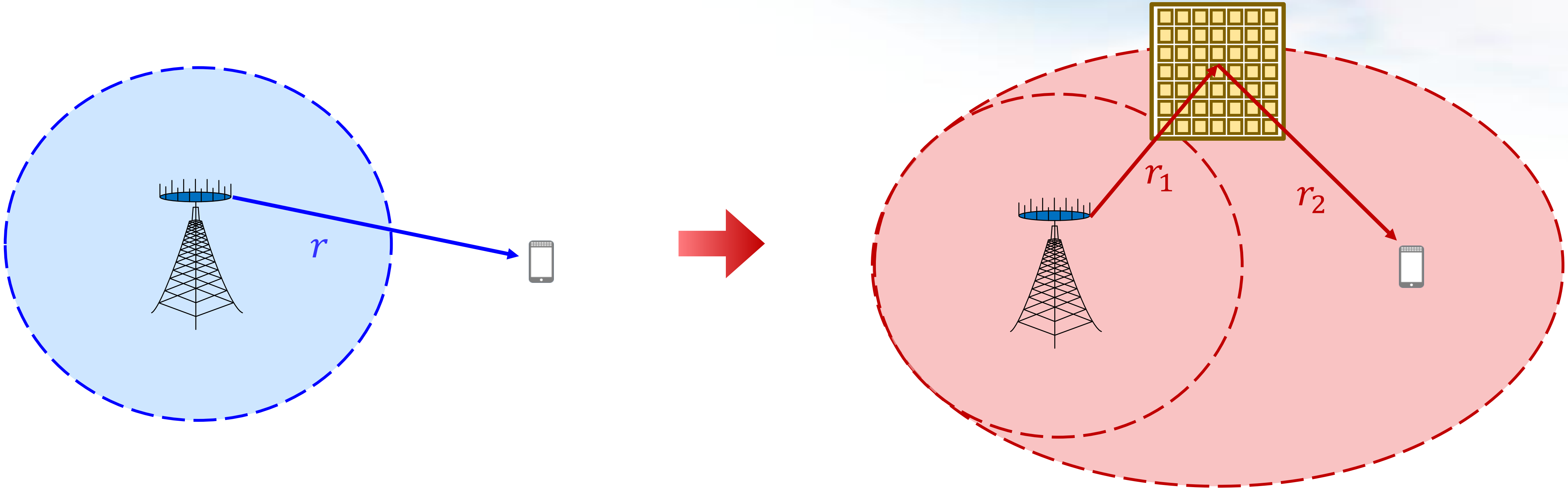

Near-field range for MIMO: $r < \frac{2D^2}{\lambda}$

Near-field range for RIS: $\frac{r_1 r_2}{r_1 + r_2} < \frac{2D^2}{\lambda}$

X. Wei, L. Dai, Y. Zhao, G. Yu, and X. Duan, "Codebook design and beam training for extremely large-scale RIS: Far-field or near-field?," *China Commun.*, vol. 19, no. 6, pp. 193-204, Jun. 2022. (**Invited Paper**)

6. AI-Aided Near-Field Transmission Techniques

- **The near-field channel model are much more complex**
  - ➢ **Non-linear channel phase in near-field compared to the linear channel phase in far-field**
  - ➢ **Much larger codebook size than the far-field codebook**

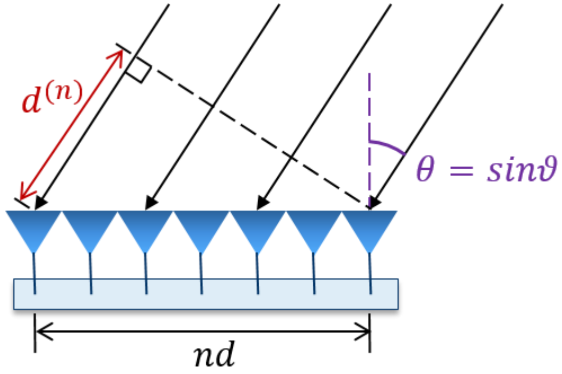

Far-field linear phase

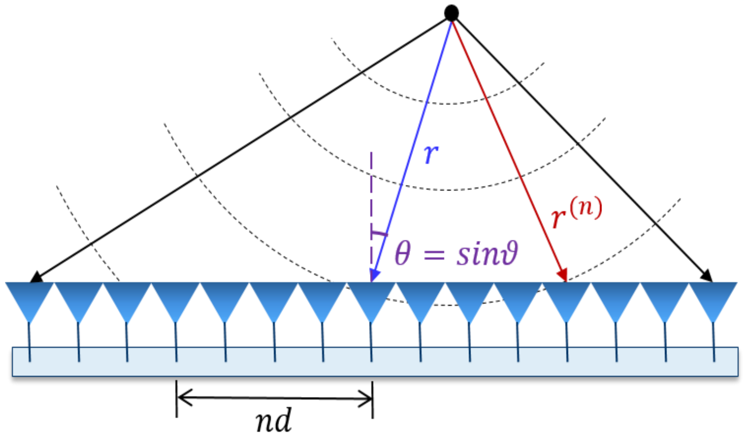

Near-field non-linear phase

Codebook size @ 100 GHz

Parameters	Far-field codebook	Near-field codebook
Number of antennas	512	512
Number of distance grids	1	20
Codebook size	512	10240

AI is promising to address this problem through non-linear neural networks

[1] X. Wei, C. Hu, and L. Dai, "Deep learning for beamspace channel estimation in millimeter-wave massive MIMO systems," *IEEE Trans. Commun.*, vol. 69, no. 1, pp. 182-193, Jan. 2021.

[2] Y. Chen, L. Yan, and C. Han, "Hybrid spherical- and planar-wave modeling and DCNN-powered estimation of Terahertz ultra-massive MIMO channels," *IEEE Trans. Commun.*, vol. 69, no. 10, pp. 7063-7076, Oct. 2021.

7. Near-Field Localization

- **Enhanced localization accuracy exploiting the distance-aware channels**
  - **The curvature of arrival (CoA) can be used to infer the source position**

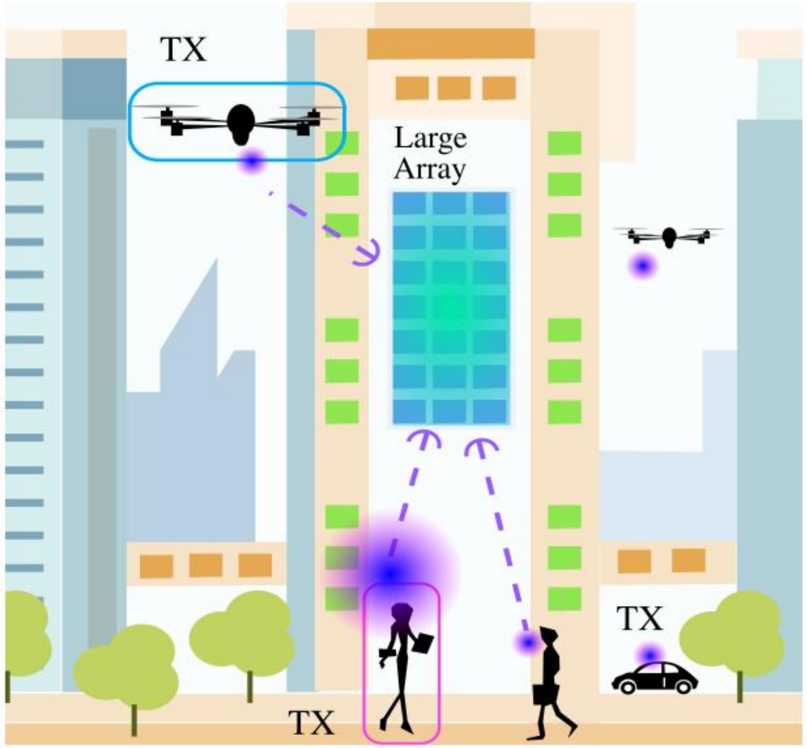

Localization scenario with ELAA

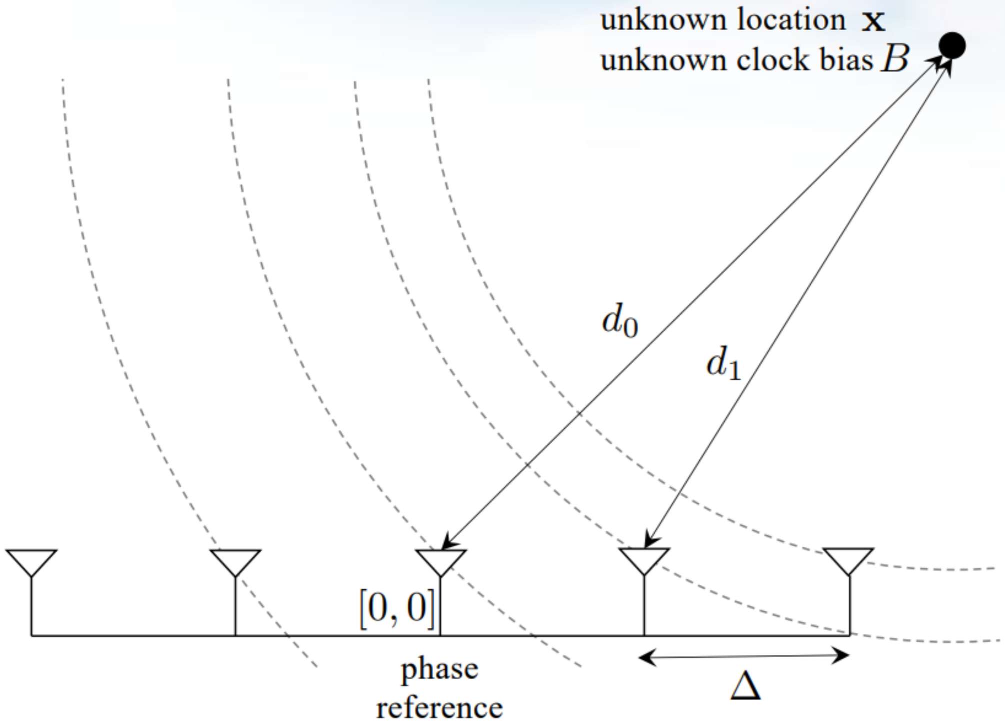

The curvature of spherical wavefront

A. Guerra, F. Guidi, D. Dardari, and P. M. Djurić, "Near-field tracking with large antenna arrays: Fundamental limits and practical algorithms," *IEEE Trans. Signal Process.*, vol. 69, pp. 5723-5738, 2021.

8. Near-Field ISAC

- **Near-field spherical wave holds the extra resolution in the distance domain**
- **Near-field propagation can potentially provide higher localization and tracking accuracy for ISAC**

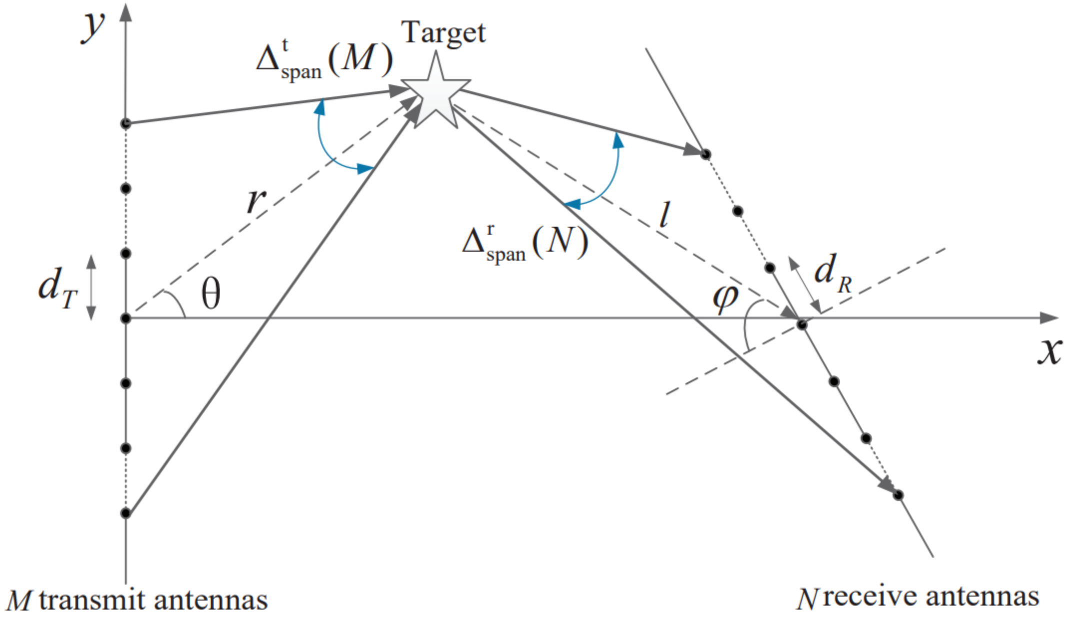

Radar sensing with extremely large-scale MIMO

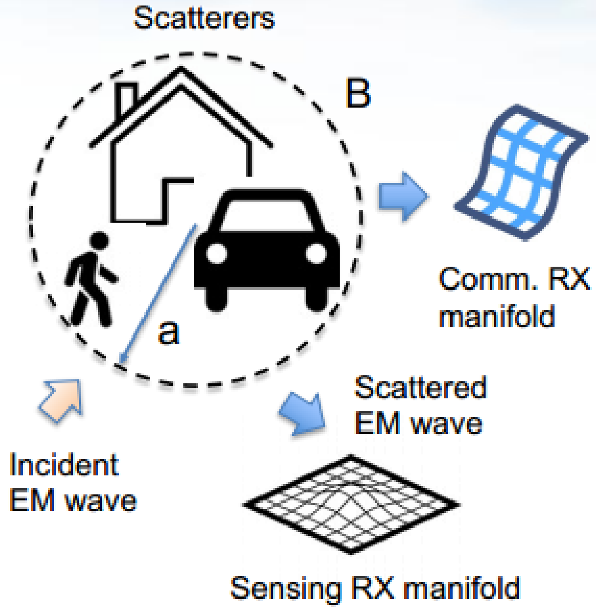

[1] A. M. Elbir, K. V. Mishra, S. Chatzinotas, and M. Bennis, "Terahertz-band integrated sensing and communications: Challenges and opportunities," *arXiv preprint arXiv:2208.01235*, Aug. 2022.

[2] H. Wang and Y. Zeng, "SNR scaling laws for radio sensing with extremely large-scale MIMO," in *Proc. 2022 IEEE International Conference on Communications Workshops (ICC Workshops)*, 2022, pp. 121-126.

9. Near-Field Holographic Imaging

- **Near-field holographic imaging with large-scale MIMO antennas**
  - **Near-field propagation would increase the number of exploitable degrees of freedom (DoF)**
  - **More informative measurements can be collected, thus leading to improved imaging capabilities**

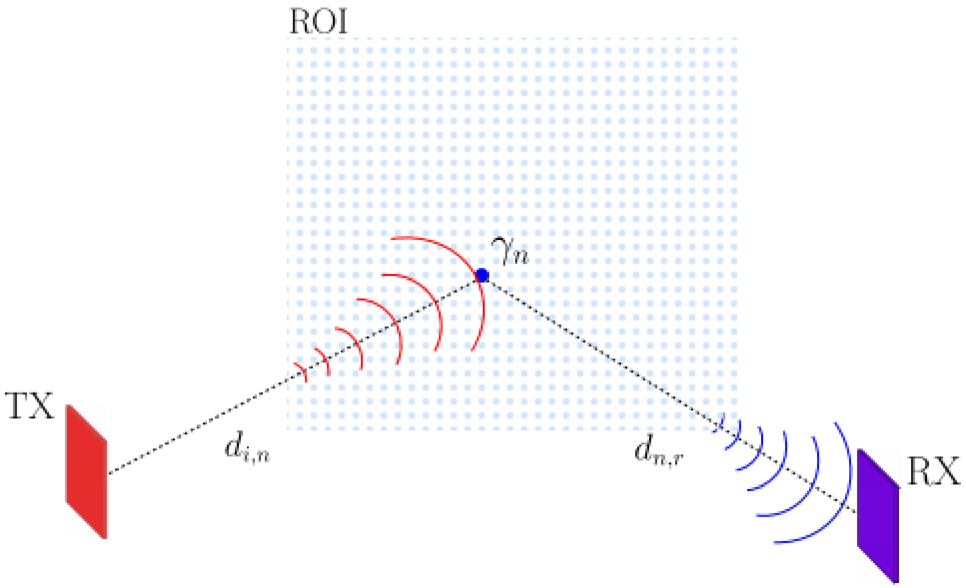

(a) LOS holographic imaging

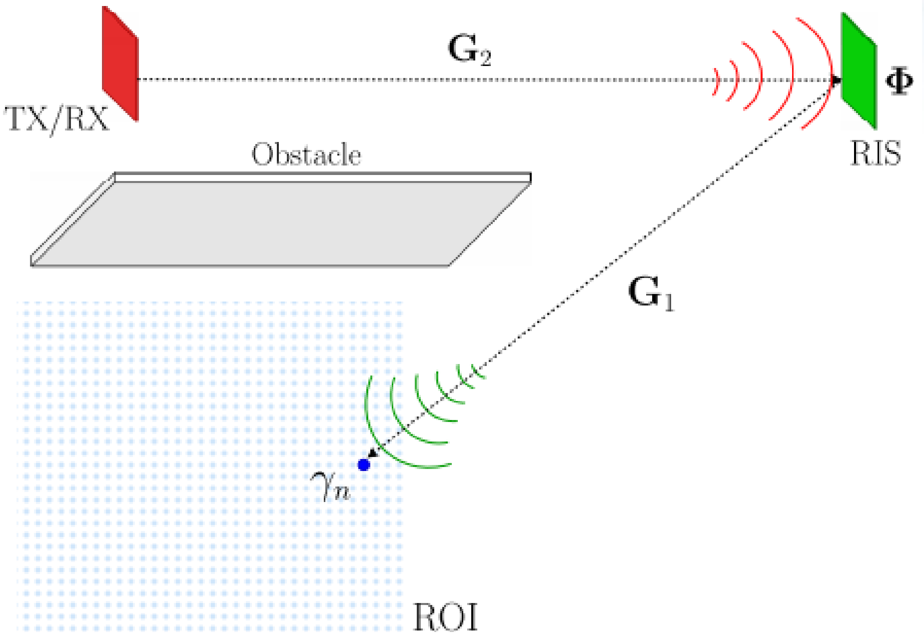

(b) NLOS holographic imaging

G. Torcolacci, A. Guerra, H. Zhang, F. Guidi, Q. Yang, Y. C. Eldar, and D. Dardari, "Holographic imaging with XL-MIMO and RIS: Illumination and reflection design," *IEEE JSTSP*, 2024.

10. Hybrid Far- and Near-Field Communications

- **Hybrid far- and near-field communications will be more practical**
  - ➢ **The environment coexists both far-field and near-field scatters**
  - ➢ **Channel modeling, channel estimation, hybrid precoding, localization, and so on**

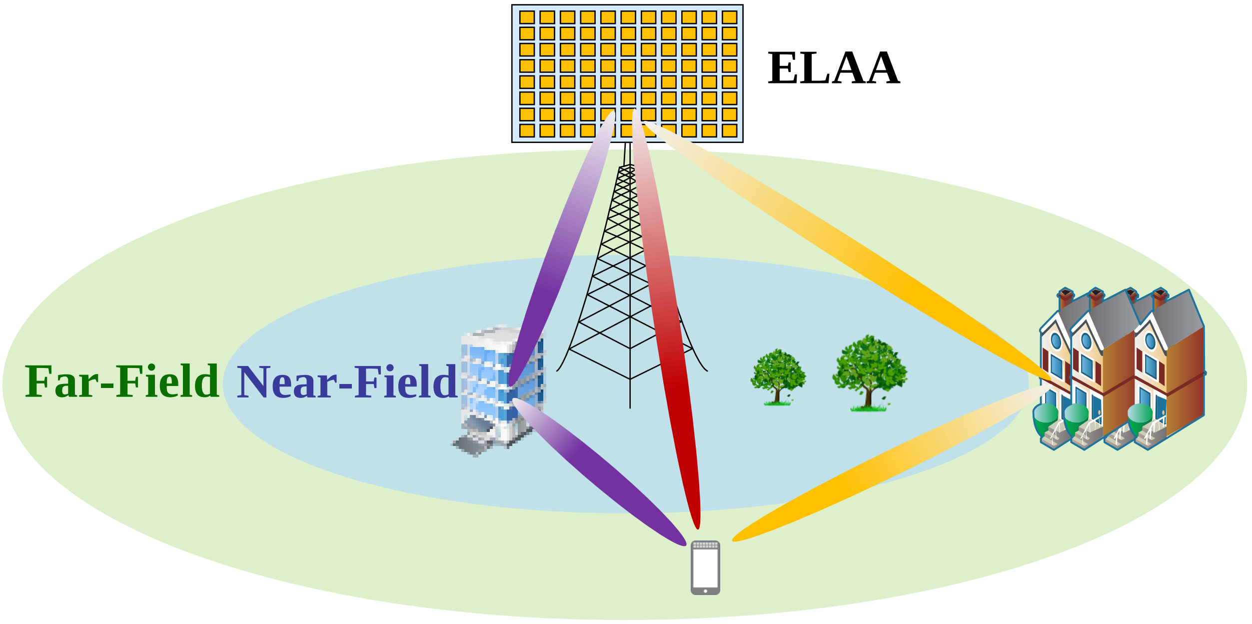

Hybrid-field communications[1]

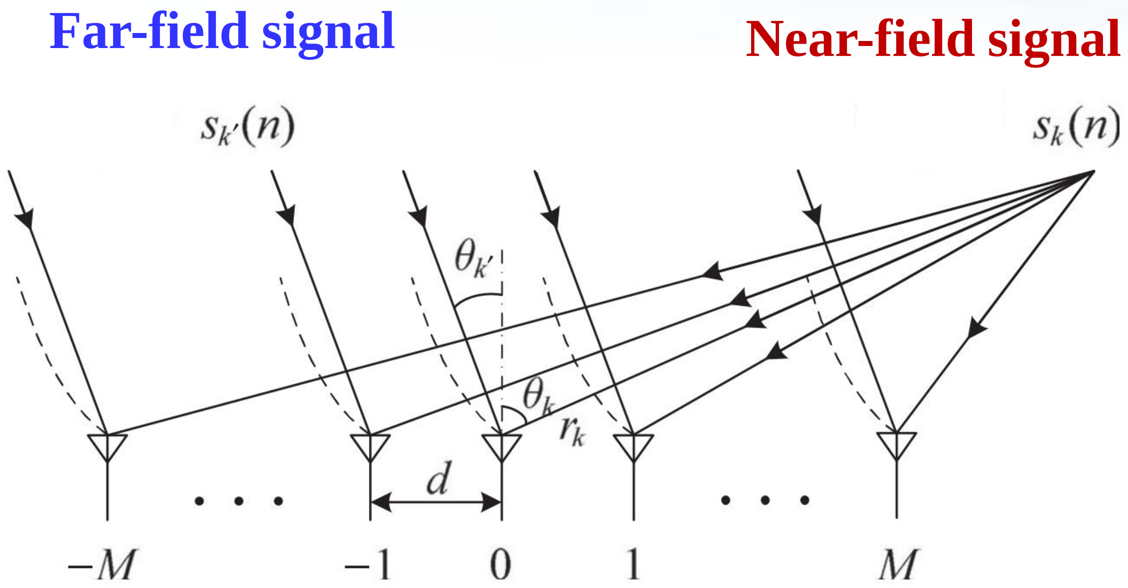

Hybrid-field localization[2]

---

[1] X. Wei and L. Dai, "Channel estimation for extremely large-scale massive MIMO: Far-field, near-field, or hybrid-field?," *IEEE Commun. Lett.*, vol. 26, no. 1, pp. 177-181, Jan. 2022.

[2] W. Zuo, J. Xin, N. Zheng, and A. Sano, "Subspace-based localization of far-field and near-field signals without eigendecomposition," *IEEE Trans. Signal Process.*, vol. 66, no. 17, pp. 4461-4476, Sep. 2018.

11. Hardware Verification

- **Extremely large antenna array prototypes**
  - **Tsinghua (2022): 2304-element ELAA, carrier 28 GHz, bandwidth 800 MHz, peak data rate 1.68 Gbps**
  - **Qualcomm (WMC 2024): 4096-element ELAA, 13 GHz, Rayleigh distance 95 m**

2304-element ELAA

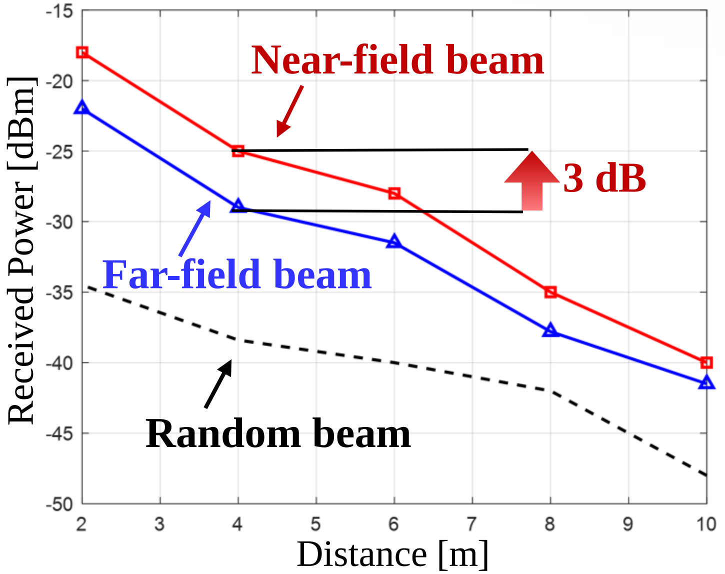

4096-element ELAA

M. Cui, Z. Wu, Y. Chen, S. Xu, F. Yang, and L. Dai, "Demo: Low-power communications based on RIS and AI for 6G," in *Proc. IEEE ICC 2022*, May 2022. (**IEEE ICC 2022 Outstanding Demo Award**)

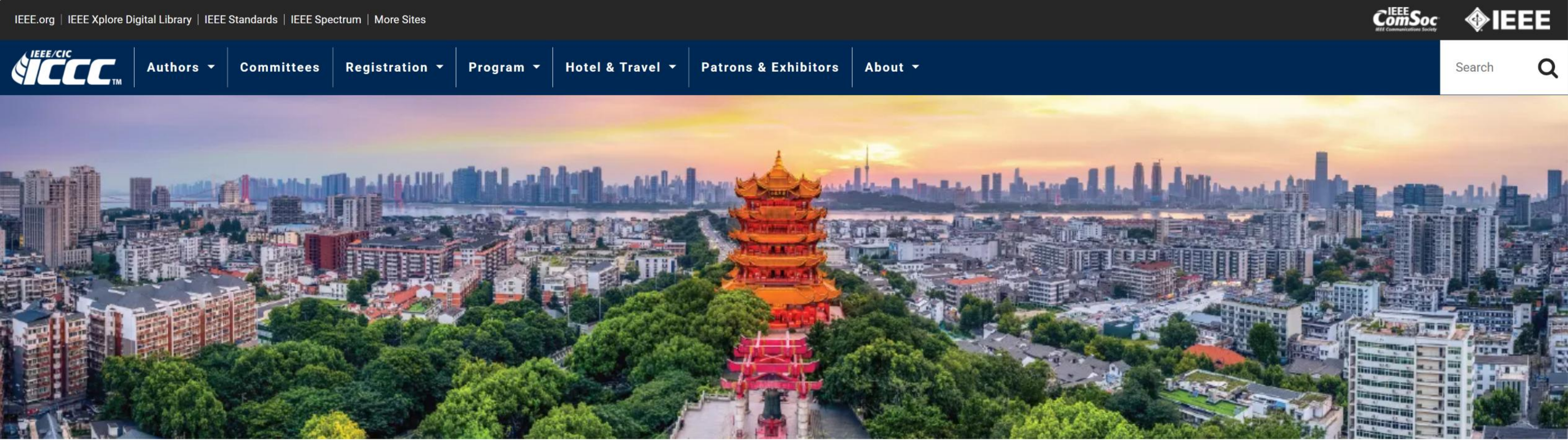

Conclusions

Conclusions

- Overview of **near-field communications** for 6G
- Fundamentals
  - Derivation of **Rayleigh distance**
  - Beamsteering vs. **beamfocusing**
- Potentials
  - Near-field **single-user capaticy enhancement**
  - Near-field **multi-user capaticy enhancement**
  - Near-field Airy beam **for blockage mitigation**
- Challenges
  - Near-field **channel estimation**
  - Near-field **beam split**
  - Near-field **grating lobes suppression**
- Future directions
  - **EIT**, distributed MIMO, **RIS**, ISAC, prototypes, …

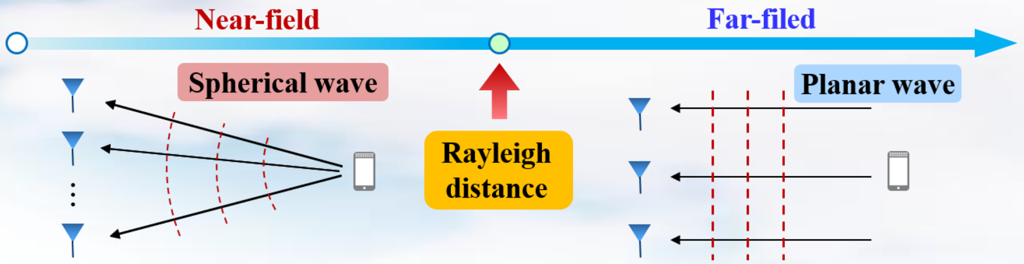

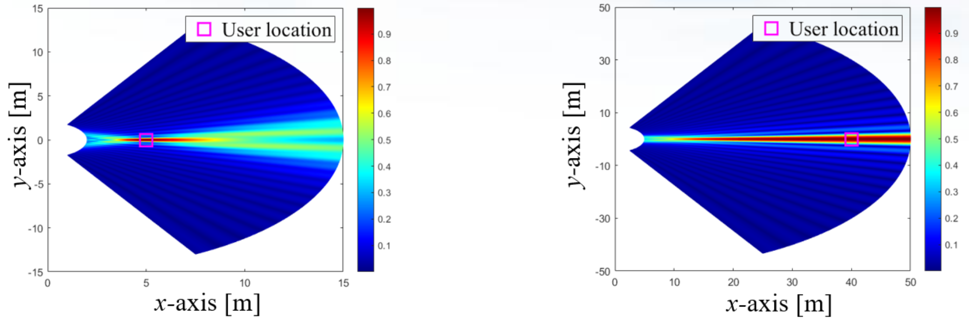

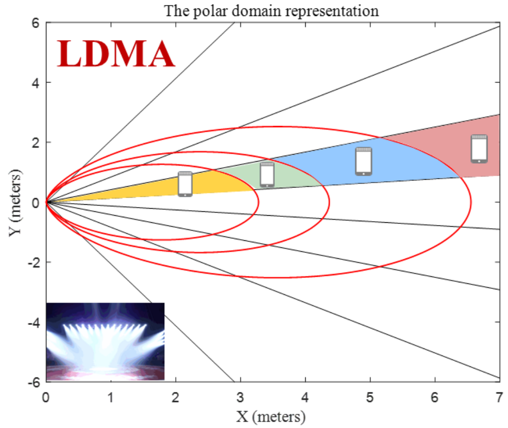

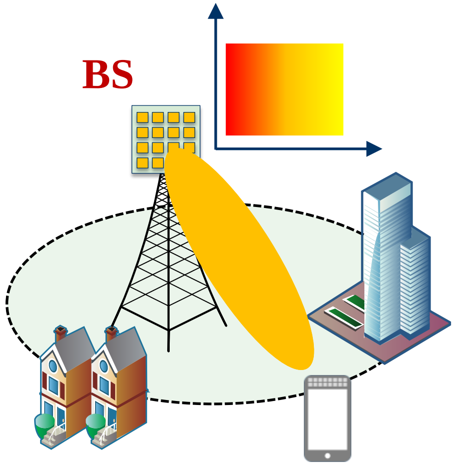

Near-Field Communication: A Double-Edged Sword

- Every coin has two sides
- Near-field communication is a double-edged sword for future 6G

Near-field communications

Potentials

Near-field communication capacity enhancement

Near-field sensing accuracy improvement

Challenges

Near-field channel estimation

Near-field beam split


0011
0101
0010
1000
1110
0101
1110
Thanks